INTRAMOLECULAR TUNNEL AND REGULATORY MECHANISMS OF ASPARAGINE SYNTHETASE (ASNS)

By

Kai Li

A DISSERTATION PRESENTED TO THE GRADUATE SCHOOL
OF THE UNIVERSITY OF FLORIDA IN PARTIAL FULFILLMENT
OF THE REQUIREMENTS FOR THE DEGREE OF
DOCTOR OF PHILOSOPHY

UNIVERSITY OF FLORIDA

2007

To my wife, Zhen, and my parents

ACKNOWLEDGMENTS

I acknowledge the financial support for the travel grants from College of Liberal Arts and Sciences and Graduate Student Council, which made it possible to present my work at several conferences.

I thank Dr. Nigel G. J. Richards, my supervisor, who guided me into enzymology research field by working on asparagine synthetase. I am grateful to my doctoral dissertation committee, Dr. Nicole A. Horenstein, Dr. Daniel L. Purich, Dr. Adrian E. Roitberg, and Dr. Jon D. Stewart, for their helpful advices on my project. Furthermore, I would like to thank Dr. Gail E. Fanucci, Dr. Ion Ghiviriga, Dr. Thomas J. Lyons and Dr. David N. Silverman for their helps.

Special thanks go to Dr. Drazenka Svedruzic, Dr. Jemy A. Gutierrez, Dr. Tania Córdova de Sintjago and Dr. Patricia Moussatche, for their helpful discussions with my projects; William Beeson and Alexandria Berry, two undergraduates, with whom I accomplished this work; Xiao He, Dr. Hui Jiang, Sangbae Lee, Mario E. Moral, and Dr. Yong Ran, for their friendship and helps.

I am grateful to my mom and stepfather for their unconditional support of any decision I made, to my parents-in-law for their care by sending me email everyday and to my wife for the happy life we shared for almost ten years.

TABLE OF CONTENTS

page

LIST OF TABLES

LIST OF FIGURES

Abstract of Dissertation Presented to the Graduate School
of the University of Florida in Partial Fulfillment of the
Requirements for the Degree of Doctor of Philosophy

THE INTRAMOLECULAR TUNNEL AND REGULATORY MECHANISMS OF ASPARAGINE SYNTHETASE (ASNS)

By

Kai Li

December 2007

Chair: Nigel G. J. Richards
Major: Chemistry

So far, more and more evidence from several actively studied polyfunctional enzymes indicate the existence of an intramolecular tunnel. Among those enzymes, ammonia/ammonium is the most common intermediate thus far. As one of these enzymes, the tunnel in asparagine synthetase B (ASB) from *Escherichia coli* is about 20 Å long. It connects two active sites, a glutaminase site and a synthetase site.

My work on asparagine synthetase (ASNS), an enzyme involved in leukemia resistance to the treatment using asparaginase, has focused on the following aspects: (1) kinetic characterization of ASNS; (2) structure activity relationships; (3) regulatory mechanisms.

In this work, I developed a first quantitative NMR based assay (K. Li et al, *Biochemistry*, 2007, ***46[****16]*, 4840-4849) and studied the efficiency of ammonia tunneling in ASB catalyzed reaction.

The function of bioactive macromolecule can only be understood under the structural context. Therefore, to study the function of the intramolecular tunnel in ASB, first I identified the tunnel residues by computational methods. Most of the tunnel residues are conserved from prokaryote to eukaryote species. The studies of several tunnel mutant showed that one of the mutants may have a blocked tunnel.

Among the family of amidotransferases, the two half reactions are strictly coupled. While ASNS can catalyze the hydrolysis of glutamine without other substrates, this raises the interest in the regulatory mechanisms of this enzyme, which prevents it from consuming glutamine and releasing free ammonia. As part of my PhD research, I investigated the mechanisms of product inhibition to this enzyme. Under physiological conditions, the activity of this enzyme may be inhibited significantly by asparagine, which prevents cells from wasting glutamine and producing toxic ammonia in *vivo*.

So far, only one crystal structure of glutamine dependent asparagine synthetase was reported. To further understand the function of ASNS, especially of human enzyme, more crystal structures are needed. Therefore, co-working with Alexandria Berry, I investigated the binding of substrate/transition state analog to hASNS and successfully prepared inhibitor bound enzyme. The prepared enzyme has been sent for crystal analysis.

CHAPTER 1

INTRODUCTION

Asparagine Synthetase (ASNS) and the Intramolecular Tunnel

With the advances in molecular biology and crystallography, many complex proteins have been structurally determined. More and more evidences show that intramolecular tunnel exists in many enzymes with multiple catalytic sites. Since the first intramolecular tunnel within tryptophan synthase was found in 1988 (*1*), tunnels within at least 11 enzymes have been demonstrated (*2, 3*). Among these tunnels, NH_3/NH_4^+ tunnels in amidotransferases are the most common. It has been determined in carbamoyl phosphate synthetase (CPS), GMP synthetase, glutamine phosphor-ribosylpyrophosphate amidotransferase (glutamine PRPP amidotransferase), asparagines synthetase B (ASB), glutamate synthase, imidazole glycerol phosphate synthase, glucosamine 4-phosphate synthase, and recently, CTP synthase (*4*). All these enzymes use glutamine as nitrogen source donor. First, glutamine is hydrolyzed into glutamate (product) and NH_3/NH_4^+ (intermediate) at one active site. Then NH_3/NH_4^+ is transported to another active site through an intramolecular tunnel for next half-reaction. It seems that all proteins that use glutamine to produce NH_3/NH_4^+ as intermediate will have this kind of intramolecular tunnel.

Among those enzymes with NH_3/NH_4^+ tunnel identified thus far, asparagine synthetase (include ASB and mammalian AS), Glucosamine 4-phosphate synthase, Glutamine PRPP amidotransferase, and glutamate synthase belong to Ntn hydrolases / class II glutamine amidotransferase subfamily, since they all have an N-terminal nucleophile – cysteine, which catalyzes the hydrolysis of glutamine (*5, 6*).

Asparagine synthetase catalyzes ATP-dependent conversion of aspartate to asparagine. The discovery of asparagine synthetase resulted from the studies about the metabolism of amino acids. Asparagine is one of the amino acids that have been lately studied. After the first

discovery of proteins with asparagine synthetase activity in the early 1950s, asparagine synthetase has been found in many species including prokaryote and eukaryote. The studies for asparagine synthetase raised even more interests because of the correlation between asparagine level in human cells and the resistance to the treatment of asparaginase in certain types of cancer cells such as acute lymphoblastic leukemia (ALL) (*7, 8*).

In *E. coli*, two unlinked genes with little similarities, *asnA* and *asnB*, encode asparagine synthetase (*9-12*). While asparagine synthetase A (ASA) from *asnA* can only use ammonium as nitrogen source, asparagine synthetase B (ASB, EC 6.3.5.4) can use both ammonium and glutamine, with a preference of glutamine. ASB belongs to class II or Ntn amidotransferase subfamily and catalyzes following reactions.

$$\mathbf{Gln + H_2O + ATP + Asp \rightarrow Glu + AMP + PPi + Asn} \qquad \mathbf{(R1)}$$

$$\mathbf{NH_3 + ATP + Asp \rightarrow AMP + PPi + Asn} \qquad \mathbf{(R2)}$$

$$\mathbf{Gln + H_2O \rightarrow Glu + NH_3} \qquad \mathbf{(R3)}$$

Because of its 37% identity to human asparagine synthetase and the same reactions that catalyzes, ASB has served as a model system to understand the biosynthesis and metabolic control of asparagine. Up to now, the function of ASB from *E. coli* has been extensively studied (*13*). Boehlein et al (1994) reported that both C1A and C1S mutant of ASB lose glutaminase activity completely, although these two mutants still can bind glutamine. This result confirms the important catalytic role of N-terminal cysteine residue in hydrolysis of glutamine. By analogy with cysteine proteases, the thiolate anion of Cys1 residue act as nucleophile (Figure 1-1) and attack the γ-carbonyl group of glutamine to form a thioester intermediate and ammonia. The thioester then reacts with water to produce glutamate. This mechanism is strongly supported by the report that a covalent intermediate during the glutaminase reaction were isolated and proposed to be γ-glutamyl thioester (*14*). In 1998, the same research group reported their studies

about the kinetic mechanism of *E. coli* ASB. Scheme 1-1 shows the kinetic mechanism based on their report. They also provided the evidence by ^{18}O transfer experiment that supports the existence of intermediate, β-aspartyl-adenylate (β-aspartyl-AMP), which reacts with NH_3/NH_4^+ produced by hydrolysis of glutamine (or NH_3/NH_4^+ from bulk solution) to synthesize asparagine (Figure 1-2).

After the crystal structure of C1A mutant of ASB was reported (*15*), there is no doubt about the existence of an intramolecular tunnel in ASB. The crystal structure clearly shows two active sites, named glutaminase site and synthetase site. Glutaminase domain comprises the N-terminal half of the protein (1-190) and synthetase domain the C-terminal half (208-553). The two halves are connected by a coil of 17 residues. The distance between two active sites is about 20 Å. Like other members of Ntn subfamily, glutamine domain is a αββα four layer sandwich structure. Glutamine binding pocket is between the two antiparallel β-sheets at one edge of the domain (Figure 1-3).

Glutaminase domain catalyzes the hydrolysis of glutamine (R3). Synthetase domain catalyzes ATP-dependent synthesis of asparagine (R2), using NH_3/NH_4^+ produced by R3. There are two possible pathways for NH_3/NH_4^+ produced at glutaminase site to get to synthetase site. One is intermolecular pathway. That is, NH_3/NH_4^+ first is released by ASB and then equilibrates with bulk solution before the synthesis reaction. The other pathway is through intramolecular tunneling. The kinetic results rule out the first one as the major pathway, if it does exist. Suppose NH_3/NH_4^+ goes through bulk solution, it will take some time for NH_3/NH_4^+ cumulating and reaching a concentration at which the synthetase activity can be detected. This means there would be a lag for the glutamine dependent synthetase activity. Furthermore, the k_{cat} value of glutamine dependent synthetase activity should be same as that of ammonia dependent activity.

This is inconsistent with the kinetic results. There must be an intramolecular pathway (tunneling) to transport NH_3/NH_4^+.

To date, ASB has been extensively studied by steady state studies (*16-24*). Although there is no doubt for the existence of tunnel in ASB, the mechanisms of ammonia tunneling are still unclear. In order to understand vectorial transport of NH_3/NH_4^+ under structural context, I explored the structure of the tunnel,

The Intramolecular Tunnel

Determination of residues that involved in NH_3/NH_4^+ tunnel by experiment is the essential step for understanding the transportational mechanisms of NH_3/NH_4^+, synchronization of the two active sites, and therefore, the catalytical mechanisms of asparagine synthetase.

41 residues were determined involving in the NH_3/NH_4^+ tunnel within ASB based on the crystal structure (PDB code: 1CT9) of C1A mutant of *E. coli* ASB. These residues can be arbitrarily divided into 3 parts, the mouth, the body, and the bottom. Figure 1-4 shows the cavity formed by these residues with Gln and AMP binding. By aligning sequences from 21 species, including bacteria, plant and animal, prokaryote and eukaryote, 21 out of 41 residues mentioned above are identical. 7 are almost absolutely conserved with only one exception. Most of the rest are substituted by similar residue such as L by I or by V (Appendix A).

Glutaminase Active Site and the Mouth of the Tunnel

Table 1-1 lists all the residues in glutamine active site of *E. coli* ASB. The distinctive feature of Ntn subfamily is that they all contain several invariant residues. Cys^{1}-Arg^{49}-Asn^{74}-Gly^{75}-Asp^{98} motif is distinctive feature of glutamine binding site of Ntn subfamily (*E. coli* ASB numbering) (Figure 1-5). Arg49 and Asp98 account for the specific binding of glutamine. Carboxyl group of glutamine forms ionic bond with Arg49 as well as hydrogen bonds with backbone of Ile52 and Val53, while the amino group interacts with two negative-charged

residues – Glu76, Asp98 and the backbone of Gly75. The distance between carboxyl O atom of Asp98 and amino N of Gln is 2.56 Å, indicating a very strong interaction. Meanwhile, Gly75 also forms a strong hydrogen bond with the carbonyl/amide group of Gln with an N-O distance of 2.53 Å. Carbonyl/amide group of Gln is also hydrogen-bonding with sidechain of Asn74. With the amino group of Cys1, these two fingerprint residues are believed to provide an oxyanion hole that stables transition state during the hydrolysis of glutamine. N/amide of Gln also interacts with carbonyl O of backbone of Leu50.

The amide group of Gln are surrounded by Ala 1 (Cys 1), Leu 50, Ile 52, Asn 74, Gly 75, Glu 76 (Figure 1-6), which form the mouth of the tunnel. These residues are highly conserved (Table 1-1, highlighted residues) and probably play an important role not only in binding of Gln and catalysis, but also in NH_3 releasing.

The Body of the Tunnel

In the interface of the two domains, Met 120, Ile 143, Asn 389, Ala 399, plus the carbonyl group of the backbone of Ala 388 form the narrow part of the tunnel, with a diameter of about 5-6 Å (Figure 1-4, table 1-2 & Figure 1-7).

His 29, Arg 30, Gly 31, Pro 32, Tyr78, Met392, Ser 393, Gly 396, Val 397, Glu 398 and Arg400 locate between the narrow part and the mouth of the tunnel (Figure 1-8A, B) and form the upper part of the tunnel. This part of the tunnel contains an absolutely conserved residue cluster in asparagine synthetases from different species, His^{29} -- Arg^{30} -- Gly^{31} -- Pro^{32} -- Asp^{33}. Arg^{30} and Gly^{31} are also fingerprint residues of Ntn subfamily. Other conserved residues in this part include Gly396 and Glu398. The residues in this part can not form a ring by themselves like the residues in the other part. They fill the gap between mouth and tunnel part 2. The size of tunnel here is bigger than other parts.

The lower part of the tunnel comprises Ile142, Leu232, Met329, Val344, Leu345, Ser346, Cys385, Ala388, Val401, Leu404 and sidechain of Glu348. Some of these residues are also in the ATP binding site (Figure 1-8C), such as Leu232, Leu345 and Ser346. Most of the residues in this part are hydrophobic (Figure 1-9) and conserved.

The Bottom of the Tunnel

This part of tunnel is formed by Asp 238, Gly 347, Glu 348, Gly 349, Ser 350, Asp 351, Glu 352, Tyr 357, Leu 380 and Asp 384. Most of the residues are in ATP binding site (Figure 1-8D). An interesting feature of this part is that almost all the residues are polar and 5 out of 10 are negative-charged residues (Figure 1-9). These negative-charged residues, plus Tyr357 form the end of the tunnel, which is presumed as the NH_3/NH_4^+ binding site. The carboxyl group of Glu 352 is right at the bottom of the tunnel and about 4-7 Å far away from AMP. This negative charge may provide the driving force to transport NH_3/NH_4^+. The α-phosphate group of AMP (ATP) is on the side of this part of tunnel (Figure 1-10).

The Interface of the Two Domains and Water

The fact that binding of ATP stimulates glutaminase activity of *E. coli* ASB suggests conformational changes during the catalysis (*17*). The signal between catalytic domains should arrive through those residues in the interface, especially those that interact with other residues from different domain (Table 1-3).

7 water molecules are in the tunnel, water 2, 3, 50, 190, 690, 709 and 861. Water 709 is the only one in the ATP binding site with AMP as the ligand. Since the kinetic data suggest no ATP hydrolyzing during catalysis, water molecules are supposed to be excluded when ATP and Asp bind the enzyme. The rest are all in the interface between the two domains.

ASB is an ideal system to study highly conserved NH_3/NH_4^+ tunnel in asparagine synthetase. With successful techniques of cloning, expression and purification (*16*), coupled with

the well-developed assay methods such as Glutaminase assay (*17*), PPi assay (*22*), and HPLC assay (*15*), the intramolecular tunnel of ASB were studied and the structure activity relationship were investigated.

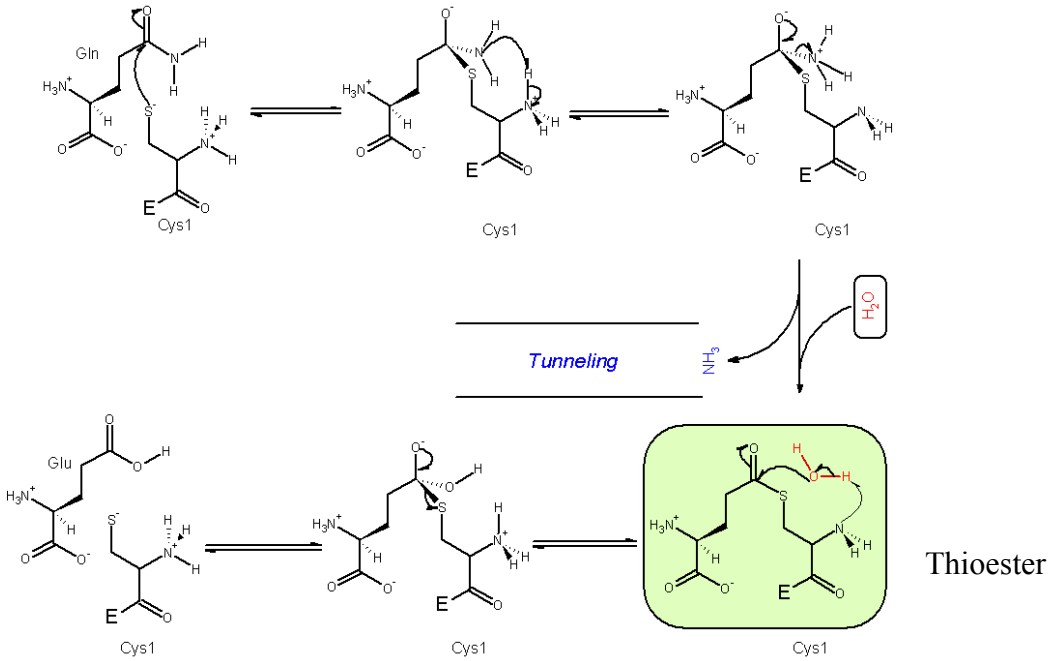

Figure 1-1. Proposed mechanism of hydrolysis of glutamine by *E. coli* asparagine synthetase B**.** The thiolate anion group of Cys1 acts as nucleophile and form an ES thioester.

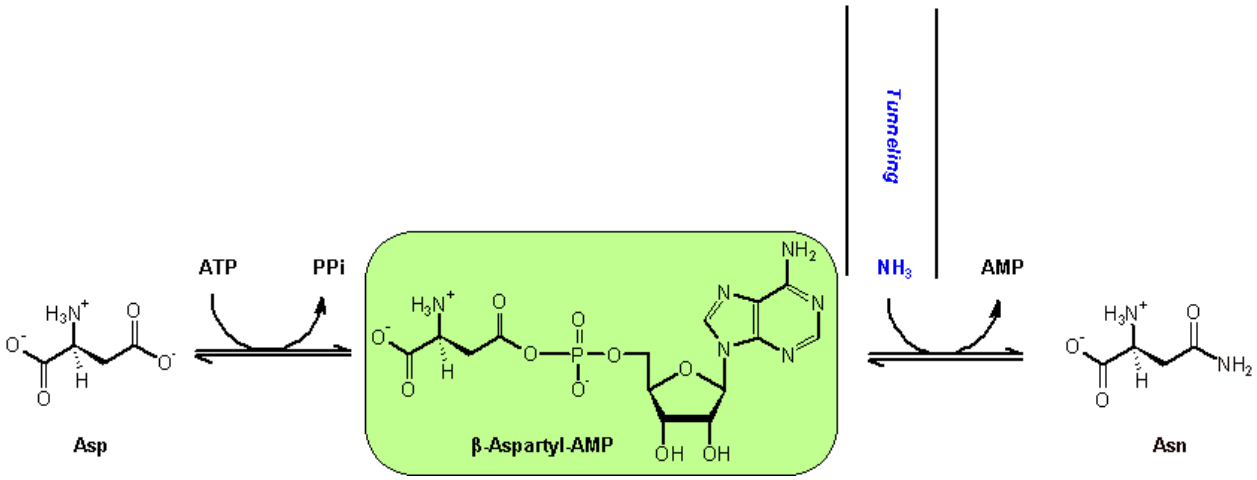

Figure 1-2. Synthesis of asparagines through an intermediate β-aspartyl-adenylate by ASB**.**

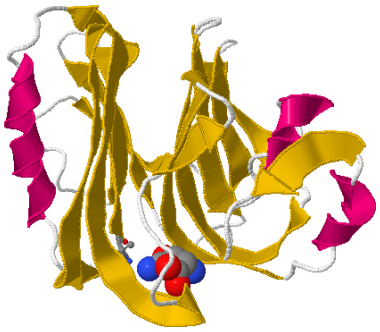

Figure 1-3. Cartoon of glutaminase domain of *E. coli* ASB. Glutamine is showed by spacefill. Ala1(Cys1) is showed by ball and stick.

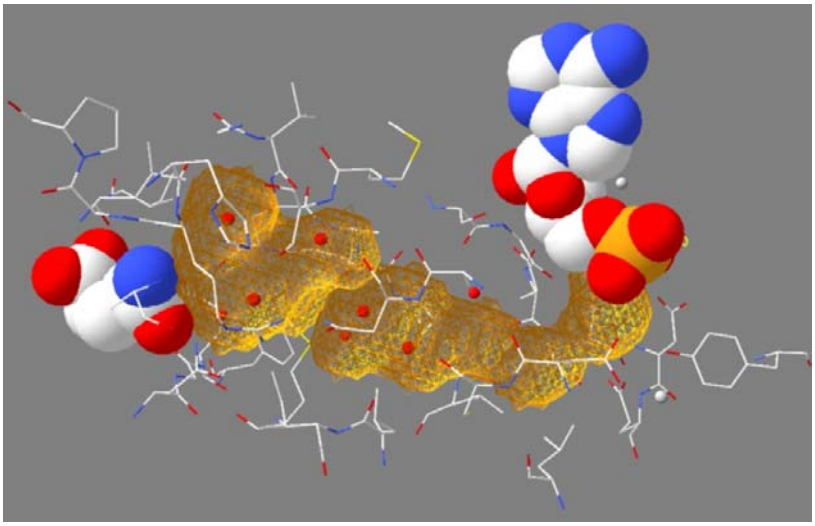

Figure 1-4. The tunnel within ASB**.** Tunnel residues are showed in sticks, colored by cpk. The cavity (tunnel) is brown. Glutamine (left) and AMP (right) are showed in spacefill, colored by cpk. Water (red) and heavy metal ions (grey) are showed in small-size of spacefill.

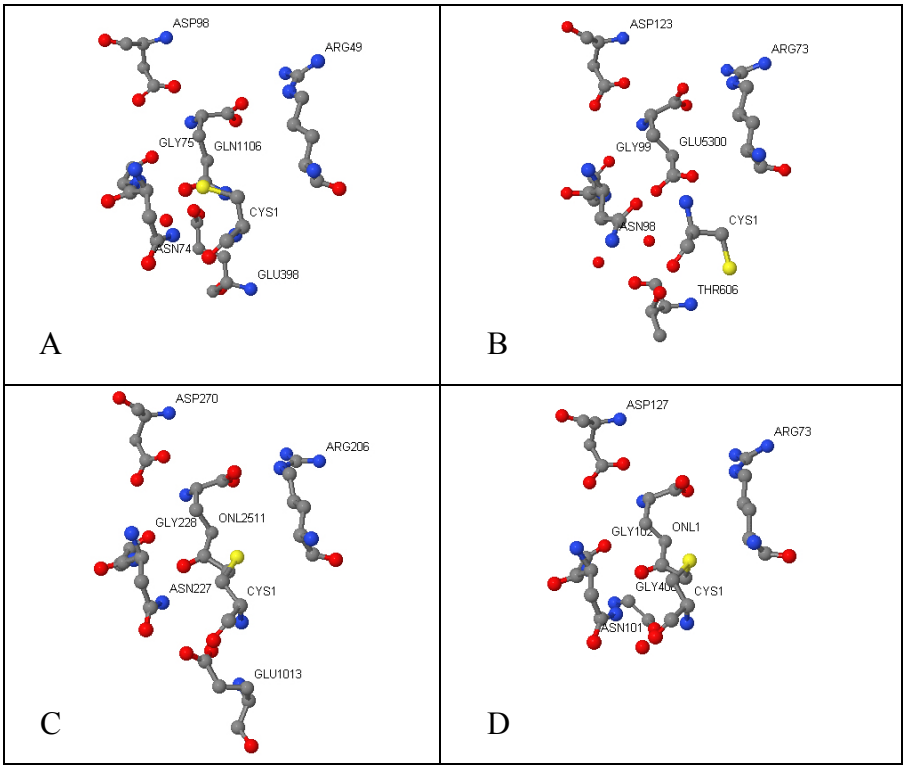

Figure 1-5. Cys1-Arg-Gly-Asn-Asp is a common motif of the glutamine binding site for Ntn subfamily of glutamine dependent amidotransferases A. asparagine synthetase B from *Escherichia coli* (PDB code: 1CT9, modified). B. Glucosamine 4-Phosphate Synthase from *Escherichia coli* (PDB code: 1JXA and 1XFF, modified). C. Glutamate Synthase From *Synechocystis Sp* (PDB code: 1OFE). D. Glutamine Phosphoribosyl-pyrophosphate (Prpp) Amidotransferase from *Escherichia coli* (PDB code: 1ECC).

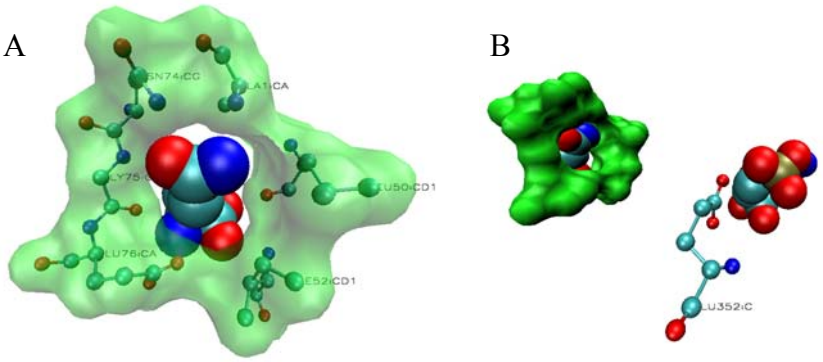

Figure 1-6. The mouth of the tunnel**.** 6 highly conserved residues, Ala 1 (Cys 1), Leu 50, Ile 52, Asn 74, Gly 75, Glu 76, surround the amide group of glutamine and form the mouth of the tunnel. A. Mouth of the tunnel with glutamine. Probe radius is 1.4 Å. B. Relative position to AMP. The mouth of tunnel is showed in green.

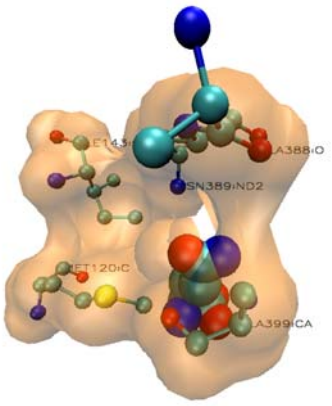

Figure 1-7. The narrowest part of the tunnel formed by M120, I143, N389, A399 and carbonyl group of A388.

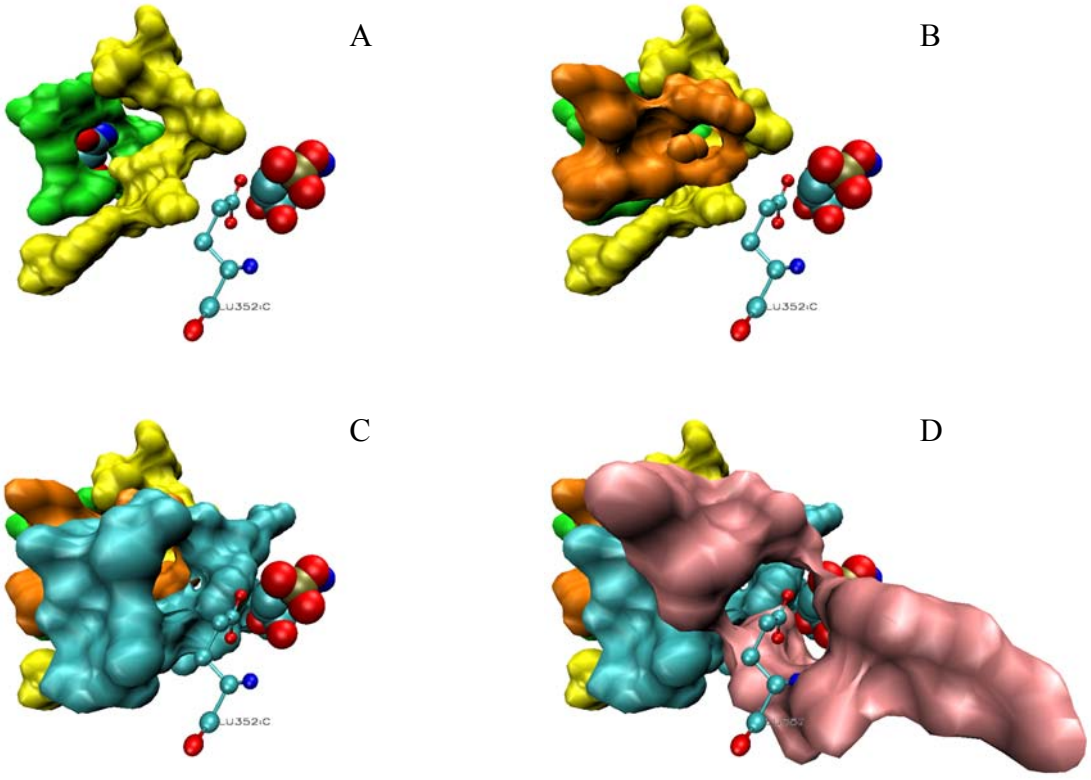

Figure 1-8. The tunnel in *E. coli* ASB. Mouth (green); Upper part (yellow); narrow part (brown); Lower part (cyan); Bottom part (pink). Gln (left) and AMP (right) are showed in spacefill; Glu352 are showed in ball and stick form and colored by cpk.

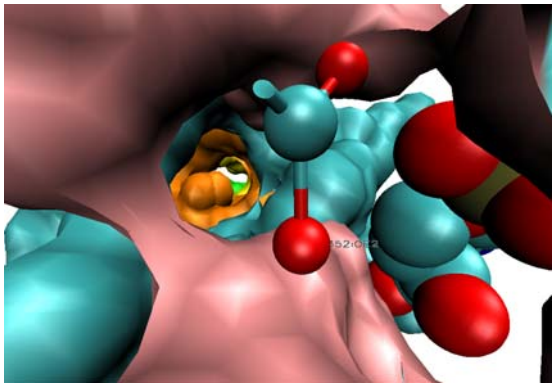

Figure 1-9. The body of the tunnel is mainly formed by hydrophobic residues (yellow) and the bottom almost totally by polar (green) and acidic (red) residues. Several basic residues (blue) close to glutamine site.

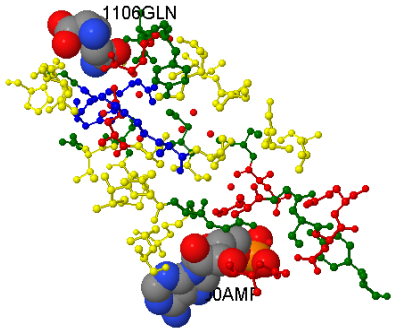

Figure 1-10. The Glu352 is right at the bottom of the tunnel. AMP (spacefill) is on one side. The hole shows the tunnel. Mouth (green); Upper part (yellow); narrow part (brown); Lower part (cyan); Bottom part (pink).

Table 1-1. Residues in Gln binding pocket and possible roles

Resname	Functional group	H-bond/salt bridge	Distance (Å)	Conservation	Roles
Ala1 (Cys1)	**backbone**	**--**	**--**	**conserved**	**Forming tunnel**
	sidechain	**--**	**--**		**Nucleophilic catalysis**
His47	sidechain	--	--	H or F	Active site
Arg49	**sidechain**	**εN-H…O1**	**3.09**	**conserved**	**specificity**
	sidechain	**ηN-H…O1**	**2.97**		
Leu50	backbone	O…H-NE	3.07	conserved	Binding of Gln, catalysis and forming tunnel?
	sidechain	--	--		
Ser51	whole	--	--	Not cons.	Active site
Ile52	backbone	N-H…O2	2.79	I or V	Binding of Gln and forming tunnel?
	sidechain	--	--		
Val53	backbone	N-H…O2	2.77	Not cons.	Gln binding?
	sidechain	--	--		
Gly58	whole	--	--	conserved	Active site?
Gln60	whole	--	--	conserved	Active site?
Leu62	sidechain	--	--	Cons. subst.	Active site
Val73	whole	--	--	Not cons.	Active site
Asn74	**backbone**	**--**	**--**	**conserved**	**Specificity and forming oxyanion hole and tunnel**
	sidechain	**ND-H…OE**	**2.97**		
Gly75	**--**	**O…H-N**	**3.12**	**conserved**	**Specificity and forming oxyanion hole and tunnel**
	--	**N-H…OE**	**2.53**		
Glu76	backbone			conserved	Gln binding and forming tunnel?
	sidechain	OE1…H-N	3.09		
Ser97	whole	--	--	S, C, V	Active site
Asp98	**backbone**	**--**	**--**	**conserved**	**Specificity**
	sidechain	**OD1…H-N**	**2.56**		
Cys99	whole	--	--	Not cons.	Active site
H_2O3	--	O-H…OE	2.80		Reactant?
H_2O30	--	O-H…O1	2.89		

Note: Those residues forming mouth of the tunnel are highlighted by yellow. Fingerprint residues of Ntn subfamily are showed in red

Table 1-2. Size of narrow part of the tunnel

Residues	Atoms	Distance (Å)
Met120 – Asn389	CE -- ND	5.58
Met120 – Asn389	SD -- ND	5.51
Ala399 – Ile143	O – CD1	6.27
Ala399 – Ile143	O – CG1	6.85

Table 1-3. Residues in the interface between two domains of *E. coli* ASB

(Those residues forming tunnel are showed in red)

Residues	Atoms	Distance (Å)	Conservation
Asp115	OD1	2.77	not
Arg193	NH1		not
Asp54	N	2.81	D or G / D or E — D-D or G-E
Asp226	OD1		
Ile52	**O**	2.74	**16I, 5V**
Asp226	N		17D, 4E
Glu76	**OE1**	2.51	**Conserved**
Glu398	**OE1**		**Conserved**
Asp33	OD1	2.76	Conserved
Lys342	NZ		18K except mammalian
Lys342	O	2.76	18K except mammalian
Glu398	**N**		**Conserved**
Gln118	NE	2.92	14D, 4Q, 1R, 1T, 1N
Asp405	OD1		conserved
His139	NE2	2.85	7P, 6A, 5H, 3T
Leu404	**O**		**Conserved**
Glu173	OE1	2.23	not
His381	ND1		15H, 5Y (mammalian), 1N
Lys162	NZ	2.89	Conserved
Glu316	OE1		Conserved
Lys162	N	2.76	Conserved
Glu316	OE1		Conserved
Met161	N	3.07	10L, 9M, 3A (mammalian)
Glu316	OE1		Conserved
Met161	N	2.89	10L, 9M, 3A (mammalian)
Glu316	OE2		Conserved
Lys390	NZ	2.66	18K, 3R (mammalian)
Glu316	OE2		Conserved
Tyr146	OH	2.71	18Y, 3F (mammalian)
Lys390	NZ		18K, 3R (mammalian)
Arg30	**NH1**	2.84	**conserved**
Asn389	**OD1**		**17N, 4D (mammalian)**
Arg30	**NH2**	3.05	**Conserved**
Asn389	**OD1**		**17N, 4D (mammalian)**
His192	--	--	not
Lys406	--	--	13K, 3R, 3H (mamm.), 2T

Scheme 1-1

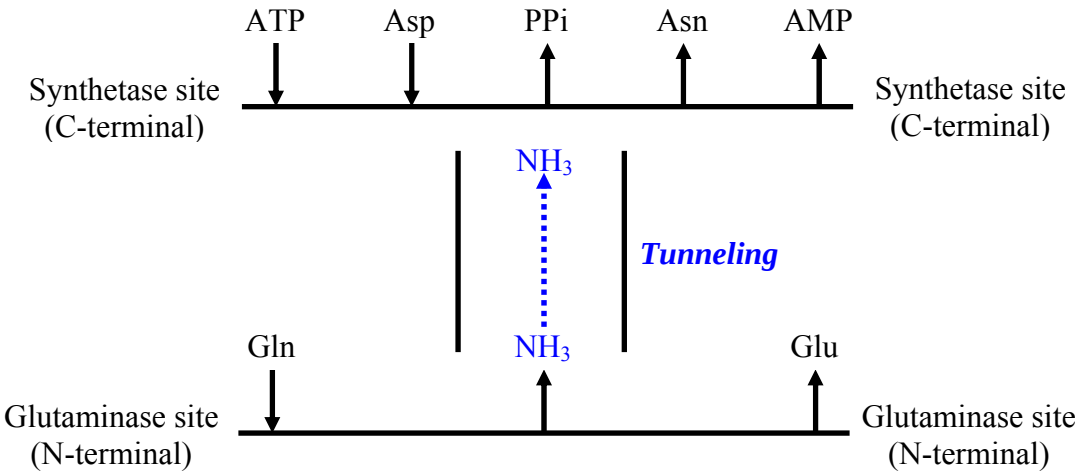
ATP
Asp
PPi
Asn
AMP
Synthetase site
(C-terminal)
Synthetase site
(C-terminal)
NH3
Tunneling
Gln
NH3
Glu
Glutaminase site
(N-terminal)
Glutaminase site
(N-terminal)

CHAPTER 2
A gHMQC-BASED NMR ASSAY FOR INVESTIGATING AMMONIA CHANNELING IN GLUTAMINE DEPENDENT AMIDOTRANSFERASES

Introduction [‡]

Glutamine-dependent amidotransferases catalyze ammonia transfer from the amide of glutamine to a variety of acceptors (*3, 5, 6, 25*). These enzymes first hydrolyze glutamine into glutamate and ammonia. The ammonia intermediate is then transferred to a second active site and reacts with other substrates to synthesize different nitrogen containing product. X-ray crystal structures of many amidotransferases has showed that this family of enzymes has multiple active sites which are separated from each other and connected with an intramolecular tunnel (*2, 15, 26-33*). The reactions catalyzed at both active sites are integrated together by intermediate transfer through this tunnel. It seems that all the glutamine dependent amidotransferases have an ammonia tunnel, with the glutaminase active site at one end and the synthetase active site at the other end. Although it has been proposed that ammonia produced by hydrolysis of glutamine is channeled efficiently into a second active site to complete the overall enzymatic reaction (*6, 34-38*), kinetic studies for relatively few glutamine-dependent amidotransferases have provide evidences to support this hypothesis (*39-42*). Perhaps the most convincing results for efficient ammonia channeling has come from ^{15}N NMR studies of carbamoyl phosphate synthetase (CPS) (*39, 43-45*), which demonstrated that no exchange happens between $^{14}NH_3$ produced in the glutamine domain of CPS and $^{15}NH_3$ present in bulk solution (*39*). In addition, pre-steady state kinetic measurements have shown the rates of ammonia utilization and glutaminase activity in CPS to be coupled, implying that only a single ammonia molecule is present in the intramolecular tunnel of the enzyme during catalytic turnover (*43*). Integrated structural,

[‡] This work was finished with the helpful discussion of an undergraduate William Beeson.

computational and experimental measurements have also provided support for active site coupling and intramolecular ammonia transfer in imidazole glycerol phosphate synthase (IGPS) (*40, 46-49*). Both CPS and IGPS are Class I amidotransferases (*6, 50*), however, and their molecular behavior may not therefore be representative of the evolutionarily unrelated Class II (*6, 51*) or Class III amidotransferases (*52*).

Glutamine-dependent asparagine synthetase (ASNS) (EC 6.3.5.4) belongs to the Class II amidotransferases, which also includes Glucosamine 4-phosphate synthase, Glutamine phosphoribosylpyrophosphate (PRPP) amidotransferase, and glutamate synthase (*5, 6*). The two domains of asparagine synthetase, glutaminase domain and synthetase domain, catalyzes the hydrolysis of glutamine (R3) and the ATP-dependent synthesis of L-asparagine from L-aspartic acid respectively (R2) (*13*), with R1 as the overall enzymatic reaction.

$$\mathbf{Gln + H_2O + ATP + Asp \rightarrow Glu + AMP + PPi + Asn} \qquad \mathbf{(R1)}$$

$$\mathbf{NH_3 + ATP + Asp \rightarrow AMP + PPi + Asn} \qquad \mathbf{(R2)}$$

$$\mathbf{Gln + H_2O \rightarrow Glu + NH_3} \qquad \mathbf{(R3)}$$

Both the mammalian and bacterial forms of the enzyme can accept free ammonia as an alternate substrate *in vitro* (*24, 53*). With ATP and aspartate, glutamine is hydrolyzed into glutamate and ammonia at glutaminase site through a thioester enzyme-substrate complex (*14*) and then the ammonia intermediate is transported through a 20 Å long, intramolecular tunnel to the synthetase site, which is accepted by β-Aspartyl-AMP, an intermediate that formed at synthetase site using ATP and Asp, to produce asparagine. In sharp contrast to the behavior of other Class II amidotransferases for which the independent catalytic sites are tightly coupled (*54-56*), without the ammonia acceptor, asparagine synthetase still can hydrolyze glutamine (*22, 57*). This lack of active site coupling in ASNS is surprising in light of observations on other amidotransferases, and raises questions about the structural integrity of the solvent inaccessible, intramolecular

tunnel that is seen in the AS-B crystal structure as the enzyme proceeds through its catalytic cycle.

We now report the use of a very convenient isotope-edited ^{1}H NMR-based assay (*58*) that we have developed to probe ammonia transfer between the two active sites in glutamine dependent asparagine synthetase from *Escherichia coli* (AS-B). This gradient heteronuclear multiple quantum coherence (gHMQC) method, which should be generally applicable for studies of other glutamine-dependent amidotransferases, has provided quantitative information on the extent to which ^{15}N is incorporated into the side chain of asparagine formed in the enzyme-catalyzed reaction. In addition, although our studies of AS-B have employed end-point measurements, the gHMQC strategy may be amenable for use in continuous assays of nitrogen transfer catalyzed by other members of this enzyme family. At least in the case of AS-B, the results of these gHMQC NMR studies show that (i) high glutamine concentrations do not suppress ammonia-dependent asparagine formation by this enzyme, and (ii) ammonia in bulk solution can undergo reaction with a thioester intermediate formed during the glutaminase half-reaction (*14, 59*). These observations are consistent with a model in which exogenous ammonia can access the tunnel in AS-B during glutamine-dependent asparagine synthesis, in contrast to expectations based on studies of Class I amidotransferases (*39, 46, 47*).

Material and Methods

Materials

Unless otherwise stated, all chemicals and reagents were purchased from Sigma (St. Louis, MO), and were of the highest available purity. 1,3-$^{15}N_2$-Uracil, ^{15}N-L-asparagine, and d_6-DMSO were purchased from Sigma-Aldrich (St. Louis, MO). The isotopic incorporation in these samples was greater than 99%. All experiments employed freshly prepared solutions of recrystallized L-glutamine (*17*). Recombinant, wild type AS-B was expressed and purified

following literature procedures (*16*). Protein concentrations were determined using a modified Bradford assay (Pierce, Rockford, IL) (*60*), for which standard curves were constructed with bovine serum albumin, and corrected as previously reported (*55*). NMR spectra were recorded on a Varian INOVA 500 instrument equipped with a 5 mm triple resonance indirect detection probe (z-axis gradients) operating at 500 and 50 MHz for ^{1}H and ^{15}N, respectively. Chemical shifts are reported in ppm relative to sodium 2,2-dimethyl-2-silapentane-5-sulfonate (DSS). The co-axial inner cell (catalog: NE-5-CIC-V) containing the external NMR standards was purchased from New Era Enterprises (Vineland, NJ).

NMR Measurements

Concentrations of ^{15}N-L-asparagine were determined using a solution of 1,3-$^{15}N_2$-uracil dissolved in d_6-DMSO as a standard, which was placed in a coaxial inner cell inserted into the 5 mm tube containing the assay sample. The amount of ^{15}N-L-asparagine was measured using a phase-sensitive, 1-D gHMQC pulse sequence (*58*), as implemented in the Varian VNMR software package (version 6.1C). NMR spectra were acquired on a Varian INOVA500 spectrometer, at a fixed temperature of 25 ^{o}C, in 256 transients with a digital resolution of 0.25 Hz/point (25966 points in the FID over a spectral window of 6492 Hz) using a relaxation delay of 1 s and an acquisition time of 2 s. The total time for acquiring each spectrum was therefore 13 min. The encoding gradient level was 37 Gauss/cm of 2.5 ms duration, and the corresponding values for the decoding gradient were 18.7 Gauss/cm and 1 ms, with a gradient recovery time was 0.5 ms. 90º pulse times used in the experiment for ^{1}H and ^{15}N were 9.6 μsec and 25.8 μs, respectively, and the ^{1}H-^{15}N coupling constant was set to a value of 87 Hz. The FID was weighted with a line broadening of 10 Hz and a Gaussian of 0.278 Hz.

Competition Experiment

Reaction mixtures consisted of 100 mM HEPPS buffer (pH 8.0), 60 mM $MgCl_2$, 10 mM

ATP, 20 mM aspartate and different concentrations of $^{15}NH_4Cl$ (pH 8.0) or glutamine in total volume of 2 mL. In experiments where the concentration of $^{15}NH_4Cl$ (pH 8.0) was varied as 2.0 mM, 5.0 mM, 25 mM, 50 mM and 100 mM, L-glutamine was fixed at 20 mM. Alternatively, when L-glutamine was varied as 0 mM, 2.5 mM, 10 mM, 20 mM and 40 mM, $^{15}NH_4Cl$ was added at an initial concentration of 100 mM. Reactions were initiated by the addition of AS-B (31 μg) and the resulting samples incubated for 10 min at 37 ^{o}C before being quenched by the addition of trichloroacetic acid (TCA) (60 μL). After centrifugation for 5 min at 3000 rpm to remove precipitated protein, the supernatant was adjusted to pH 5 by the addition of 10 M aq. NaOH and an aliquot of this solution (650 μL) transferred to a 5 mm NMR tube for analysis. At higher pH values, amide NH exchange precluded the derivation of any quantitative relationship between peak area and ^{15}N-Asn concentration. The standard samples contained 100 mM HEPPS buffer (pH 8.0), 60 mM $MgCl_2$, 10 mM ATP, 100 mM $^{15}NH_4Cl$ (pH 8.0), 20 mM glutamine and different concentrations of ^{15}N-L-Asn from 0.25 mM to 5 mM, without adding AS-B.

^{15}N Exchanging Experiment

Reaction mixtures consisted of 100 mM HEPPS buffer (pH 8.0), 60 mM $MgCl_2$, 10 mM ATP and different concentrations of $^{15}NH_4Cl$ (pH 8.0) or glutamine in total volume of 2 mL. In experiments where the concentration of $^{15}NH_4Cl$ (pH 8.0) was varied as 2.0 mM, 5.0 mM, 25 mM, 50 mM and 100 mM, L-glutamine was fixed at 20 mM. Alternatively, when L-glutamine was varied as 0 mM, 2.0 mM, 5.0 mM, 10 mM, 20 mM, 40 mM and 80 mM, $^{15}NH_4Cl$ was added at an initial concentration of 100 mM. Reactions were initiated by the addition of AS-B (62 μg) and the resulting samples incubated for 10 min at 37 ^{o}C before being quenched by the addition of trichloroacetic acid (TCA) (60 μL). After centrifugation for 5 min at 3000 rpm to remove precipitated protein, the supernatant was adjusted to pH 5 by the addition of 10 M aq. NaOH and an aliquot of this solution (650 μL) transferred to a 5 mm NMR tube for analysis. At higher pH

values, amide NH exchange precluded the derivation of any quantitative relationship between peak area and ^{15}N-Asn concentration. The standard samples contained 100 mM HEPPS buffer (pH 8.0), 60 mM $MgCl_2$, 10 mM ATP, 100 mM $^{15}NH_4Cl$ (pH 8.0), 20 mM glutamine and different concentrations of ^{15}N-L-Asn from 0.10 mM to 5 mM, without adding AS-B.

HPLC-Based Determination of Total L-Asparagine

In order to obtain an estimate of total L-asparagine in the final reaction mixtures, we employed an HPLC-based end-point assay (*15*). Hence, an aliquot of each mixture (40 μL) was diluted (200 μL final volume) with 400 mM aq. Na_2CO_3, pH 9, containing 10% DMSO and 30% dinitrofluorobenzene (DNFB) (as a saturated solution in EtOH). The resulting solutions were heated at 50 °C for 45 min to permit reaction of DNFB with the amino acids to yield their dinitrophenyl (DNP) derivatives. **Caution**: Extreme care should be taken when handling solutions of 2,4-dinitrofluorobenzene in organic solvents because this reagent is a potent allergen and will penetrate many types of laboratory gloves (*46*). Aliquots of each assay mixture (20 μL) were analyzed by reverse-phase HPLC (RP-HPLC) using a C_{18} column and a flow-rate of 0.7 mL/min. The DNP-derivatized amino acids were eluted using a step gradient of 40 mM formic acid buffer, pH 3.6, and CH_3CN. In this procedure, the initial concentration of the organic phase (CH_3CN) was 14%, which was maintained over a period of 26 min before the amount of CH_3CN was increased to 80% over a period of 30 s, and elution continued for a further 8 min. Eluted amino acid DNFB derivatives were monitored at 365 nm and identified by comparison to authentic standards. Under these conditions, DNP-asparagine exhibited a retention time of approximately 25 min, and could be quantified on the basis of its peak area. Calibration curves were constructed using solutions of pure L-asparagine derivatized in the same manner as the samples.

Kinetic Simulations

Simulations were performed using the GEPASI software package (*61, 62*).

Results and Discussion

Two mechanisms can be envisaged for nitrogen transfer from the glutaminase to the synthetase active sites in AS-B (Figure 2-1). In the first, ammonia is directly transferred between the two active sites through an intramolecular tunnel (*2, 15, 26-33*). This proposal, which is hypothesized to occur in all other glutamine-dependent amidotransferases (*6, 34-38*), is supported by X-ray crystallographic observations on the bacterial enzyme (*15*). A second model can be envisaged, however, in which ammonia is released into bulk solution prior to re-entering the synthetase site and reacting with the β-aspartyl-AMP intermediate. We therefore sought a simple and rapid kinetic assay to distinguish between these possibilities, which might also be applicable in experiments aimed at developing structure-function relationships for residues defining the tunnel observed in AS-B. Early work on CTP synthetase (*41, 63, 64*) and GMP synthetase (*65*) aimed at investigating this problem employed the pH-dependence of synthetase activity when glutamine and ammonia (or alternate substrates such as hydroxylamine) were both present in solution. We elected to employ an alternate, and somewhat more straightforward, strategy, however, in which the glutamine-dependent asparagine synthetase reaction was performed in the presence of exogenous $^{15}NH_4Cl$. In particular, we hoped to employ ^{15}N NMR spectroscopy to determine the extent of ^{15}N incorporation into asparagine as a function of glutamine concentration, as previously reported in studies on CPS (*19*). The low sensitivity of the ^{15}N nucleus proved to be a significant limitation to our efforts, mandating a substantial investment of spectrometer time in order to obtain spectra with sufficiently high signal-to-noise for any quantitative measurements, thereby severely limiting the number of conditions under which competition studies could be carried out. We therefore investigated the use of a phase-

sensitive 1D gHMQC experiment to measure the extent to which ^{15}N was incorporated into asparagine when AS-B was incubated with aspartate and ATP in the presence of both glutamine (containing nitrogen isotopes at natural abundance) and $^{15}NH_4Cl$.

NMR Assay

In gHMQC spectra, resonances are only observed for hydrogen nuclei that are (i) attached to ^{15}N nuclei, and (ii) are not in fast exchange. The chemical shifts for ^{15}N-amide protons are: ^{15}N-Asn (δ_{NHcis} = 7.58 (dd) and $\delta_{NHtrans}$ = 6.86 (dd), J = 90 Hz); ^{15}N-Gln (δ_{NH1} = 7.53 (dd) and δ_{NH2} = 6.81 (dd), J = 90 Hz). Hence, this NMR strategy permits a 30-fold increase in sensitivity over direct acquisition of ^{15}N spectra. In addition, and very importantly for the goals of these experiments, the time needed to acquire ^{15}N-edited ^{1}H NMR spectra was approximately three orders of magnitude faster than for the equivalent measurements using ^{15}N NMR spectroscopy. We were therefore able to obtain very "clean" ^{1}H NMR spectra for assay mixtures containing AS-B because the signals for protons on free $^{15}NH_3$ and $^{15}NH_4^+$ were not observed (Figure 2-2). Accurate integration of signals relative to those from an internal standard ($^{15}N_2$-uracil dissolved in d_4-DMSO) was also possible, and standard curves relating the observed peak area of amide proton signals to the concentration of ^{15}N-asparagine present in solution under a variety of conditions were easily obtained (Figure 2-3). All of these results were carefully validated by independent measurements of asparagine using an HPLC-based assay (*23*).

Competition Experiments

Having established that the amount of ^{15}N-asparagine formed in the reaction could be quantitated using gHMQC spectroscopy, we studied whether the incorporation of ^{15}N from exogenous $^{15}NH_4Cl$ into asparagine could be suppressed by L-glutamine in the synthetase reaction catalyzed by AS-B. If ASB was incubated with both ^{14}N-glutamine and $^{15}NH_4Cl$ at the presence of other substrates and cofactor, both ^{14}N-asparagine and ^{15}N-asparagine would be

produced. ^{14}N-asparagine was produced by $^{14}NH_3$ intermediate that goes through an intramolecular tunnel. And ^{15}N-asparagine was formed by $^{15}NH_3$ from free solution. $^{15}NH_3$ may compete with $^{14}NH_3$ from ^{14}N-glutamine as nitrogen donor. Therefore, quantitative analysis of both ^{15}N-asparagine and ^{14}N-asparagine in the reaction mixture gives information about the capability of ASB to utilize different nitrogen source (scheme 2-1). If ammonia can not access the active site with the presence of glutamine, all the asparagine would be ^{14}N product at saturating concentration of glutamine. In this case, free ammonia is suppressed by glutamine. The ratio of ^{14}N asparagine to ^{15}N asparagine would be infinite. This ratio will be decreasing with the extent of suppression becomes less. When there is no suppression at all, the $^{14}NH_3$ will compete with $^{14}NH_3$ freely. If ammonia tunneling is fast and efficient enough, then the ratio of ^{14}N asparagine to ^{15}N asparagine would be determined by the ratio of production rates using ammonia and glutamine. That is,

$$\frac{[^{14}N-Asn]}{[^{15}N-Asn]}=\frac{v_{14}}{v_{15}}=\frac{(k_{cat}/K_{m-tunneling})[\mathrm{Gln}][E]}{(k_{cat}/K_{m-binding})[^{15}NH_3][E]}\propto\frac{[\mathrm{Gln}]}{[^{15}NH_3]}\approx\frac{[\mathrm{Gln}]}{[^{15}NH_3]_i}$$

Therefore,

$$\frac{[^{14}N-Asn]}{[^{15}N-Asn]}\propto\frac{[G\ln]}{[^{15}NH_3]_i}\ \text{or}\ \frac{[^{14}N-Asn]}{[^{15}N-Asn]}=A\times\frac{[G\ln]}{[^{15}NH_3]_i}$$

Alternatively, if the tunnel is not efficient, the ratio of ^{14}N asparagine to ^{15}N asparagine would decreases. Most of the asparagine would be labeled form and the ratio of $^{14}N/^{15}N$ in asparagine would be close to zero if the $^{14}NH_3$ intermediate leaks and equilibrates with $^{15}NH_3$ from bulk solution, since $[^{15}NH_3]$ was much bigger than $[^{14}NH_3]$. Hence, we studied the competition in the presence of both $^{14}NH_3$ and ^{14}N-glutamine as nitrogen donors. Under experimental conditions,

the final concentration of asparagine formed was 1-2 mM. The dependence of ^{15}N incorporation into the product amide on the initial concentration of L-glutamine was determined using the NMR assay we developed and HPLC assay (Table 1), after correcting the amount of ^{15}N in L-asparagine to allow for the natural abundance of ^{15}N in L-glutamine. A similar set of experiments in which L-glutamine was fixed at 20 mM and $^{15}NH_4Cl$ varied over a range of initial concentrations was also carried out (Table 2-1).

Somewhat unexpectedly, in light of the behavior reported for CPS in a similar competition experiment (*19*), we did not observe complete suppression of ^{15}N incorporation at saturating concentrations of L-glutamine ($K_{M(app)}$: 0.69 mM (*53*)). Instead, the $^{14}N/^{15}N$ incorporation ratio exhibited saturation behavior, reaching a limiting value of 1.2 ± 0.2 as the concentration of L-glutamine was increased (Figure 2-4A). The ammonia-dependence of the $^{14}N/^{15}N$ incorporation ratio when the initial concentration of L-glutamine was fixed at 20 mM was also examined and again showed substantial ^{15}N incorporation even at non-saturating concentrations of $^{15}NH_3$ (Figure 2-4B). Any calculation of the expected $^{14}N/^{15}N$ ratio in the side chain of the product by the simple comparison of the V/K values for the two nitrogen sources is complicated, however, by the fact that L-asparagine inhibits the glutaminase activity of ASNS with an apparent K_I of 50-60 μM (*34*, *41*) while having no significant impact on ammonia-dependent synthetase activity at 1 mM concentration (*41*; also see supporting information). Thus, the rate of ammonia-dependent L-asparagine synthesis is unaffected by the presence of L-asparagine over the period of our competition experiment, while that for glutamine-dependent synthetase activity decreases over time (Figure 2-4C). The effects of this differential inhibition are reflected in the total amount of L-asparagine formed after a given time under the assay conditions, which depends on whether one or both nitrogen sources are present. As a result, the total amount of L-asparagine

formed in 10 minutes is greater when both exogenous ammonia and glutamine are present in solution than when glutamine is employed as the sole nitrogen source (Table 2-1). This also explains the observation that total L-asparagine is increased when ammonia is added to a solution containing a saturating amount (20 mM) of L-glutamine because ammonia-dependent activity is not inhibited by the reaction product binding to the glutaminase active site. Given this complication in understanding the apparent inability of L-glutamine to prevent ^{15}N incorporation into asparagine, we sought to model the theoretical $^{14}N/^{15}N$ incorporation ratio as a function of either L-glutamine or ammonia concentration by kinetic simulations of the competition experiment. In keeping with hypotheses developed from previous studies on CPS (*19*) and IGPS (*20*), we assumed that exogenous $^{15}NH_3$ and L-glutamine could not bind simultaneously to the E.ATP.Asp ternary complex required for synthetase activity (*40*, *41*). The assignment of rate constants was accomplished (*40*) on the basis of (i) direct NMR and HPLC measurements of L-asparagine production rate under the assay conditions (k_2, k_4, k_7 and k_{10}), and (ii) literature data on the steady state kinetics of AS-B (k_{-1}, k_{-3}, k_{-6} and k_{-9}) (*40*, *53*). All second order ‘‘on’’ rate constants were defined as 10^8 $M^{-1}s^{-1}$, although this does not account for conformational changes that might take place on substrate binding. Perhaps more importantly, we assumed that (i) the presence of L-asparagine in the glutaminase active site of the enzyme does not affect rate constants associated with ammonia-dependent synthetase activity (k_4, k_7 and k_{10}), and (ii) the “off” rate of asparagine from the inhibitory site is not affected by bound ammonia (k_{-11} and k_{-12}). The only remaining unknown rate constants (k_{-11} and k_{-12}) in this simple model could then be estimated from the observed K_I for L-asparagine in the glutamine-dependent synthetase reaction. Although this kinetic model exhibits a time-dependent decrease in the rate of nitrogen incorporation from L-glutamine to give ^{14}N-L-asparagine in the competition assay (Figure 2-4C),

it does not qualitatively reproduce the saturation behavior of the $^{14}N/^{15}N$ incorporation ratio as the concentration of L-glutamine is increased in the presence of a fixed amount of $^{15}NH_4Cl$ (Figure 2-4A). The lack of quantitative agreement between the experimental and simulated $^{14}N/^{15}N$ incorporation ratios likely arises from an over-estimation of the affinity of the AS-B glutaminase domain for L-asparagine, and we therefore conclude that both nitrogen sources can be present on the enzyme simultaneously.

^{15}N exchange Experiments

Evidence to support (i) the conclusion from the kinetic simulations, and (ii) the hypothesis that $^{15}NH_3$ might be able to access the N-terminal glutaminase site (and presumably the intramolecular tunnel) when L-glutamine was also present came from the observation of peaks in the isotope-edited gHMQC spectrum with chemical shift values that were different from those of the resonances arising from the amide protons of ^{15}N-asparagine (Figure 2-2B). The acquisition of ^{1}H spectra for the reaction mixture in the *absence* of isotopic editing, but with suppression of the water signal, showed that these unexpected peaks were satellites of the broad signal from the amide protons in ^{14}N-L-glutamine (Figure 2-5). As a result, we concluded that these signals arose from amide protons bonded to ^{15}N in the side chain of L-glutamine. Control experiments established that $^{14}N/^{15}N$ exchange did not occur in the absence of AS-B, and so this reaction was examined in more detail by incubating the enzyme with $^{15}NH_4Cl$ in the presence of glutamine and ATP. Under these conditions, the rate of ^{15}N-substituted glutamine formation (i) showed saturation behavior with respect to glutamine at a fixed concentration (100 mM) of $^{15}NH_4Cl$ (Figure 2-6), and (ii) was linearly dependent on the concentration of exogenous $^{15}NH_4Cl$ (data not shown).

A kinetic model was constructed to describe the $^{14}N/^{15}N$ exchange (Figure 2-7A), which gave the following equation for partitioning of the thioester intermediate at the steady-state to

yield ^{15}N-L-glutamine (see supporting information):

$$v = \frac{k_1 k_2 [E]_T [Gln][^{15}NH_4^+]}{(k_1[Gln] + k_2[^{15}NH_4^+] + k_3[H_2O])} \qquad \text{(Eqn. 1)}$$

Here *v* is the rate of ^{15}N-glutamine production via the exchange reaction in the presence of ATP but the *absence* of aspartate, and k_1, k_2 and k_3 are microscopic rate constants with estimated values of 5.1 $mM^{-1}s^{-1}$, 7.8 x 10^{-3} $mM^{-1}s^{-1}$ and 1.06 x 10^{-4} $mM^{-1}s^{-1}$, respectively, assuming that hydrolysis of the thioester intermediate is the rate-limiting step in the glutaminase reaction. Using these values in our model for the exchange reaction gave excellent agreement between the observed concentrations of ^{15}N-glutamine and those expected from kinetic simulation at a variety of NH_4Cl concentrations (Figure 2-7B). Having established a firm understanding of this reaction in the absence of aspartate, we next examined whether the overall rate of ^{14}N/^{15}N exchange was altered when AS-B was undergoing catalytic turnover to yield asparagine. A similar analysis to that described above showed that our kinetic model gave excellent agreement with experimental values (data not shown) when the microscopic rate constants k_1, k_2 and k_3 were assigned values of 9.6 $mM^{-1}s^{-1}$, 1.8 x 10^{-2} $mM^{-1}s^{-1}$ and 8.8 x 10^{-5} $mM^{-1}s^{-1}$, respectively. The similarity of these rate constants to those determined for ^{14}N/^{15}N exchange in the absence of aspartate suggests that the molecular mechanism of the reaction is identical under both sets of conditions.

The simplest explanation for ^{14}N/^{15}N exchange is that ^{15}N-substituted glutamine is formed by reaction of exogenous $^{15}NH_3$ with a thioester intermediate formed in the N-terminal active site during the enzyme-catalyzed hydrolysis of glutamine (Scheme 2-2) (*14, 59*). This is an intriguing finding because a similar ^{14}N/^{15}N exchange reaction involving the side chain amide of L-glutamine was not observed in similar competition experiments employing CPS (*19*), although it is possible that the amounts of ^{15}N-substituted glutamine formed might have been too small for detection by ^{15}N NMR spectroscopy. In addition, this phenomenon has not been described

previously, to the best of our knowledge, for any other glutamine-dependent amidotransferase. The molecular pathway by which $^{15}NH_3$ gains access to the N-terminal, glutaminase site remains to be determined. Hence, it is possible that exogenous ammonia can access the N-terminal domain directly as a consequence of the enzyme adopting a conformation in which the tunnel linking the two active sites is solvent accessible. Alternatively, ammonia might enter the intramolecular tunnel linking the two active sites after entering the C-terminal domain. In both mechanisms, ammonia could displace water molecules in the tunnel prior to glutamine binding and the adoption of the "closed" conformation observed in the crystal structure of the enzyme.

Conclusions

In summary, we have reported a sensitive, quantitative and reproducible isotope-edited ^{1}H NMR assay for monitoring the incorporation of ^{15}N into the side chain amide of L-asparagine. Spectra can be obtained rapidly thereby permitting the examination of a wide variety of conditions for these steady-state competition experiments. The application of this assay to the reaction catalyzed by AS-B has shown, somewhat unexpectedly, that high concentrations of glutamine can not suppress the incorporation of ^{15}N from exogenous $^{15}NH_3$. This result, in combination with our observation that exogenous ammonia can trap the thioester intermediate in the glutaminase reaction, is consistent with a model in which the putative ammonia channel linking the N- and C-terminal active sites can be accessed by $^{15}NH_3$ molecules at some point during catalytic turnover. This behavior seems to contrast with previous findings concerning ammonia channeling in Class I amidotransferases, such as CPS (*19*) and IGPS (*20*), which appear to have been optimized during evolution for (i) high nitrogen transfer efficiency (*19*), and (ii) tight kinetic coupling of glutaminase and synthetase activities (*20*, *23*). In part, this may be a consequence of the ability of asparagine to inhibit non-productive glutaminase activity, which might have relaxed any evolutionary pressure to construct intra-domain interactions needed for

efficient kinetic coupling of catalysis in the two active sites of asparagine synthetase.

Any interpretation of the inability of saturating glutamine to suppress ammonia-dependent synthetase activity in terms of molecular structure is complicated by the observed solvent inaccessibility of the intramolecular tunnel that is observed in the high-resolution crystal structure of AS-B (*12*). We have shown previously, however, that coupling of the glutaminase and synthetase activities of the enzyme appears to break down as the glutamine concentration is increased (*40*), perhaps because of a conformational change that permits the release of ammonia ($^{14}NH_3$) from one or both of the glutaminase sites. It is therefore possible that molecules of exogenous ammonia ($^{15}NH_3$) might be able to gain access to the synthetase site when the enzyme adopts this conformation, with the result that high concentrations of L-glutamine fail to suppress ^{15}N incorporation to the extent seen for other amidotransferases.

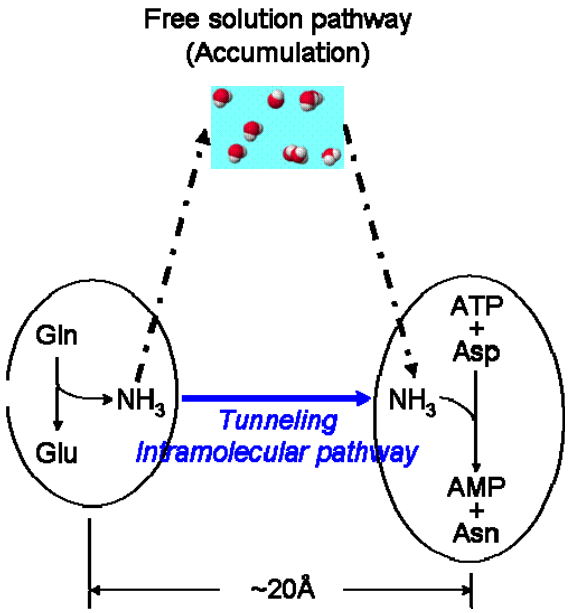

Figure 2-1. Two possible pathways for the ammonia transfer to reach synthetase site. One is intramolecular pathway, in which ammonia intermediate go through an intramolecular tunnel after being released from glutaminase site, without exposes to solution. The second pathway is free solution pathway. The ammonia is released to the free solution first, and then binds to synthetase site. In the latter pathway, the concentration of ammonia in the solution is very low at beginning, increases with time, and finally reaches maximum. This would produce a lag in the plot of synthetase activity versus time, which can be ruled out by kinetic studies after separate active sites are confirmed.

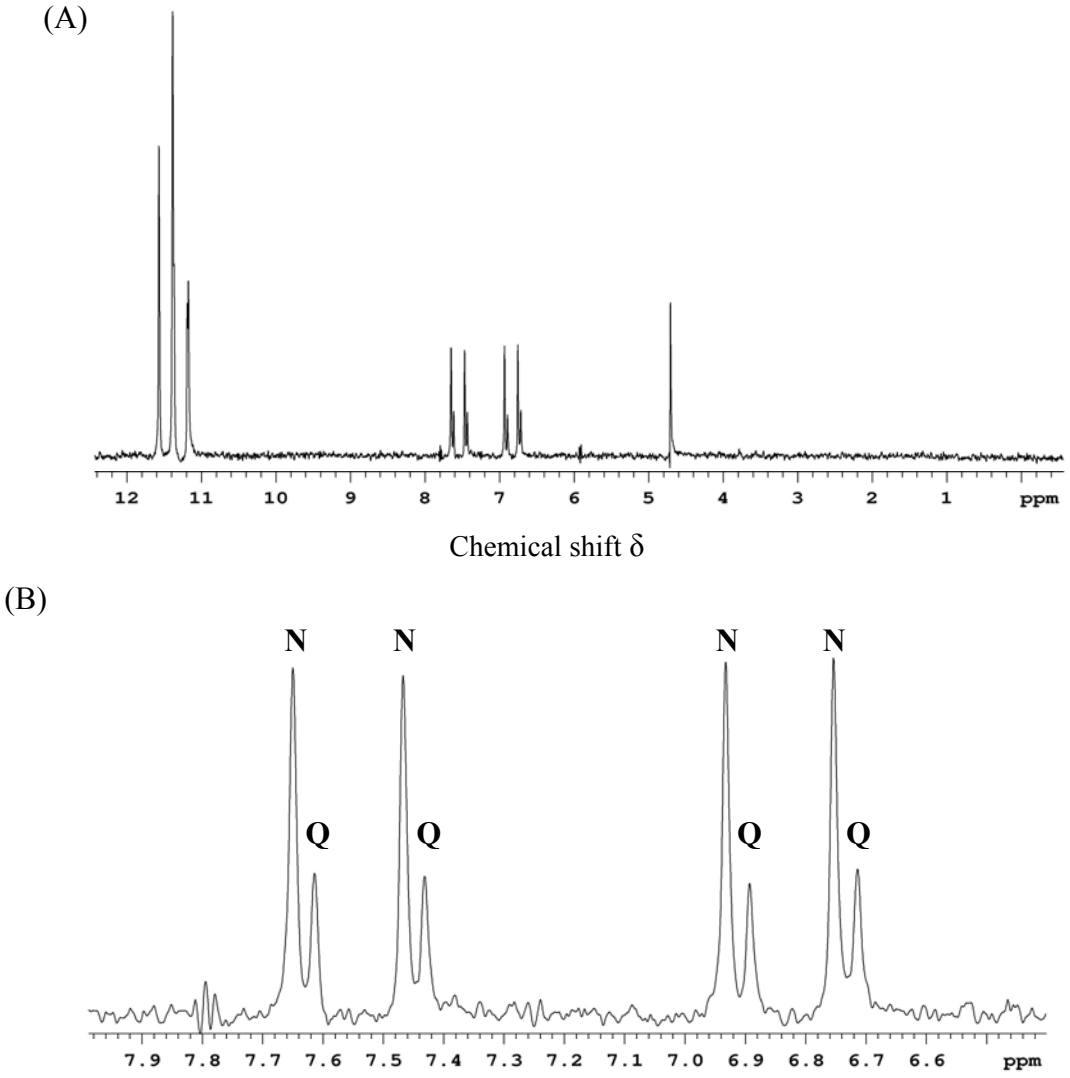

Figure 2-2. gHMQC ^{1}H-NMR spectrum. (A) "Clean" ^{1}H-NMR spectrum obtained by gHMQC. Only ^{15}N-amide protons were showed in the spectrum. For the samples used in this work, these peaks (from left to right) stands for $^{15}N_2$-uracil ($\delta > 11.00$ ppm), ^{15}N-amides (glutamine or asparagine, δ: 6.50 – 7.80 ppm) and solvent (H_2O, $\delta = 4.70$ ppm) respectively. The peak areas of ^{15}N-glutamine or ^{15}N-asparagine are relative to the total peak area of $^{15}N_2$-uracil in d_4-DMSO, which was set to 100. (B) The ^{15}N-amide peaks. ^{15}N-Asn ($\delta_{NHcis} = 7.58$ ppm (dd) and $\delta_{NHtrans} = 6.86$ ppm (dd), J = 90 Hz); ^{15}N-Gln ($\delta_{NH1} = 7.53$ ppm (dd) and $\delta_{NH2} = 6.81$ ppm (dd), J = 90 Hz)

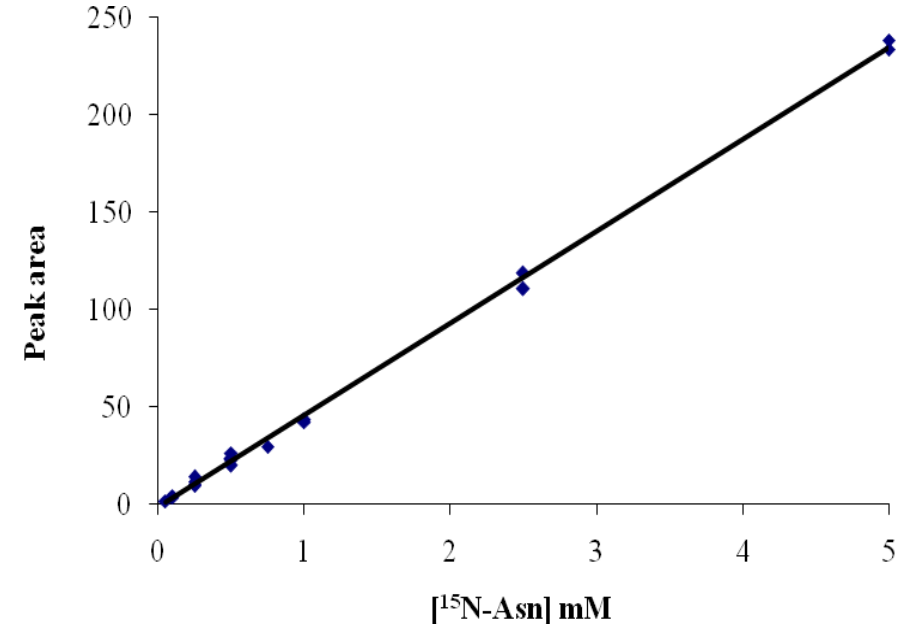

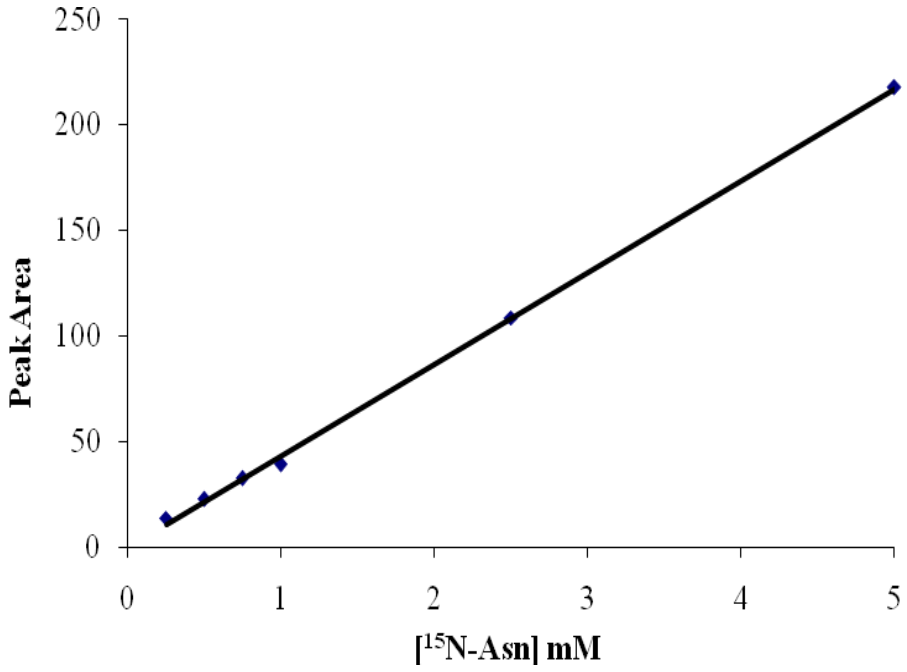

Figure 2-3. Standard curves. (A) Standard curve for exchange experiment. The concentrations of ^{15}N-Asn added were 0.05 - 5.0 mM. R^2 = 0.9986. Detection limit < 50 μM. (B) Standard curve for competition experiment. The concentrations of ^{15}N-Asn was varied from 0.25 - 5.0 mM. R^2 = 0.9991. Detection limit < 50 μM.

Scheme 2-1

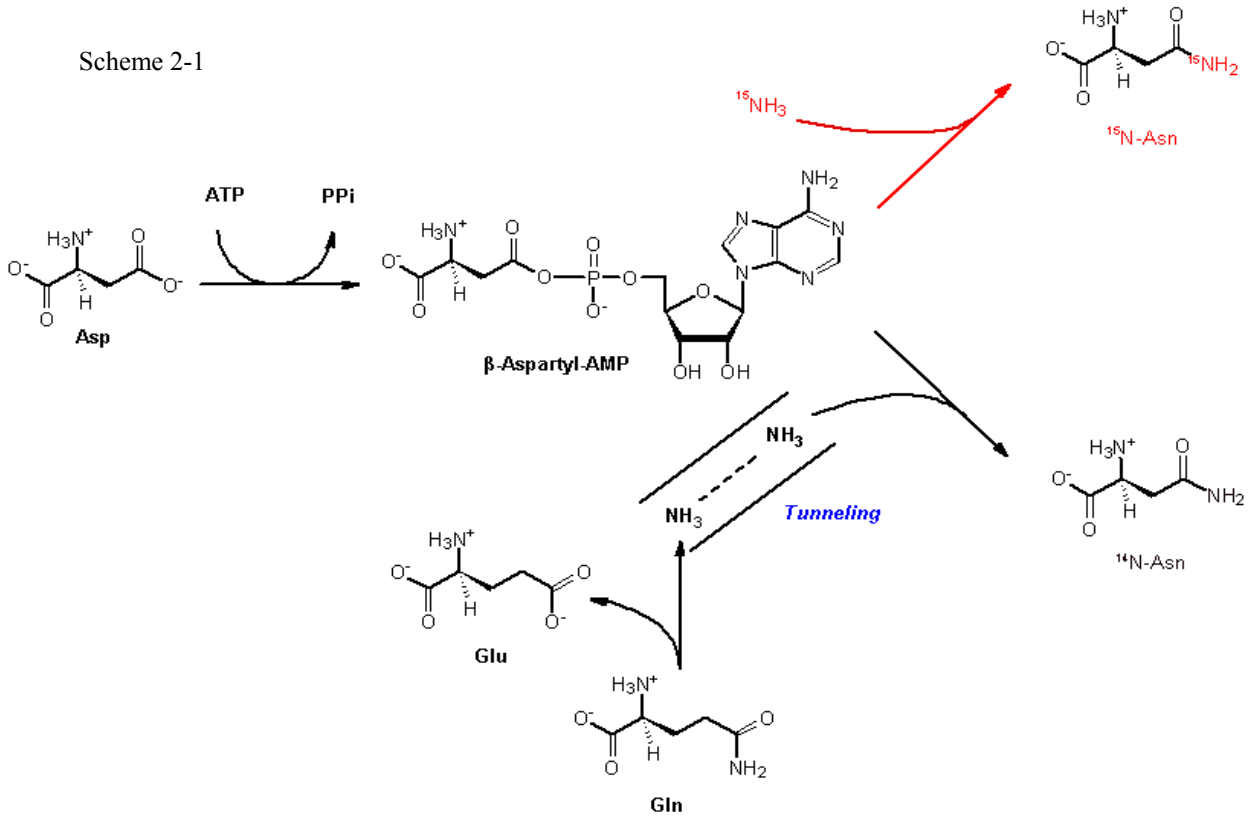
ATP
PPi
Asp
β-Aspartyl-AMP
$^{15}NH_3$
^{15}N-Asn
NH_3
NH_3
Tunneling
^{14}N-Asn
Glu
Gln

A

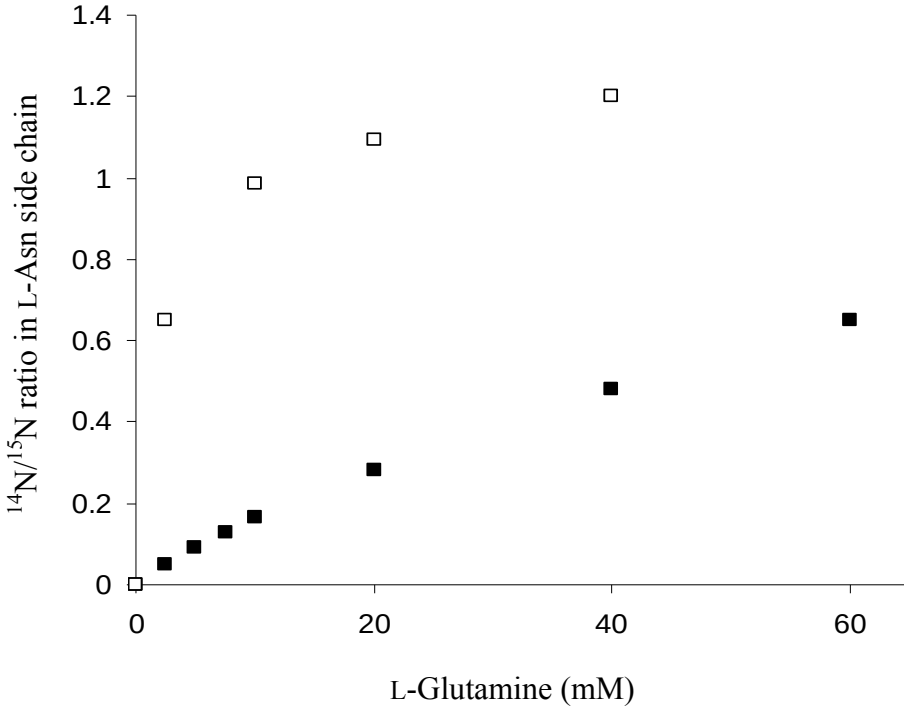
1.4
1.2
1
0.8
0.6
0.4
0.2
0
0
20
40
60
$^{14}N/^{15}N$ ratio in L-Asn side chain
L-Glutamine (mM)

B

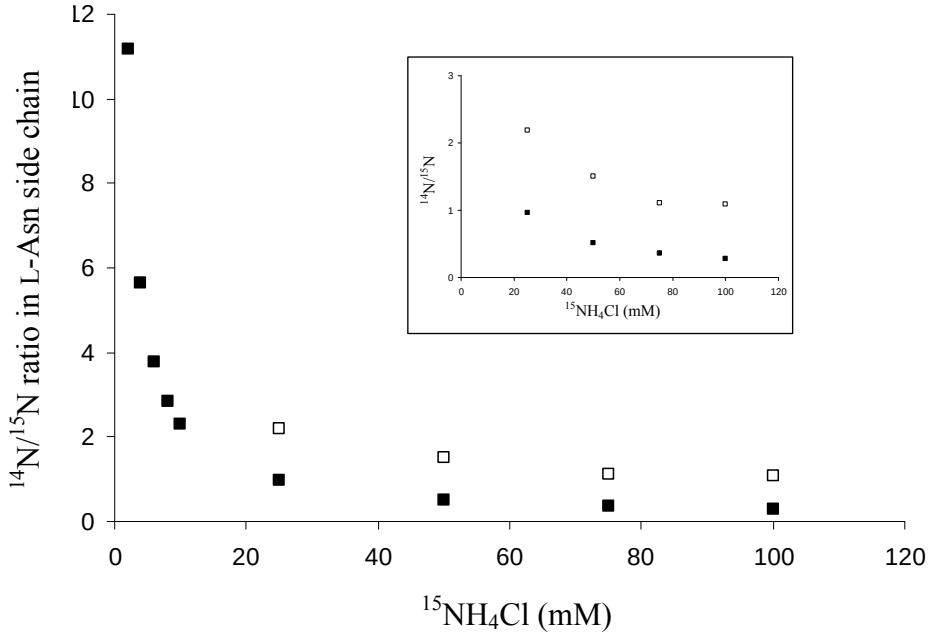
12
10
8
6
4
2
0
0
20
40
60
80
100
120
$^{14}N/^{15}N$ ratio in L-Asn side chain
$^{15}NH_4Cl$ (mM)
3
2
1
0
$^{14}N/^{15}N$
0
20
40
60
80
100
120
$^{15}NH_4Cl$ (mM)

C

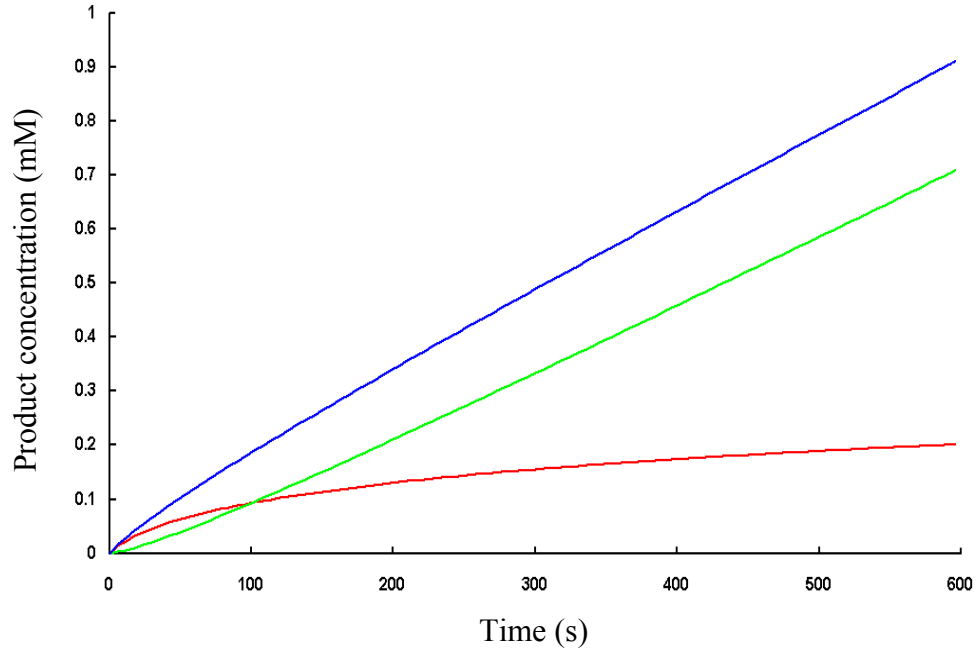

Figure 2-4. $^{14}N/^{15}N$ incorporation ratios in L-asparagine formed by the AS-B synthetase reaction under competition assay conditions. (A) Comparison of the experimentally observed (□) and simulated (■) $^{14}N/^{15}N$ incorporation ratio in 100 mM HEPPS buffer, pH 8, containing 10 mM MgATP, 20 mM aspartate and 100 mM $^{15}NH_4Cl$. (B) Comparison of the experimentally observed (□) and simulated (■) $^{14}N/^{15}N$ incorporation ratio in 100 mM HEPPS buffer, pH 8, containing 10 mM MgATP, 20 mM aspartate and 20 mM L-glutamine. The inset shows an expanded view of the plot for the experimental $^{14}N/^{15}N$ ratios. (C) Kinetic simulation of the time-dependent formation of total L-asparagine (blue), ^{14}N-L-asparagine (red) and ^{15}N-L-asparagine (green) showing the impact of differential inhibition of the two synthetase reactions by L-asparagine.

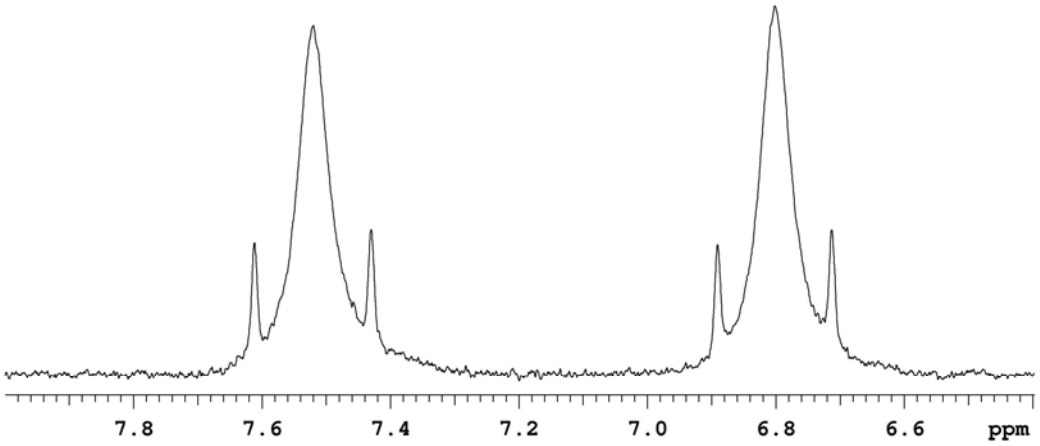

Figure 2-5. Normal ^{1}H-NMR spectrum that shows amide protons from both ^{15}N-glutamine (product, sharp peak) and ^{14}N-glutamine (reactant, sharp peak). The spectrum was acquired after water suppression at 25 ^{o}C. Acquisition time was 5s. Number of transients was 128.

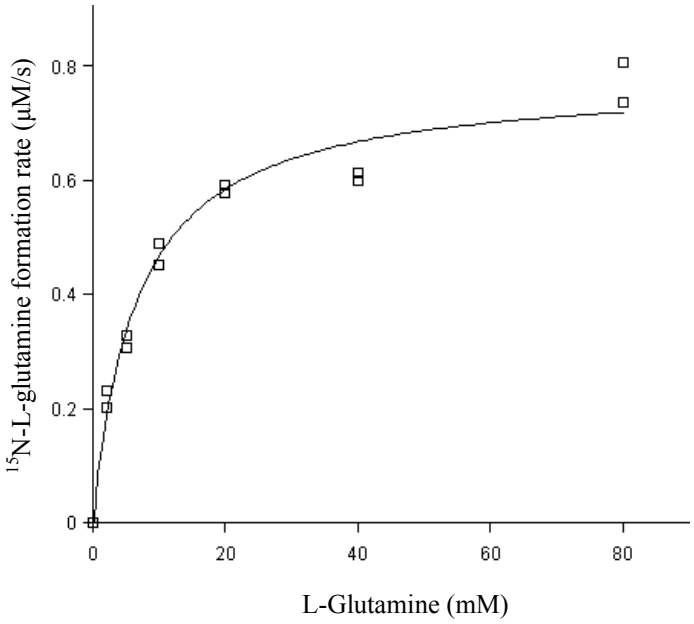

Figure 2-6. Glutamine-dependence of the exchange of $^{15}NH_3$ into L-glutamine under exchange assay conditions**.** Exchange reactions were performed in 100 mM HEPPS buffer, pH 8, containing 60 mM $MgCl_2$, 10 mM ATP and 100 mM $^{15}NH_4Cl$ (2 mL total volume), and each data point represents an average of duplicate experiments.

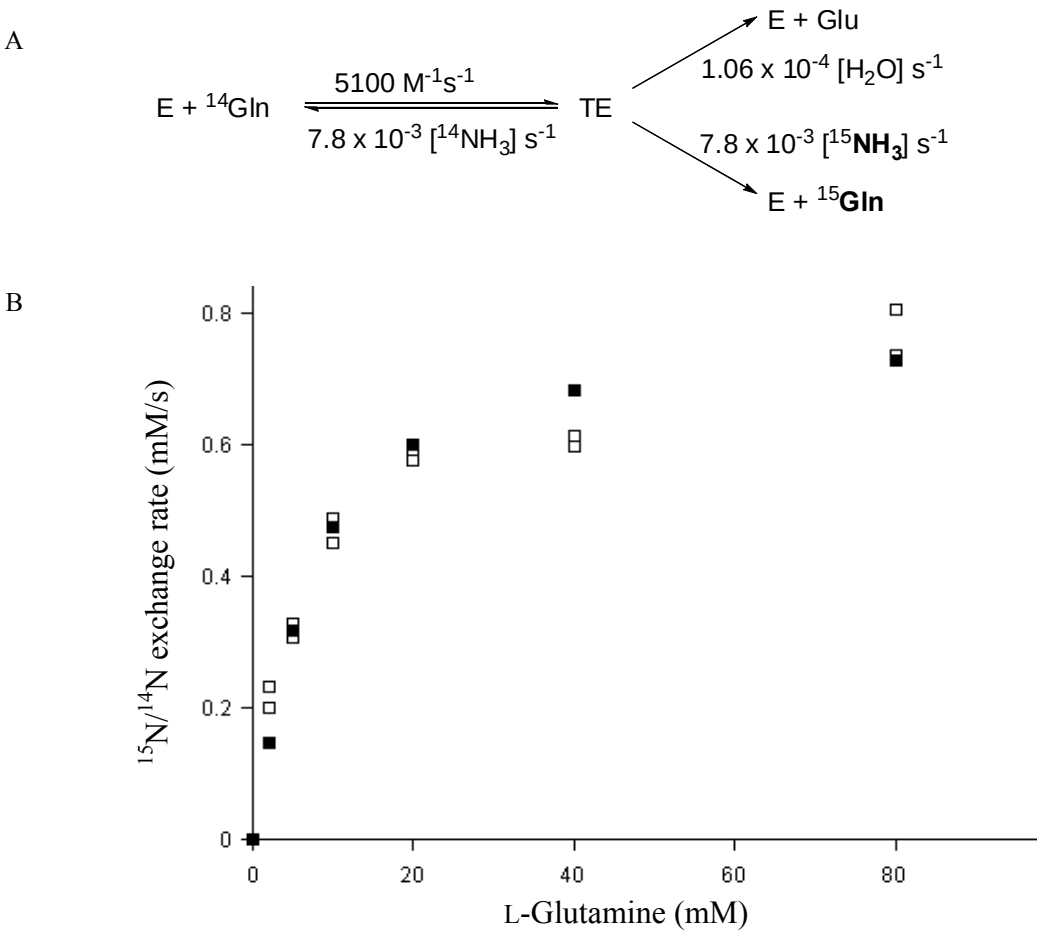

Figure 2-7. Exchange of $^{15}NH_3$ into L-glutamine during the glutaminase reaction catalyzed by AS-B. (A) Kinetic model employed in the simulations of this exchange process. (B) Comparison of the experimentally observed (□) and simulated (■) rate of $^{15}NH_3$ exchange into L-glutamine when AS-B is incubated in 100 mM HEPPS buffer, pH 8, with L-glutamine and 100 mM $^{15}NH_4Cl$ in the absence of ATP and aspartate.

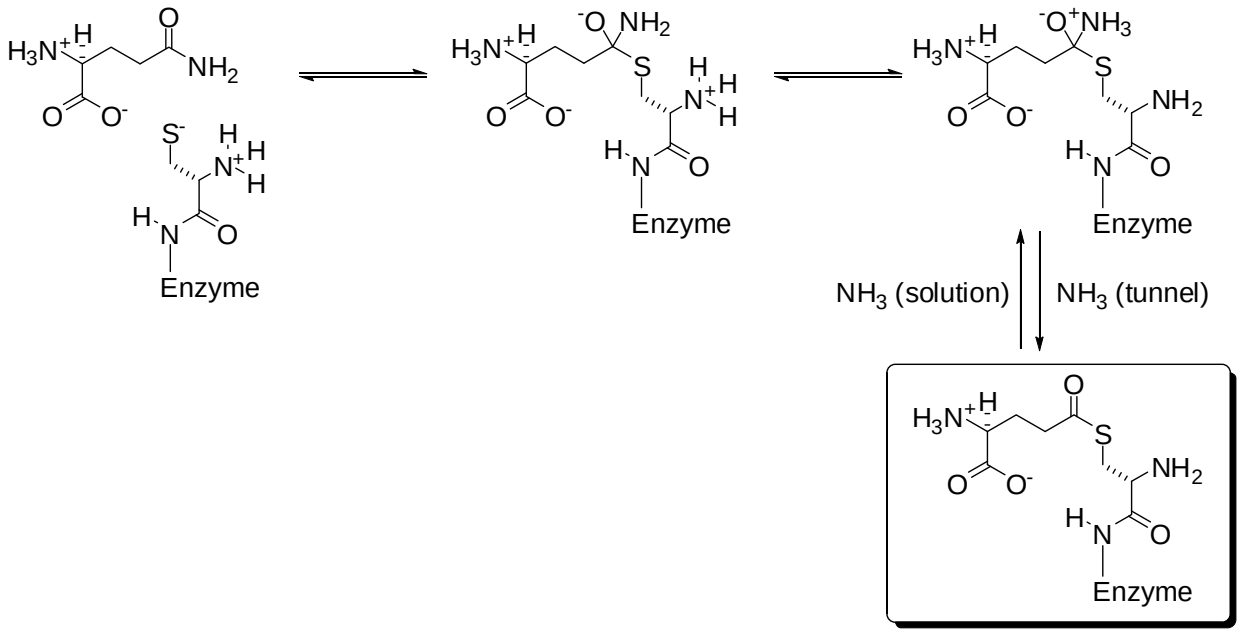

Scheme 2-2. Hypothetical mechanism for formation of a thioester intermediate during the ASNS-catalyzed hydrolysis of L-glutamine. Note that the N-terminal amino group is thought to function as the general acid/base in the reaction (*17, 55*), although direct evidence for this proposal remains to be obtained in the case of ASNS. The thioester intermediate (TE), which subsequently reacts with water to give glutamate, is drawn within a "shadowed" box.

Table 2-1 AS-B catalyzed incorporation of ^{15}N into L-asparagine in the steady-state competition assays.[a]

Gln (mM)	$^{15}NH_4Cl$ (mM)	^{15}N-Gln (mM)[b]	^{15}N-Asn (mM)[b,c]	Total Asn (mM)[d]	^{14}N-Asn/^{15}N-Asn
0	100	ND[e]	0.83 ± 0.03	0.83 ± 0.03	0
2.5	100	ND[e]	0.71 ± 0.02	1.22 ± 0.06	0.65 ± 0.08
10	100	0.18 ± 0.01	0.66 ± 0.02	1.30 ± 0.06	1.0 ± 0.1
20	100	0.26 ± 0.01	0.67 ± 0.01	1.4 ± 0.1	1.1 ± 0.2
40	100	0.34 ± 0.01	0.63 ± 0.03	1.4 ± 0.1	1.2 ± 0.2
20	0	ND[e]	ND[e]	0.76 ± 0.04	NA[e]
20	25	0.12 ± 0.01	0.29 ± 0.01	0.94 ± 0.03	2.2 ± 0.1
20	50	0.16 ± 0.02	0.44 ± 0.02	1.09 ± 0.05	1.5 ± 0.1
20	75	0.19 ± 0.01	0.62 ± 0.07	1.19 ± 0.07	1.1 ± 0.1
20	100	0.26 ± 0.01	0.67 ± 0.01	1.4 ± 0.1	1.1 ± 0.2

[a] All reactions contained 10 mM MgATP, 20 mM aspartate, 60 mM $MgCl_2$ and 490 nM AS-B in 100 mM HEPPS buffer, pH 8 (2 mL total volume).

[b] As determined by gHMQC NMR spectroscopy. Errors are estimated on the basis of measurements employing known concentrations of authentic ^{15}N-Asn.

[c] This value is corrected for the amount of ^{15}N-Asn that would be formed from ^{15}N-Gln at natural abundance, but the contribution of ^{14}N-Asn formed from any $^{14}NH_3$ released from the enzyme, as a result of the glutaminase activity of AS-B, is assumed to be negligible.

[d] Mean value and standard deviation computed from two separate determinations on duplicate samples using reverse-phase HPLC.

[e] ND – not detected; NA – not applicable.

CHAPTER 3
CHARACTERIZATION OF A TUNNEL MUTANT

Introduction

The crystal structure of C1A mutant of *Escherichia coli* asparagine synthetase B showed that the two active sites are separated by a 20 Å distance. The biochemical studies on ASB, with structural evidence, support the presence of an intramolecular ammonia tunnel in this enzyme. To investigate the channeling mechanism of ammonia in asparagine synthetase under the structural context, the tunnel residues need to be identified and their key roles in ammonia tunneling need to be elucidated. The tunnel residues were determined by computing the molecular surface of the protein, with a probing radius at 1.4 Å. Do these residues form the real tunnel that ammonia intermediate goes through? Futhermore, since most of them are conserved in different species including bacterial, fungus, plants, insect and mammalian, which indicates they are important to either the structure or the function of the tunnel. Then what kind of roles do they play in ammonia tunneling? To provide some insight to these questions, I performed biochemical studies on ASB. The strategy here is to characterize tunnel mutants in which ammonia transfer is affected by either blockage or leakage of the tunnel. The hypothesis are: if the tunnel is blocked or perforated by mutations without affecting the active sites, glutaminase activity and ammonia dependent synthetase activity of the mutants will not be significantly affected, compared to that of wild type, while its glutamine dependent synthetase activity will decrease.

The putative tunnel is arbitrarily divided into three parts: the mouth, the body and the bottom. The residues in the mouth and the bottom part are within the active sites. Therefore, only those residues in the body part were considered. Among these residues, Ala388 is one of the conserved residues. Its backbone forms the narrow part of the tunnel, with other residues. And its

side chain points into the tunnel (Figure 3-1). Since the side chain of alanine is a methyl group, mutation of this residue to another one with bigger side chain such as Leu may block the tunnel. Based on this hypothesis, the A388L mutant was prepared and characterized.

Material and Methods

Materials

The experiments were performed as described in Chapter 2 Materials and Methods part.

The primers of A388L mutant were ordered from idtdna.com. QuikChange® Site-Directed Mutagenesis Kit for PCR were from Stratagene. *Pfu*Turbo™ DNA polymerase, 10× reaction buffer, dNTP mix and XL1-blue supercompetent cells were from the mutagenesis kit. *Dpn* I restriction enzyme was from New England Biolab. Wizard® Plus Midipreps DNA Purification System for plasmid purification was from Promega.

Unless otherwise stated, all chemicals and reagents were purchased from Sigma (St. Louis, MO), and were of the highest available purity. 1,3-$^{15}N_2$-Uracil, ^{15}N-L-asparagine, and d_6-DMSO were purchased from Sigma-Aldrich (St. Louis, MO). The isotopic incorporation in these samples was greater than 99%. All experiments employed freshly prepared solutions of recrystallized L-glutamine (*17*). NMR spectra were recorded on a Varian INOVA 500 instrument equipped with a 5 mm triple resonance indirect detection probe (z-axis gradients) operating at 500 and 50 MHz for ^{1}H and ^{15}N, respectively. Chemical shifts are reported in ppm relative to sodium 2,2-dimethyl-2-silapentane-5-sulfonate (DSS). The co-axial inner cell (catalog: NE-5-CIC-V) containing the external NMR standards was purchased from New Era Enterprises (Vineland, NJ).

Primers were designed and analyzed using Gene Runner ver3.05 (Hastings Software). The sequences of A388L primers are 5'-GAC TGC GCG CGT CTG AAC AAA GCG ATG TC-3' and 5'-GA CAT CGC TTT GTT CAG ACG CGC GCA GTC-3 for sense and antisense primer

respectively. The plasmid for mutant expression was prepared by PCR using a pET-21c(+) plasmid with *Escherichia coli asnB* gene inserted into its *Nde* I restriction site as the DNA template. The template plasmid contains total 7103 bps (5441 bps for empty plasmid plus 1662 bps for *asnB* gene) with a marker for ampicillin resistance. QuikChange® Site-Directed Mutagenesis Kit was used for PCR and cloning. The plasmid with *asnB* gene mutant was purified using Wizard® Plus Midipreps DNA Purification System. Recombinant, A388L ASB mutant was expressed and purified following literature procedures (*16*). Protein concentrations were determined using a modified Bradford assay (Pierce, Rockford, IL) (*60*), for which standard curves were constructed with bovine serum albumin, and corrected as previously reported (*55*).

Competition Experiment

Reaction mixtures consisted of 100 mM HEPPS buffer (pH 8.0), 60 mM $MgCl_2$, 10 mM ATP, 20 mM aspartate and different concentrations of $^{15}NH_4Cl$ (pH 8.0) or glutamine in total volume of 2 mL. In experiments where the concentration of $^{15}NH_4Cl$ (pH 8.0) was varied as 10 mM, 25 mM, 50 mM, 75 mM and 100 mM, L-glutamine was fixed at 20 mM. Alternatively, when L-glutamine was varied as 0 mM, 2.5 mM, 5mM, 10 mM, 20 mM and 40 mM, $^{15}NH_4Cl$ was added at an initial concentration of 100 mM. Reactions were initiated by the addition of A388L ASB mutant (30 μg) and the resulting samples incubated for 10 min at 37 ^{o}C before being quenched by the addition of trichloroacetic acid (TCA) (60 μL). After centrifugation for 5 min at 3000 rpm to remove precipitated protein, the supernatant was adjusted to pH 5 by the addition of 10 M aq. NaOH and an aliquot of this solution (650 μL) transferred to a 5 mm NMR tube for analysis. At higher pH values, amide NH exchange precluded the derivation of any quantitative relationship between peak area and ^{15}N-Asn concentration. The standard samples contained 100 mM HEPPS buffer (pH 8.0), 60 mM $MgCl_2$, 10 mM ATP, 100 mM $^{15}NH_4Cl$ (pH

8.0), 20 mM glutamine and different concentrations of ^{15}N-L-Asn from 0.05 mM to 2.5 mM, without adding ASNS.

NMR Measurements and HPLC assay

See Chapter 2 Materials and Methods part.

Results and Discussion

After the A388L ASB mutant was prepared, the kinetic parameters were first determined using enzyme assays (Beeson, unpublished data). Since the pyrophosphate assay, which is used for determination of synthetase activity of the enzyme, gave a low k_{cat} value due to a possible pyrophosphatase contamination, the k_{cat} values for both glutamine dependent and ammonia dependent synthetase activity were reexamined to fit NMR results. As expected, the specificity of A388L mutant to glutamine based on its glutaminase activity changed by less than 2 fold compared to the results for wild type ASB. This change resulted mainly from the decrease of K_m values. Its specificity for ammonia based on the ammonia dependent synthetase activity had little change. Both k_{cat} and K_m decreased a little. For its glutamine dependent synthetase activity, the specificity for glutamine dropped by 8 fold, with k_{cat} decreased by 5 fold (Table 3-1).

When both $^{15}NH_4Cl$ and glutamine present in reaction mixture, the ^{14}N-asparagine/^{15}N-asparagine ratio for A388L mutant was less than that of WT ASB, with either varied glutamine from 2.5 mM to 40 mM (Figure 3-2A) or varied ammonia from 50 mM to 100 mM (Figure 3-2B). In general, these results are consistent with the result above that glutamine dependent synthetase activity decreased significantly, with no significant change of its ammonia dependent synthetase activity. However, the ^{14}N-asparagine/^{15}N-asparagine production ratio catalyzed by the A388L mutant is not proportional to that catalyzed by the WT enzyme. With $^{15}NH_4^+$ at 100 mM, the ^{14}N-asparagine/^{15}N-asparagine ratio decreased by about 10 folds when the concentration of glutamine was below 10 mM, while with higher glutamine, it decreased by about 4 folds.

When varying ammonium, this ratio didn't change proportionally either. Especially at low concentration of ammonium, its value was close to that of WT ASB. These results may be caused by the overall effect of 1) the asparagine inhibition of glutaminase activity; 2) the suppression of the ammonia utilization by glutamine, and 3) glutamine inhibition.

The production of ^{14}N-asparagine by A388L mutant decreased significantly compared to WT ASB, while the production of ^{15}N-asparagine had no big change, when either varying glutamine or varying ammonium (Figure 3-3, 3-4). Furthermore, the production of ^{15}N-glutamine increased slightly for the mutant (Figure 3-5), which is consistent with the increased specificity of glutamine for its glutaminase activity. The ^{14}N-asparagine/^{15}N-asparagine ratio, and the production of ^{14}N-asparagine, ^{15}N-asparagine and ^{15}N-glutamine, as well as the kinetic results determined by enzyme assays, support that the mutation of Ala388 to Leu may block the tunnel. Ala388 is in the narrowest part of the tunnel. It is not only at the interface of the two domains, but also one of the non-polar residues close to the glutaminase sites that consists of mainly polar residues (Figure 3-6). Its side chain, a methyl group, is not likely to involve in interactions with other residues, as aromatic residues or charged residues usually do. However, mutation of this alanine to leucine resulted in the possible blockage of the tunnel, which may suggest that this part of the tunnel may act as the gate of the tunnel.

Conclusions

Based on the tunnel residues determined by computational methods, a tunnel mutant was prepared, in which a conserved alanine residue was mutated to leucine. The glutaminase activity and ammonia dependent synthetase activity of this A388L mutant are similar to that of WT ASB, while its glutamine dependent synthetase activity dropped by about 8 fold. The kinetic studies of this mutant experimentally support that the identified tunnel residues by computational methods are those forming the intramolecular ammonia tunnel. Furthermore, the NMR studies on this

mutant, together with the kinetic results, suggest that the mutation may result in the blockage of the tunnel.

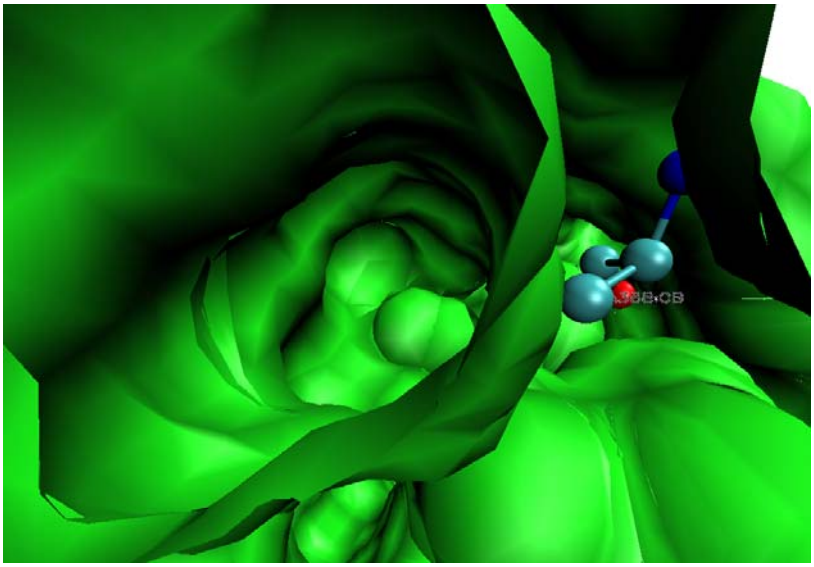

Figure 3-1. One of the conserved tunnel residues, Ala388. The backbone of A388 forms the narrow part of the tunnel with several other tunnel residues. Its side chain points into the tunnel close to the glutaminase site.

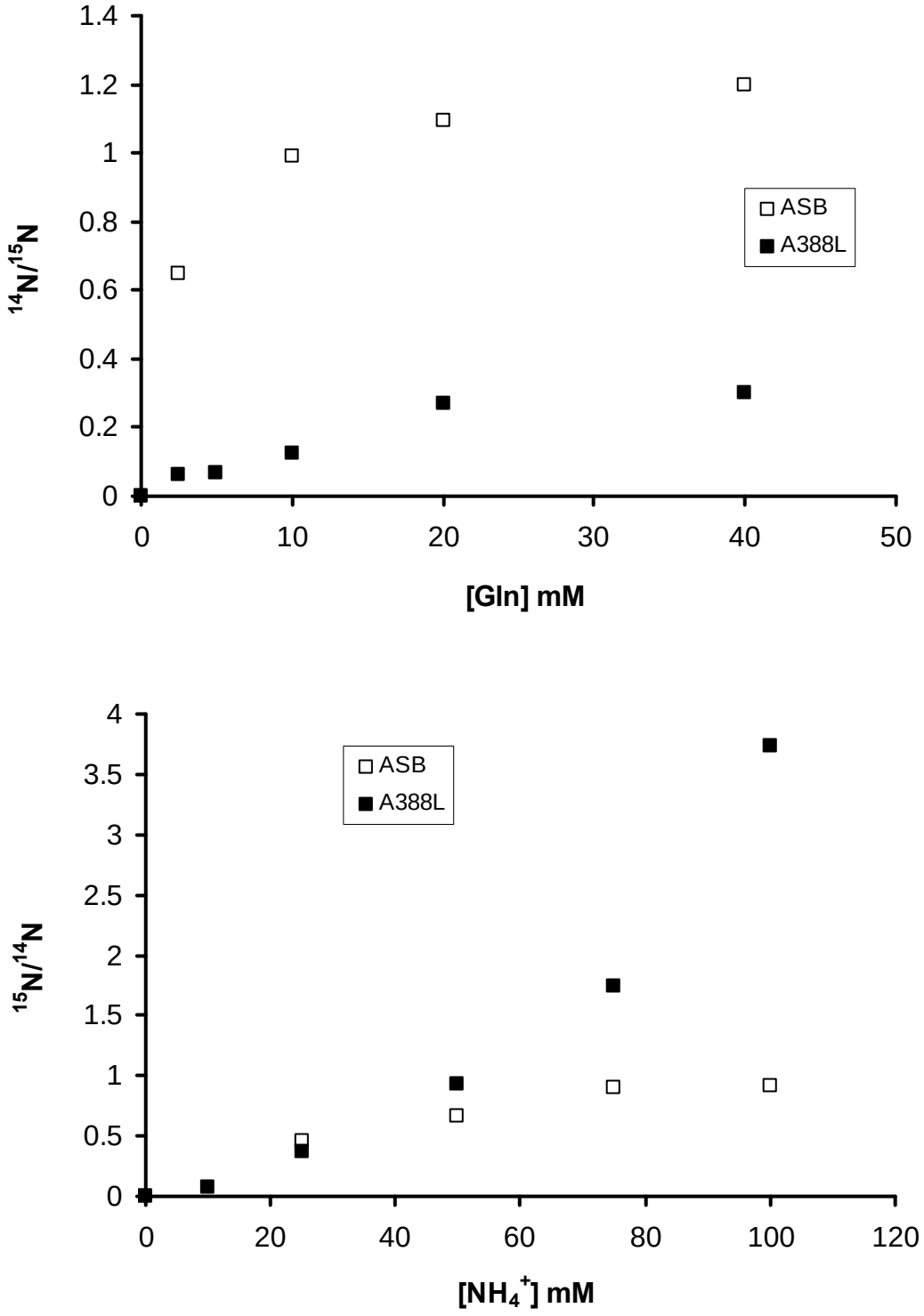

Figure 3-2. Competition results for A388L ASB mutant, as well as WT ASB. Filled square: A388L; blank square: WT ASB. In general, the ^{14}N-asparagine/^{15}N-asparagine ratio decreased due to the mutation of alanine to leucine. A) varying glutamine; B) varying ammonium.

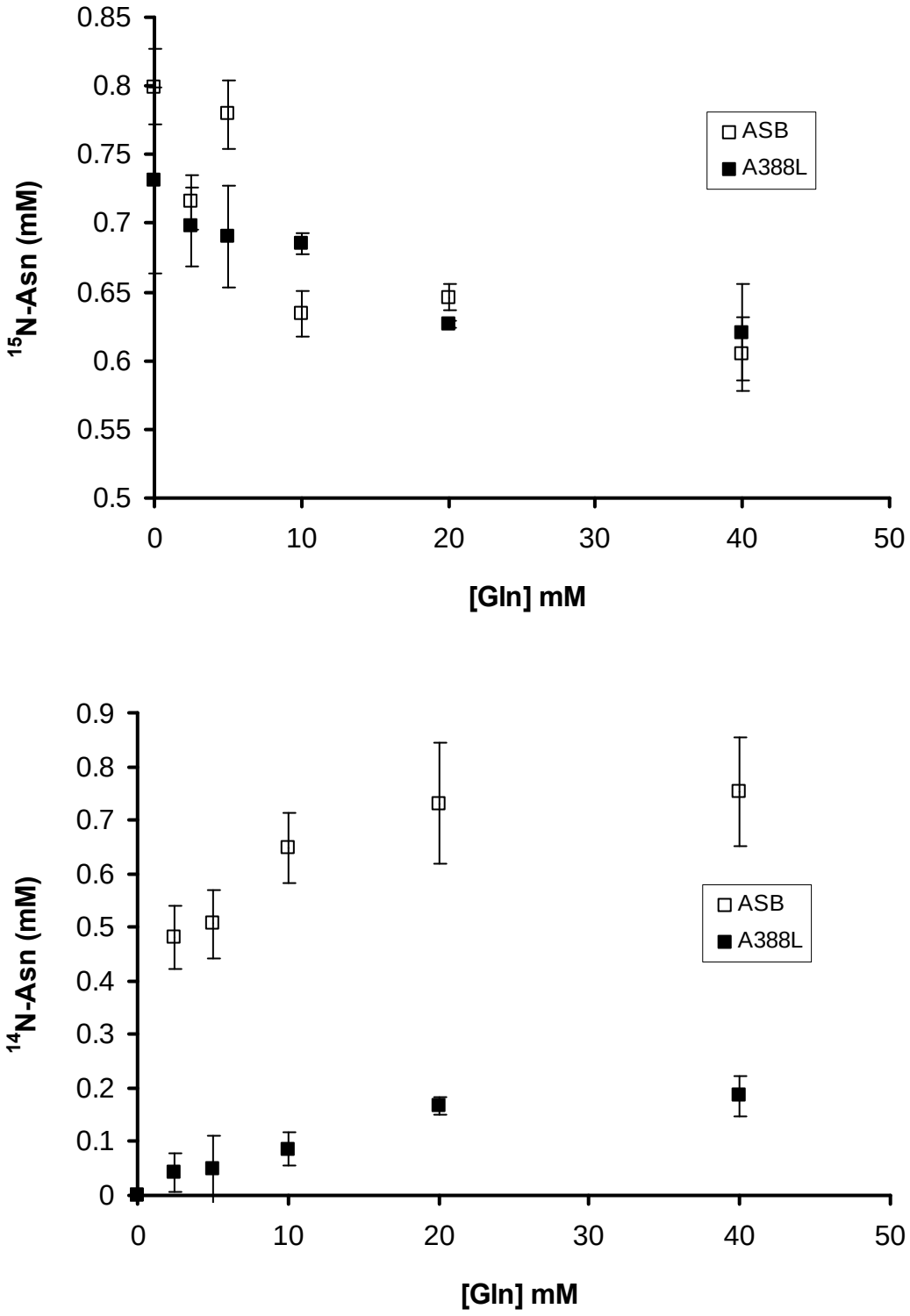

Figure 3-3. Production of asparagine catalyzed by A388L ASB mutant and WT ASB with varied glutamine. Filled square: A388L; blank square: WT ASB. In general, the ^{14}N-asparagine decreased significantly due to the mutation of alanine to leucine. A) production of ^{15}N-asparagine; B) production of ^{14}N-asparagine.

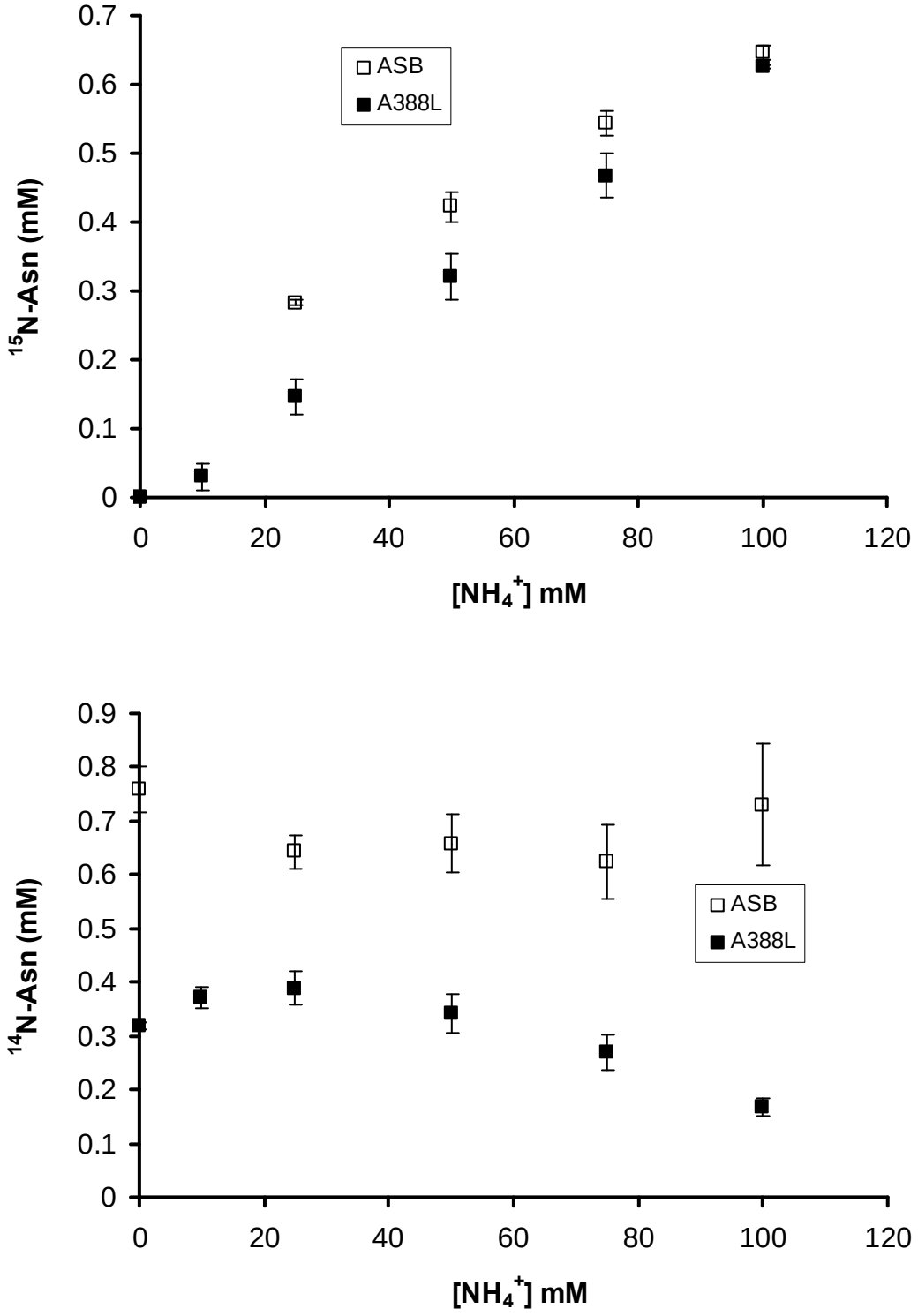

Figure 3-4. Production of asparagine catalyzed by A388L ASB mutant and WT ASB with varied ammonium. Filled square: A388L; blank square: WT ASB. In general, the ^{14}N-asparagine decreased significantly due to the mutation of alanine to leucine. A) production of ^{15}N-asparagine; B) production of ^{14}N-asparagine.

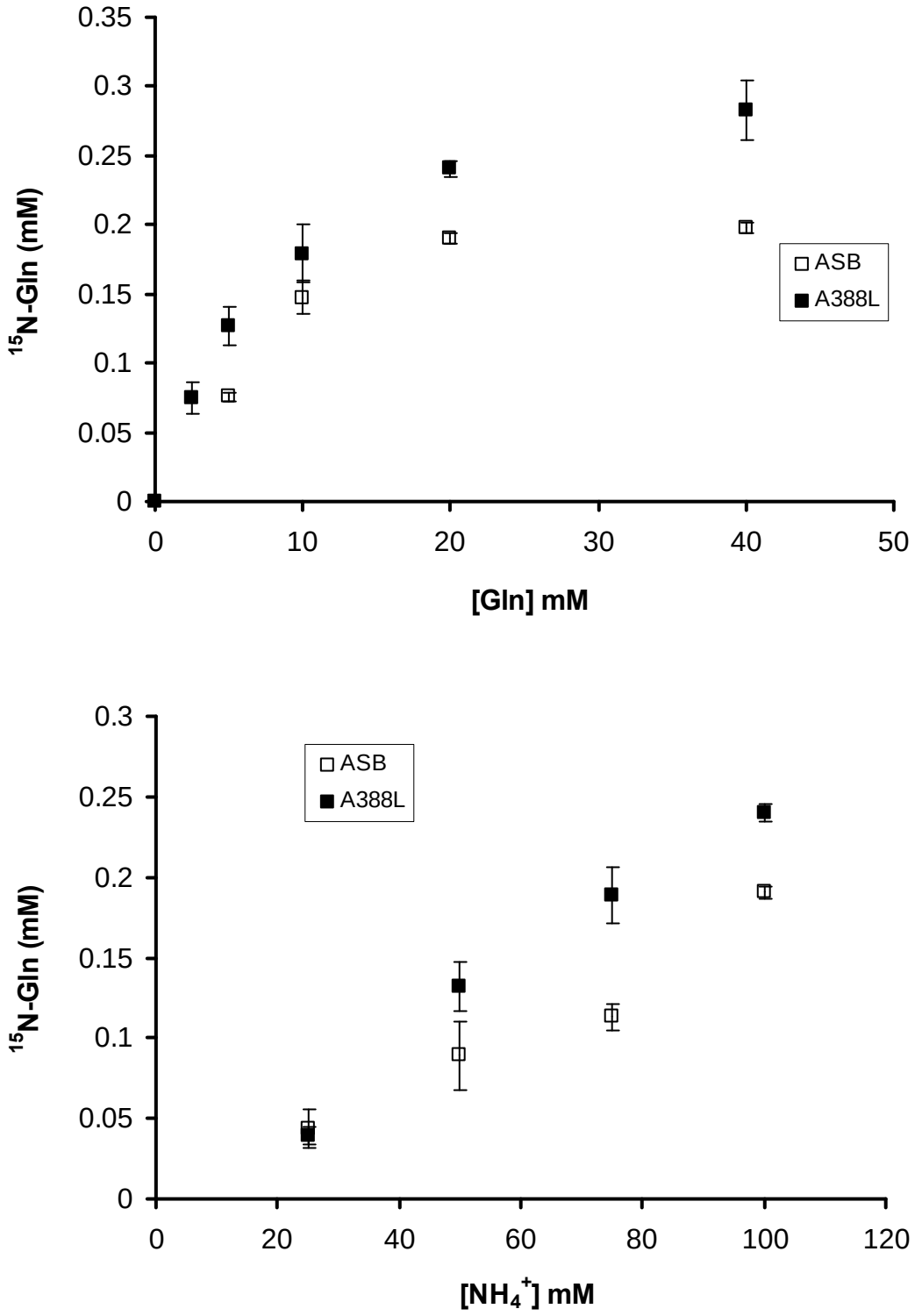

Figure 3-5. The nitrogen exchange catalyzed by A388L mutant and WT ASB. Filled square: A388L; blank square: WT ASB. In general, the production of ^{15}N-glutamine increased due to the mutation of alanine to leucine. A) varying glutamine; B) varying ammonium.

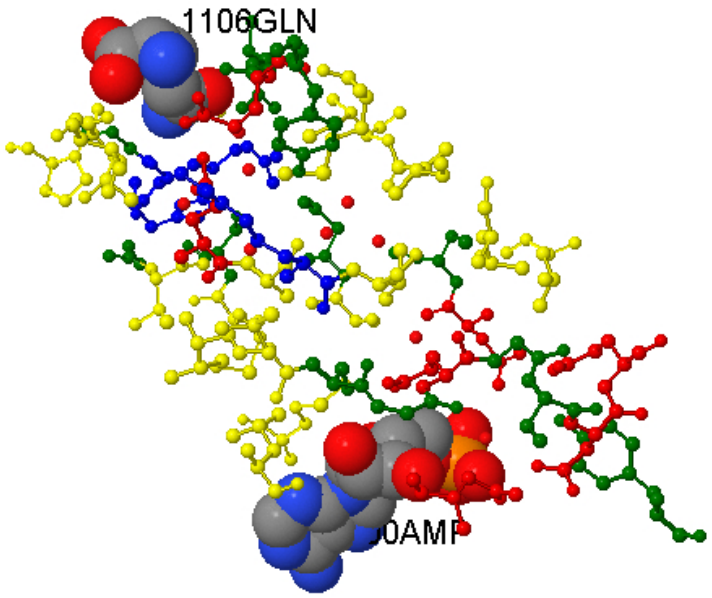

Figure 3-6. The polarity of the tunnel residues. Yellow: non-polar residues; green: polar residues; blue: basic residues; red: acidic residues. Both AMP (bottom) and glutamine (top) showed in balls.

Table 3-1. The kinetic parameters for glutaminase activity, ammonia dependent synthetase activity and glutamine dependent synthetase activity of both wild type ASB and A388L mutant

	WT ASB			A388L mutant		
	k_{cat} (s^{-1})	K_m (mM)	k_{cat}/K_m ($M^{-1}s^{-1}$)	k_{cat} (s^{-1})	K_m (mM)	k_{cat}/K_m ($M^{-1}s^{-1}$)
Glutaminase activity	3.38	1.67	2000	3.12	0.87	3600
Ammonia dependent synthetase activity	3.19	17	190	2.34	15	160
Glutamine dependent synthetase activity	2.94	0.69	4300	0.57	1.06	540

CHAPTER 4
ASPARAGINE INHIBITION TO ASPARAGINE SYNTHETASES AND ITS EFFECT ON THE QUATERNARY STRUCTURE OF THE ENZYMES

Introduction [‡]

Glutamine-dependent (EC 6.3.5.4) asparagine synthetase belongs to amidotransferase superfamily(*5, 6*), and was found in all kinds of species including archaeon, bacteria, fungi, plant, and animals (*13*). Based on the structure and function of its glutaminase domain, asparagine synthetase was classified as class II amidotransferase, which consists of three other amidotransferases, glutamine PRPP amidotransferase, glucosamine 4-phosphate synthase, and glutamate synthase. This enzyme has two domains, glutaminase domain and synthetase domain, which are connected by a single loop (*15*). It catalyzes ATP-dependent synthesis of L-asparagine from L-aspartic acid using either glutamine or ammonium as nitrogen source. At glutaminase site, the amide nitrogen of glutamine is hydrolyzed into ammonia intermediate through a thioester enzyme-substrate complex, with glutamate as one of the products (*14*). Ammonia is then transported through an intramolecular tunnel to synthetase site and reacts with β-Aspartyl-AMP, an intermediate that formed by ATP and Asp at synthetase site, to produce asparagine. Alternatively, this enzyme can also use free ammonia as nitrogen donor. Unlike other class II amidotransferases (*54, 66-68*), the hydrolysis of glutamine is not strictly coupled with the synthesis of final product *in vitro* (*17*). Without ATP and Asp, asparagine synthetase can consume glutamine and release toxic ammonia. Furthermore, the glutaminase activity of bacterial enzyme is even stimulated by the presence of ATP without producing asparagine (*17*). These observations raise the interest in the regulation of glutaminase activity of asparagine

[‡] Li designed the inhibition experiments. Inhibition to ASB part was performed by Li and an undergraduate, William Beeson. Inhibition to hASNS was performed by William Beeson himself. Li and Beeson did the kinetic analysis. Li did the simulation. Li designed and performed the SEC experiments and analyed the results.

synthetase *in vivo* to prevent the waste of glutamine and the releasing of free ammonia.

Kinetic studies of asparagine synthetase have been extensively performed in the last 20 years, especially for *Escherichia coli* enzyme (ASB) (*2, 3, 7, 8, 11, 22, 24, 35, 57, 69-72*). The glutaminase activity of asparagine synthetase can be affected by chloride ions (*72*), ATP or asparagine (*22, 24*). With a K_I value of about 100 μM, asparagine may play an important role in preventing unnecessary hydrolysis of glutamine under physiological conditions. Therefore, we investigated the possible mechanisms for asparagine inhibition to the glutaminase activity of *Escherichia coli* ASB and hASNS from both structural and kinetic aspects. Our results showed that asparagine inhibited the hydrolysis of glutamine by ASB and hASNS through different mechanisms and had different effect on the quaternary structure of these two enzymes.

Materials and Methods

Materials

Unless otherwise stated, all chemicals and reagents were purchased from Sigma (St. Louis, MO). L-Glutamine was recrystallized prior to use as previously described (*53*). Wild-type *Escherichia coli* ASB and recombinant, C-terminally tagged human AS were expressed in and purified from a baculo virus/insect cell expression system as previously described (*16, 57*).

Enzyme Assays

Kinetic constants were determined by incubating purified, recombinant asparagine synthetase in reaction mixtures in which one substrate was varied and all others were at saturating concentrations. Asparagine synthetase was added to 200 μL reaction mixtures containing 100 mM HEPPS, pH 8.0, 100 mM NaCl, 8mM $MgCl_2$, and varying amounts of L-glutamine (0-50 mM). The reaction mixture was incubated at 37 ^oC for 10 minutes and then quenched with 30 μL of 20% w/v trichloroacetic acid. Each quenched reaction mixture was added to a premixed 770 uL solution containing 300 mM glycine, 250 mM hydrazine, pH 9.0,

1.5 mM NAD^+, and 1 mM ADP. Glutamate production was assayed by adding 2 μL of L-glutamic acid dehydrogenase to the mixture and monitoring absorption spectrophotometrically at 340 nm for 60 minutes. Measurements at specific substrate concentrations were performed in duplicate or triplicate, and the initial rate data was analyzed by curve-fitting using computer-based methods to determine the V_{max} and K_M constants.

Asparagine Inhibition Studies

Product inhibition studies were carried out on the wild-type *E. coli* ASB (3.1 μg) and recombinant, C-terminally tagged hAS (3.0 μg) using the enzyme assay described above, but with a fixed amount of asparagine (0-0.5 mM for ASB and 0-1.0 mM for hASNS) added to each run. The apparent K_M and V_{max} values were analyzed by curve-fitting using standard computer-based methods.

Size Exclusion Chromatography to Determine the Quaternary Structure of Asparagine Synthestases.

Gel filtration chromatography was performed on Rainin Dynamax HPLC system using a Phenomenex BIOSEP SEC-S2000 column (300 x 7.8 mm with 75 x 7.8 mm guard column, particle size: 5 μm; pore size: 145 Å) with detection wavelength at 280nm and flow rate at 1.0 mL/min. The molecular weight is calculated based on a standard curve of a series of marker proteins with different molecular weights purchased from Sigma. Unless stated otherwise, stock enzymes for *Escherichia coli* asparagine synthetase B (ASB) or human asparagine synthetase were directly injected for analysis with a volume of 5 μL.

The Effect of Asparagine on the Quaternary Structure of ASB and hAS

The enzyme was analyzed as described above using a mobile phase that contained 50mM Tris-H_2SO_4 buffer at pH 7.0 with different concentrations of asparagine (0-5.0 mM). All sample points have at least two repeats.

SEC Studies of ASB with Different Amount of ASB

The enzyme was analyzed by SEC using a mobile phase that contained 50mM Tris-H_2SO_4 buffer at pH 7.0 with different injection volume of 3.1 mg/mL stock solution (2.5-40 μL).

Results

Product Inhibition

The glutaminase activity of ASB was studied with varying amounts of asparagine present (0.025 – 0.5 mM). The apparent K_M for glutaminase reaction increased with increasing asparagine concentration. Figure 4-1A shows a replot of apparent K_M respect to glutamine vs concentration of asparagine. The increase of K_M with increasing concentration of inhibitor results from the binding of asparagine to the free enzyme. However, the regression line is not linear but more like polynomial. The presence of asparagine in the reaction mixture affected not only the apparent K_M value, but also the k_{cat} value of the glutaminase reaction, which decreased as the concentration of asparagine was increased (Figure 4-1B). This result provides the evidence that asparagine binds to enzyme-substrate complex. Therefore, asparagine is a mixed inhibitor to ASB with respect to glutamine. The glutaminase activity of human enzyme was also studied with varying amounts of asparagine present (0.05 – 1.0 mM). The inhibition results showed clearly that asparagine is a competitive inhibitor to glutamine. The maximum glutaminase activity stayed constant with a value of 3.6 s^{-1} in term of monomer. And the apparent K_M versus concentration of asparagine is a straight line with determined inhibition constant as 0.11 ± 0.2 mM (Figure 4-1C).

Asparagine Affects the Quaternary Structure of ASB, But Not Human Enzyme

The nonlinear relationship of apparent K_M for ASB vs concentration of asparagine indicates more than one binding site for asparagine. In the crystal structure of ASB C1A mutant (PDB code: 1CT9), the enzyme exists as dimer form with glutamine bound to it (*15*). Each

subunit has two separated active sites, glutaminase site and synthetase sites. The distance between the two sites is about 20 Å. For better understanding of the inhibition mechanisms to ASB by asparagine from the structural point of view, we studied the quaternary structure of the enzyme by SEC with or without the presence of asparagine in the mobile phase.

It was reported that the activity of asparagine synthetases was affected by chloride ion and pH (*72*). There was no significant difference for the SEC results of asparagine synthetases using either Tris-HCl or Tris-H_2SO_4 at pH 7.0, or within the pH range of 7.0-7.9 (unpublished data). Here we choose Tris-H_2SO_4 at pH 7.0 as the mobile phase. The molecular weight (MW) was calculated using a standard curve (Figure 4-2). Using 50 mM Tris-H_2SO_4 buffer at pH 7.0, two peaks were observed in the size exclusion chromatogram of ASB, with retention times of 9.15 and 9.51 minutes respectively. The calculated MWs for these two peaks are 120kD and 84kD respectively (Figure 4-3A). After adding asparagine in the mobile phase, the retention time of the higher MW ASB peak changed, which indicates asparagine affects the quaternary structure of ASB. With the presence of asparagine in the mobile phase, two peaks with RT at 8.79 and 9.49 minutes were observed. The calculated MWs for the two peaks are 171kD and 85kD respectively, with higher MW for the peak with shorter retention time (Figure 4-3A). Under experimental conditions, the retention times of these two peaks were independent of the concentration of asparagine added, with the lowest concentration at 0.1 mM (Table 4-1). The true MW of one subunit of ASB is about 62.5kD based on its gene sequence. Therefore, the 9.50 minutes peak (calculated MW: ~85 kD) with or without asparagine is very likely the monomer form of ASB, with the 8.79 minutes peak (calculated MW: 171 kD) the dimer form (Table 4-2). And the intermediate peak at 9.15 minutes (calculated MW: 120 kD) without the presence of asparagine may result from quick exchanges between the forms. That is, equilibrium exists

between the monomer and dimer form. This conclusion was supported by the SEC results using different amount of enzyme without asparagine in mobile phase (Figure 4-4).

Besides the retention time, asparagine also affects the individual peak area and height. While the total area of the monomer and dimer peaks had almost no change with different concentrations of asparagine in the mobile phase, the dimer peak area and height increased with increasing asparagine, which supports that asparagine thermodynamically stabilizes the dimer form. The plot of percentage of dimer peak area in total ASB peak area vs. concentration of asparagine behaves like a Michaelis-Menten curve (Figure 4-5). At low concentrations of asparagine, the peak area of dimer ASB and the peak height ratio increase rapidly with the increasing concentration of asparagine. At high concentrations of asparagine, the curve gradually levels off and indicates the saturating status. The estimated binding constant of asparagine is about 0.10 mM. In our results, a monomer peak was always observed. In other words, ASB did not completely converted to dimer at high concentration of asparagine (5 mM). One possible reason is that partial protein has no chance to collide with each other and form dimer during elution. Regardless of this, we can conclude that with asparagine present in the mobile phase, both dimer and monomer peak showed in the chromatogram and the dimer is stabilized by asparagine binding at the experimental conditions.

Under the same conditions, the quaternary structure of hASNS was studied without asparagine or with 5 mM asparagine in the mobile phase. Most of enzyme exists as dimer form with retention time at 8.75 minutes. With 5 mM asparagine, no detectable changes were observed for the retention time and the peak area (Figure 4-3B).

The Equilibrium between the Dimer and Monomer Form of ASB.

When the mobile phase contains no asparagine, the SEC chromatogram showed one

monomer peak and one intermediate peak, while no dimer peak. Based on these results, we came up the idea that the ASB monomer and dimer form equilibrium at experimental conditions. However, this peak may results from the overlapping of the two forms of enzyme peaks. To confirm our hypothesis, we performed SEC studies using different amount of the enzyme without the presence of asparagine in the mobile phase.

The ratio of both peak area and peak height for the two peaks (intermediate/monomer) increased with more enzyme injected. Furthermore, the retention time of intermediate peak is closer to that of dimer peak. All these results support that more dimer formed at higher concentration of enzyme and the two forms of enzyme are in a dynamic equilibrium (Figure 4-4).

Construction of Asparagine Inhibition Model

The inhibition model for ASB (scheme 4-1A) was constructed based on the following considerations: 1. The dimer form is the active form. The active form of ASB was seldom addressed in previous studies. To date, the only 3D structural information of ASB was reported by Larsen et al(*15*). In their studies, the C1A mutant of ASB is a homogenous dimer with one glutamine bound to each glutaminase site. Since the mutated residue is at the end of N-terminal domain and plays catalytic role rather than structural role, we can consider this structure is close to that of the wild type enzyme. Therefore, it is reasonable to assume that the dimer is the active form of the enzyme. Furthermore, this hypothesis was supported by our result that glutamine also stabilizes the dimer form of ASB like asparagine (unpublished data). Because the dimer form of ASB was stabilized at low concentration of asparagine and its substrate glutamine has the similar effect on its quaternary structure, the amount of dimer form can be considered constant at most of the experimental conditions with both asparagine and glutamine present. Therefore, although our results showed equilibrium exists between the two forms of enzyme, we didn't include the

equilibrium part in the model for the purpose of simplicity. 2. One subunit of asparagine synthetase has two possible asparagine binding sites, glutaminase active site and synthetase active site because the space-filled model of the crystal structure of C1A mutant showed no third cavities that may bind the third asparagine molecule. Hence, the dimer form of asparagine has four possible asparagine binding sites. 3. The first asparagine binding site to the free enzyme is a glutaminase site. The first asparagine binding site is not likely to be at the synthetase domain because ammonia dependent synthetase activity is much less affected by 1 mM of asparagine than that to the inhibition glutamine dependent synthetase activity. This is also supported by the fact that asparagine is an analog of glutamine. 4. The result that k_{cat} value decreased with increasing concentrations of asparagine (Figure 4-1B) indicates that asparagine binds to enzyme-substrate (EEGln) complex. No matter how many asparagine binding sites there are in one molecules of free enzyme, the apparent k_{cat} can be deduced as:

$$k_{cat}' = \frac{1 + \frac{\gamma k_3[I]}{\gamma k_{cat} + k_4}}{1 + \frac{k_3[I]}{\gamma k_{cat} + k_4}} \times k_{cat}$$

Where γ is a factor resulting from the effect of asparagine binding on the turn over number for the reaction from AsnEEGln complex to glutamate; k_3 andn k_4 are the forward and backward rate constants for the bindiing of asparagine to enzyme-substrate complex (EEGln) respectively. By fitting γ, $\frac{k_3}{\gamma k_{cat} + k_4}$ and k_{cat} to the experimental results using KaleidaGraph, we got γ value close to zero (0 ± 0.3 mM). This means that the AsnEEGln complex is hardly turn over to glutamate. Therefore, we can simplify the model as showed in scheme 4-1B. The corresponding apparent k_{cat} is:

$$k_{cat}' = \frac{1}{1+\frac{k_3[I]}{k_4}} \times k_{cat} = \frac{1}{1+\frac{[I]}{K_{Ii}}} \times k_{cat}$$

Where K_{Ii} is the dissociation constant of AsnEEGln complex into asparagine and EEGln, which was fitted as 0.33 ± 0.04 mM; k_{cat} was fitted as 7.4 ± 0.2 s^{-1} for dimer form, consistent with the previously reported value. 5. Based on the results that apparent K_M value versus the concentration of asparagine is positively related but not a straight line, several possible models were proposed regarding the number of asparagine molecule binding to the free enzyme (Scheme 4-2). If there is only one asparagine binding site in the free enzyme (Scheme 4-2A), the apparent K_M versus the concentration of asparagine is a hyperpola when K_{Is} is different than K_{Ii}.

$$K_M' = \frac{1+\frac{[I]}{K_{Is}}}{1+\frac{[I]}{K_{Ii}}} \times K_M$$

If more than one asparagine binding sites in the free enzyme, the apparent K_M versus the concentration of asparagine is more like a polynomial line with second order for two binding sites model (Scheme 4-2B), third order for three sites (Scheme 4-2C), and so on.

$$K_M' = \frac{1+\frac{[I]}{K_{Is1}}+\frac{[I]^2}{K_{Is1}K_{Is2}}}{1+\frac{[I]}{K_{Ii}}} \times K_M \qquad \text{two binding sites model}$$

$$K_M' = \frac{1+\frac{[I]}{K_{Is1}}+\frac{[I]^2}{K_{Is1}K_{Is2}}+\frac{[I]^3}{K_{Is1}K_{Is2}K_{Is3}}}{1+\frac{[I]}{K_{Ii}}} \times K_M \qquad \text{three binding sites model}$$

Among these models, the best fit to the experimental results is the three sites model. The two sites model fits the data with the concentration of asparagine below 0.2 mM, not for higher

concentration, which implys the third order term. We could not directly get all three dissociation constants by fitting except K_{Is1} (0.09 ± 0.01 mM) and $K_{Is1}K_{Is2}K_{Is3}$ (0.0039 ± 0.0002 mM^3). However, we can estimate K_{Is2} and K_{Is3} using the fitted value of K_{Is1}. The final value for K_{Is2} and K_{Is3} are 0.7 ± 0.2 mM and 0.06 ± 0.02 mM respectively.

The model for asparagine inhibition to hASNS is much simpler since it is a competitive inhibitor to the enzyme. Only one molecule of asparagine can bind to the free enzyme. And it doesn't bind EGln complex. The inhibition constant was determined as 0.11 ± 0.02 mM.

Discussion

As mentioned above, the crystal structure of C1A mutant of ASB suggests the active form of this enzyme is dimer. This is supported by our results from chromatography studies, in which the binding of glutamine drove the enzyme to the dimer form, similar to asparagine. Based on this, we constructed the kinetic model for the asparagine inhibition to ASB. Our kinetic results and the simulated model tells us the apparent Km values of ASB for glutamine was affected significantly by the presence of asparagine and this may results from one molecule of free enzyme can binds at least three asparagine molecules. Consider the fact that no other possible asparagine binding site was found in the crystal structure of C1A mutant except the two active sites of each subunit, the simulated model further support that the active form of ASB is a dimer.

Communication between domains and/or subunits and allosteric regulation is a common phenomenon for biological macromolecules. Previous studies showed that binding of ATP at synthetase domain of ASB stimulates its glutaminase activity, indicating a communication between its two catalytic domains(*17*). In this study, asparagine stabilized the dimer form of ASB and drove the monomer/dimer equilibrium to the dimer side tells us that the interaction between subunits became stronger with asparagine binding to the enzyme, implying conformational changes and possible communication at the interface. This is also supported by

the three binding sites model for asparagine inhibition since all these asparagine binding sites are impossible in the same subunit of ASB. The inhibition mechanism of hASNS by asparagine is different from that of ASB. Aspargine is a simple competitive inhibitor for hASNS under the same experimental conditions. The SEC results showed hASNS is present as dimer at the experimental condition. Its quaternary structure was not affected by 5 mM asparagine, which is about 50 times of inhibition constant. Therefore, the two subunits work independently and do not communicate with each other.

In order to find possible structural basis for the communication during asparagine inhibition, we checked those interacting residues in the interface of the two subunits. The major interaction between the two subunits of ASB is that the guanidium group of Arg334 forms H-bonds with a loop that closes to glutaminase active site (Figure 4-6). This loop includes a cluster of absolutely conserved amino acid residues (H29R30G31P32D33), which involves in formation of ammonia tunnel. The backbone of G31 and P32 and the side chain of S35 interact with the 3 nitrogen atoms in the guanidium group of R334 (Figure 4-6A). Close to Arg334, two other residues from synthetase domain and one from glutaminase domain may also play a role in the interaction of the two subunits. Arg334 is followed by another positive residue, Lys335. Its amine group does not contact with the HRGPD loop, but exposed to bulk solution and interact with several water molecules. However, the indole ring of Trp34 from glutaminase domain of the other subunits inserts into the two long side chains of Arg334 and Lys335. With another indole ring from Trp395, a sandwich structure is formed with the side chain of Arg334 in the middle, probably helping Arg334 position correctly and forming hydrogen bonds with HRGPD loop, especially Trp395 with the indole ring parallel to the side chain of Arg334. All these residues are in highly conserved sequence region for all kinds of species, from bacterial to fungus, from plant

to mammals (Figure 4-7). It is also important to point out that the HRGPD loop has XGPXXXGX sequence. The two glycine residues make this loop more flexible to adopt different conformations. Based on sequence alignment, most of the species uses the same set of residues as *Escherichia coli*, from bacterial to plant, while mammals have different residues at the corresponding positions. In mammalian species, Trp34 is replaced by an Ala. This small side chain causes less steric hindrance compared to the indole ring of Trp34 and makes the dimer form more favorable for hASNS. Interestingly, a lysine residue in mammalian enzyme is at the corresponding position of Arg334 in ASB. The one carbon shorter side chain may suggest a closer contact between the two subunits in human enzyme. Consequently, the tryptophan 395 is changed to a smaller aromatic residue, histidine. In the HRGPD loop, no second glycine residue is present for mammalian enzyme, which has less conformational flexibility. All these differences may provide a structural basis for the different quaternary structures of ASB and hASNS and allosteric effect upon asparagine binding of ASB.

Using the inhibition models we constructed above, the apparent activity was simulated with the concentration of asparagine and glutamine varying from 0.1 mM to 2 mM for both ASB and hASNS (Figure 4-8). This ranged of concentration was selected based on the physiological concentration of glutamine and asparagine in blood, which is about 0.6 mM and 0.1 mM respectively. Here for the convenience of comparison with the glutaminase activity without any inhibition, the enzyme activity with no asparagine was also simulated, although it is impossible for cell to have no asparagine at all. The hydrolysis of glutamine is depressed significantly for both enzymes, with more inhibition effect on ASB. At concentration of 0.6 mM glutamine and 0.1 mM asparagine, about 55% of enzyme activity is lost because of product inhibition for ASB and 40% for hASNS. This means even at normal conditions, the glutaminase activity of

asparagine synthetase is suppressed significantly. If the asparagine concentration is above 0.3 mM, less than 10% activity will be left for ASB and less than 30% for hASNS. The presence of asparagine prevents the enzyme from hydrolyzing glutamine at its maximum rate and producing less toxic ammonia. As a regulator, asparagine regulates not only the function of asparagine synthetase, but also the expression of the corresponding gene (*73*). In some prokaryote cells, such as *Escherichia coli*, asparagine can be synthesized by ammonia dependent asparagine synthetase using ammonia instead of glutamine. Experimental results showed that ammonia utilizing enzyme is also regulated by asparagine through similar strategy (*74*, *75*). Like glutamine, asparagine is one of the principal and non-essential amino acids involved in the storage and transport of nitrogen. The balance between glutamine and asparagine is directly affected by this enzyme. Recently, the regulatory patterns of asparagine synthetases in *Helianthus annuus* (sunflower) were reported by Herrera-Rodríguez et al (*76*-*79*). Three genes encode asparagine synthetase, HAS1, HAS1.1 and HAS2. The expression of these genes is regulated by light, carbon and nitrogen availability with different sensitivities. The asparagine level is higher than glutamine during germination and cotyledon senescence. During these stages, most of asparagine synthetases was encoded from HAS2. For leaf senescence, all three genes work together and the asparagine level is lower than glutamine. These results imply the importance of asparagine synthetase in keeping the relative asparagine and glutamine level.

Conclusions

Product inhibition of asparagine synthetase is a common strategy in all species to regulate the conversion from glutamine to asparagine. However, the inhibition mechanism for *Escherichia coli* ASB is different from that of hASNS. The multi-site inhibition to ASB by asparagine and the changes of its quaternary structure after asparagine binding suggest conformational changes at the interface of the two subunits and communications between them.

Under same conditions, hASNS showed no such properties. At room temperature, ASB and hASNS showed different quaternary structure. The former is a mixture of dimer and monomer with equilibrium between these two forms, while the latter presents as dimer. This structural difference may result from the different residues at the interface of the subunits. The flexible conformation of ASB provides the structural basis for allosteric communication. Glutamine and asparagine are the two major sources to storage and transport nitrogen in *vivo*. The regulation of the reaction that synthesizes asparagine from glutamine by asparagine inhibition may have important physiological meanings.

Scheme 4-1

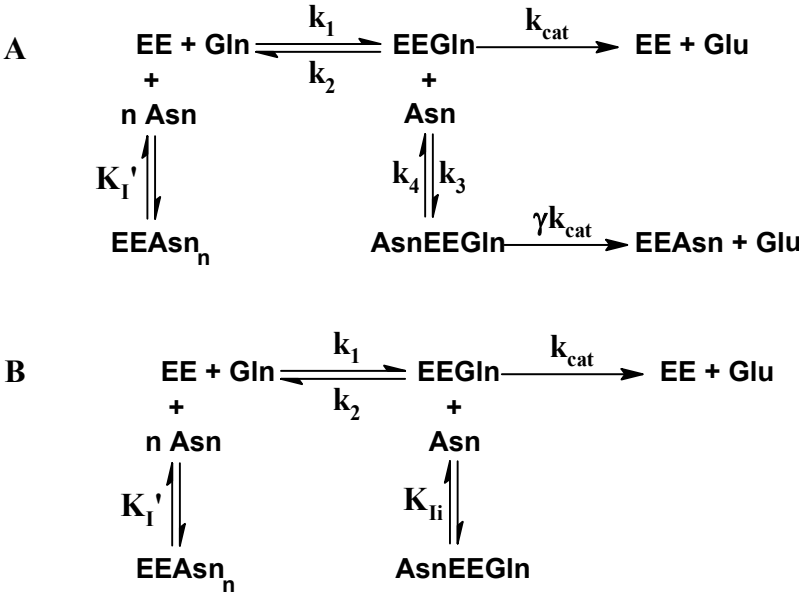
A
EE + Gln
k1
k2
EEGln
kcat
EE + Glu
+
n Asn
+
Asn
KI'
k4
k3
EEAsnn
AsnEEGln
γkcat
EEAsn + Glu
B
EE + Gln
k1
k2
EEGln
kcat
EE + Glu
+
n Asn
+
Asn
KI'
KIi
EEAsnn
AsnEEGln

Scheme 4-2

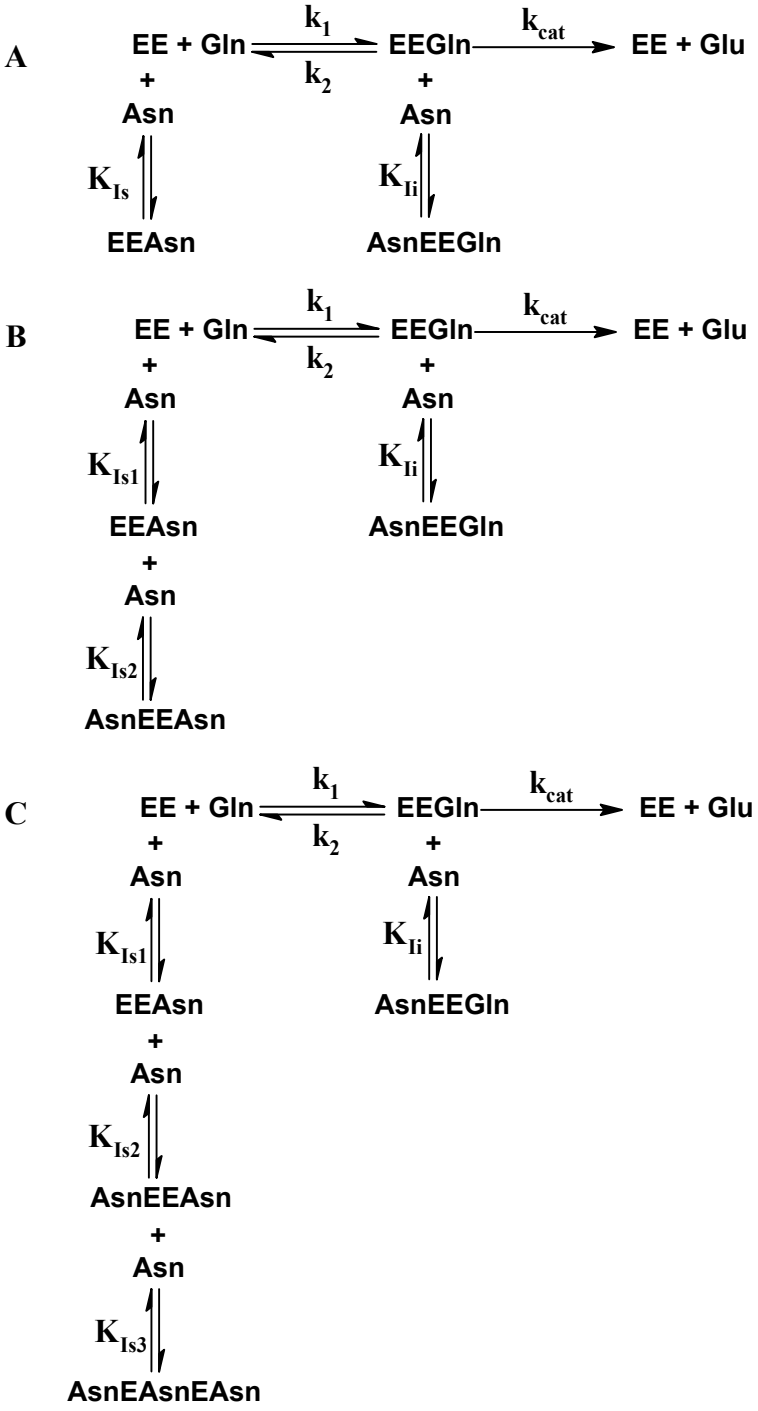
A
EE + Gln
k1
k2
EEGln
kcat
EE + Glu
+
Asn
KIs
EEAsn
KIi
AsnEEGln
B
EE + Gln
k1
k2
EEGln
kcat
EE + Glu
+
Asn
KIs1
EEAsn
KIi
AsnEEGln
+
Asn
KIs2
AsnEEAsn
C
EE + Gln
k1
k2
EEGln
kcat
EE + Glu
+
Asn
KIs1
EEAsn
KIi
AsnEEGln
+
Asn
KIs2
AsnEEAsn
+
Asn
KIs3
AsnEAsnEAsn

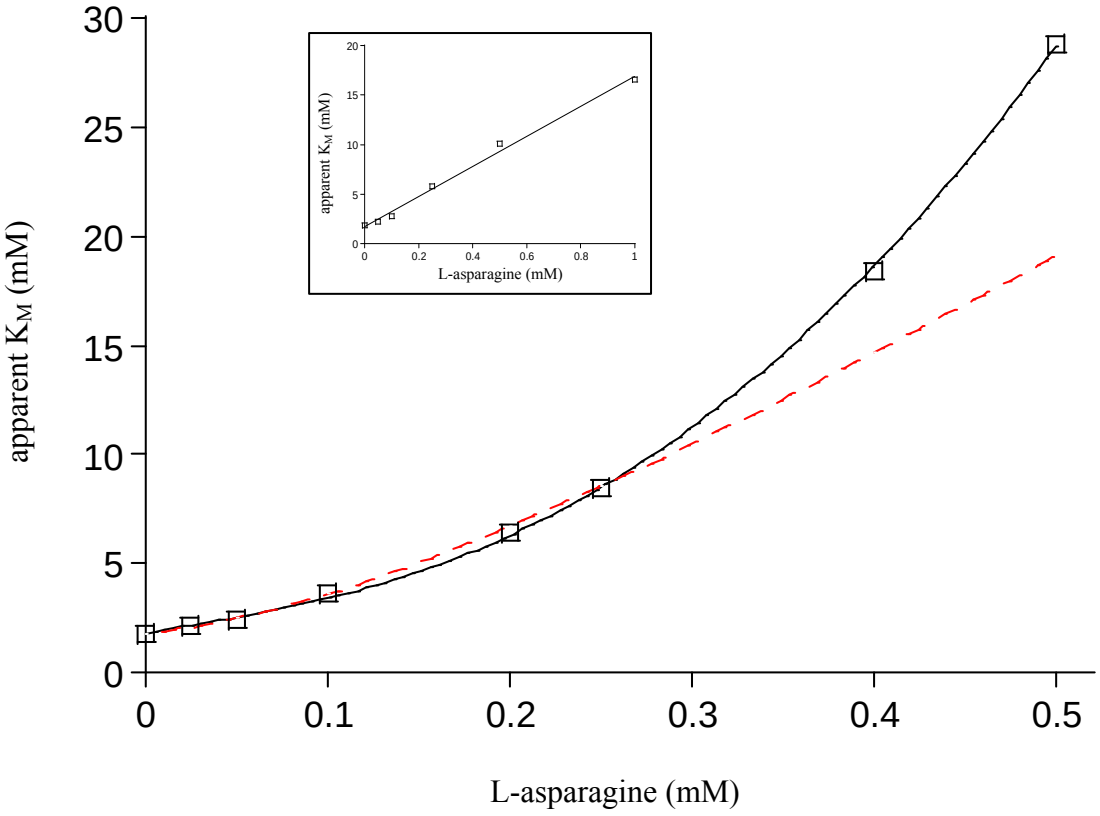

Figure 4-1. Kinetic studies of asparagine inhibition to ASNS
A. apparent K_M (mM) vs [Asn] mM

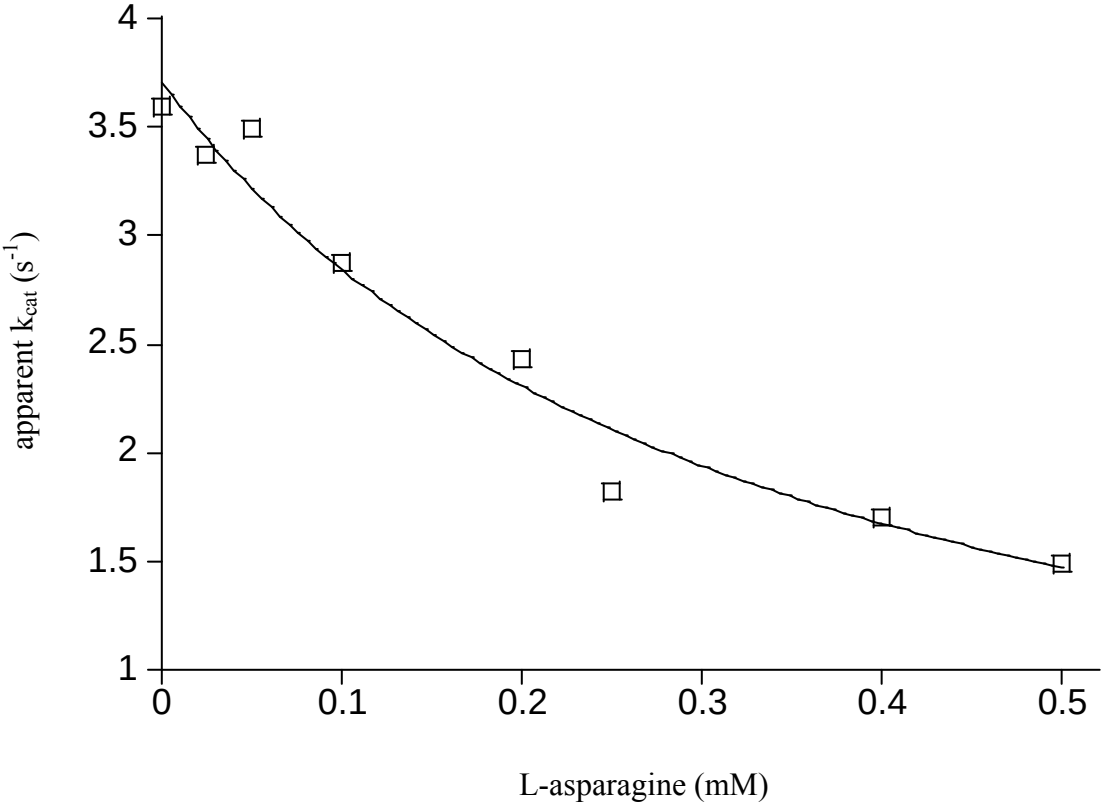

Figure 4-1 B. apparent k_{cat} (s^{-1}) vs [Asn] mM

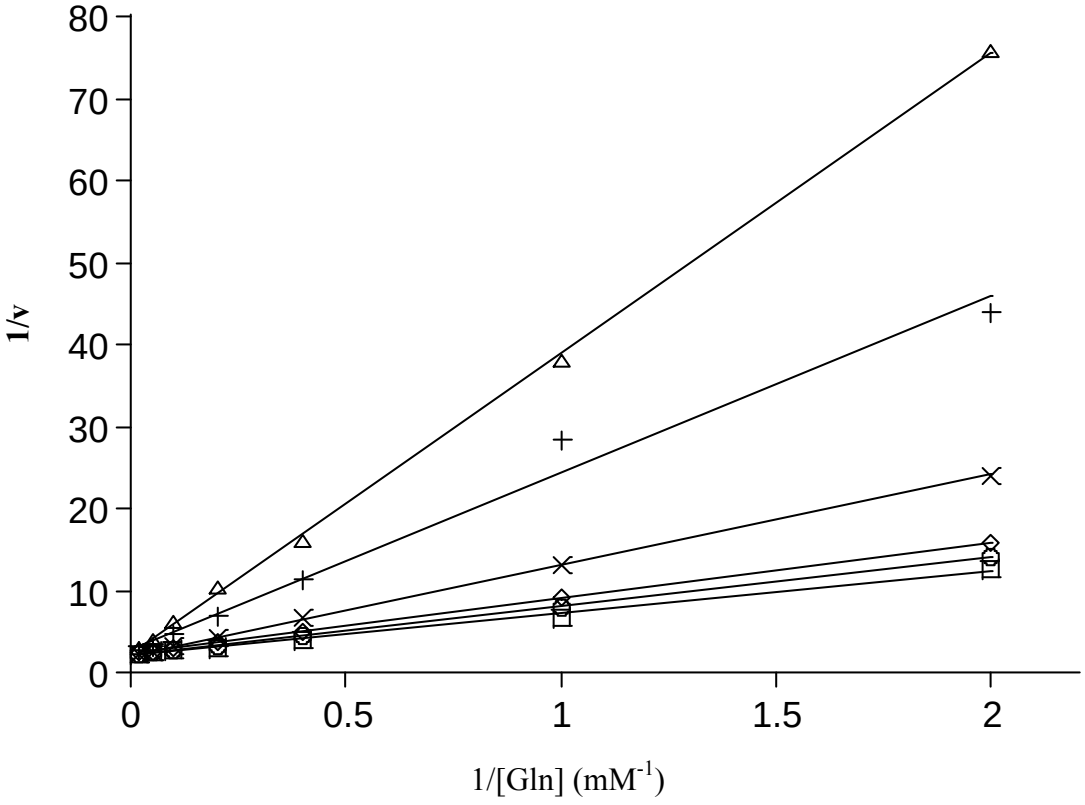

[Asn]: 0, 0.05, 0.1, 0.25, 0.5, 1 mM

Figure 4-1 C. 1/v vs [Gln] mM^{-1}

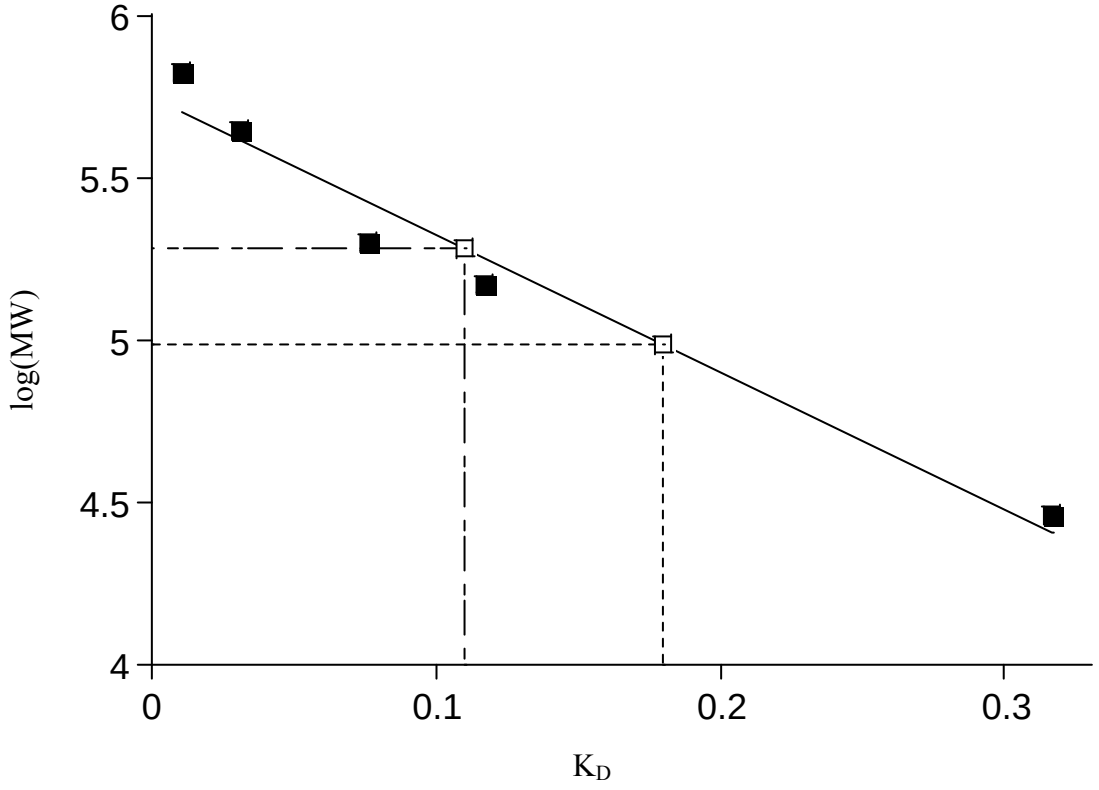

Figure 4-2. SEC standard curve: log(MW) vs K_D

$$K_D = \frac{V_e - V_o}{V_c - V_o}$$

V_e is elution volume; V_c is column volume; V_o is void volume

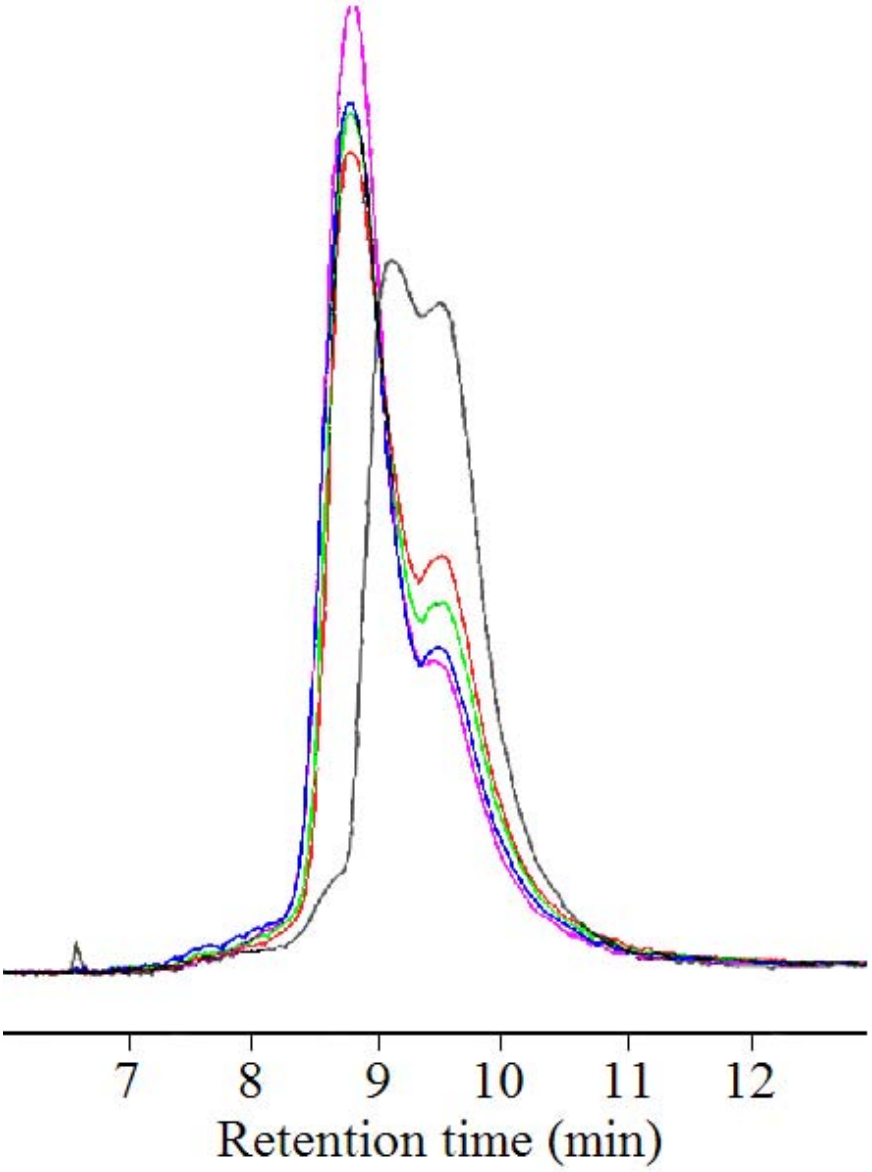

Figure 4-3. SEC analysis of quaternary structure of ASNS with different concentration of asparagine in mobile phase
A. SEC analysis of quaternary structure of ASB

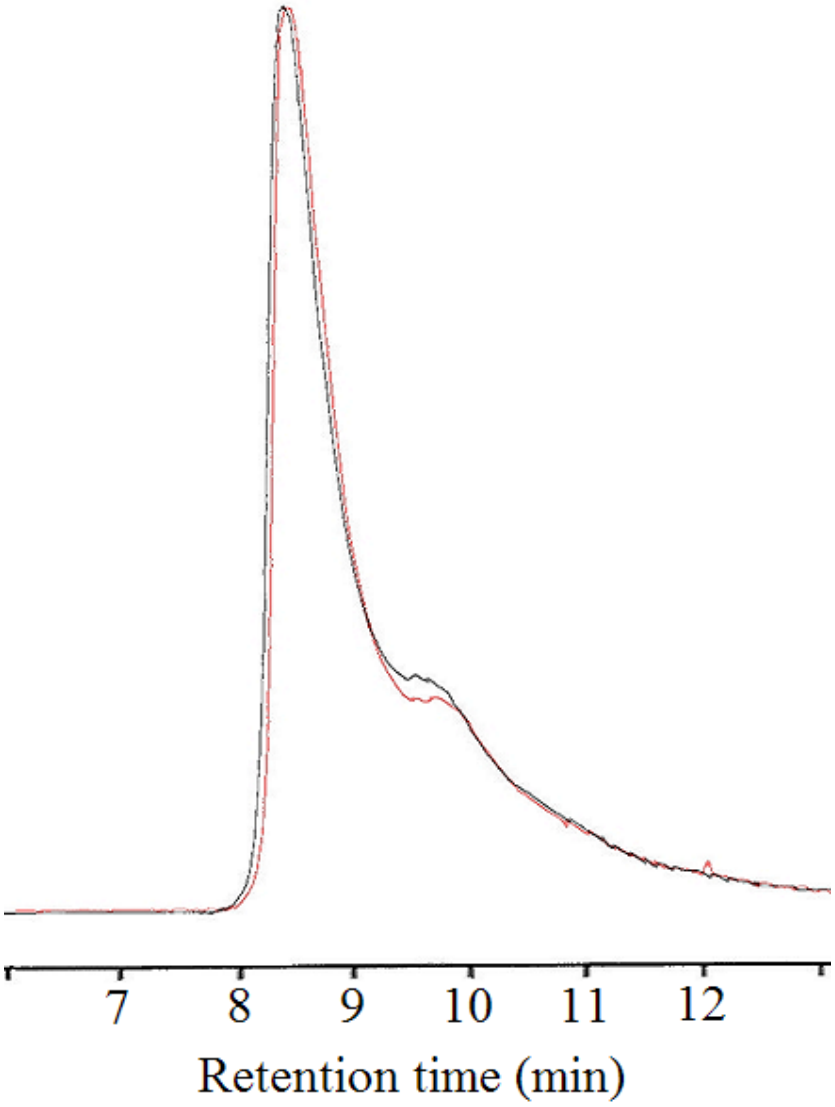

Figure 4-3 B. SEC analysis of quaternary structure of hASNS with (black) or without 5 mM asparagine (red) in mobile phase

Table 4-1. Retention time of ASB peaks in SEC studies

The peaks of ASB and their retention time (RT) with/without asparagine in mobile phase

[Asn] mM	R.T. (min)					
	Peak 1	Average (min)	Peak2	Average (min)	Peak3	Average (min)
0	9.410		9.086			
0	9.485		9.098			
0	9.458		9.131			
0	9.551	9.51 ± 0.06	9.180	9.15 ± 0.05		
0	9.596		9.225			
0	9.551		9.200			
0	9.498		9.146			
0.10	9.561				8.861	
0.10	9.556				8.873	
0.25	9.546				8.831	
0.25	9.516				8.801	
0.50	9.491				8.771	
0.50	9.481	9.49 ± 0.05			8.768	8.79 ± 0.05
1.0	9.520				8.800	
1.0	9.493				8.788	
5.0	9.416				8.726	
5.0	9.410				8.748	
5.0	9.425				8.713	

Table 4-2. The calculated MW and predicted structure of ASB corresponding to each peak

Mobile phase	With Asn	Without Asn	With/without Asn
R.T. (min)	8.79	9.15	9.50
Calculated MW (kD)	171	120	85
Possible structure	Dimer	Quick exchange between dimer and monomer form	Monomer
True MW (kD)	125	-	62.5
Calc. MW/true MW	1.37	-	1.36

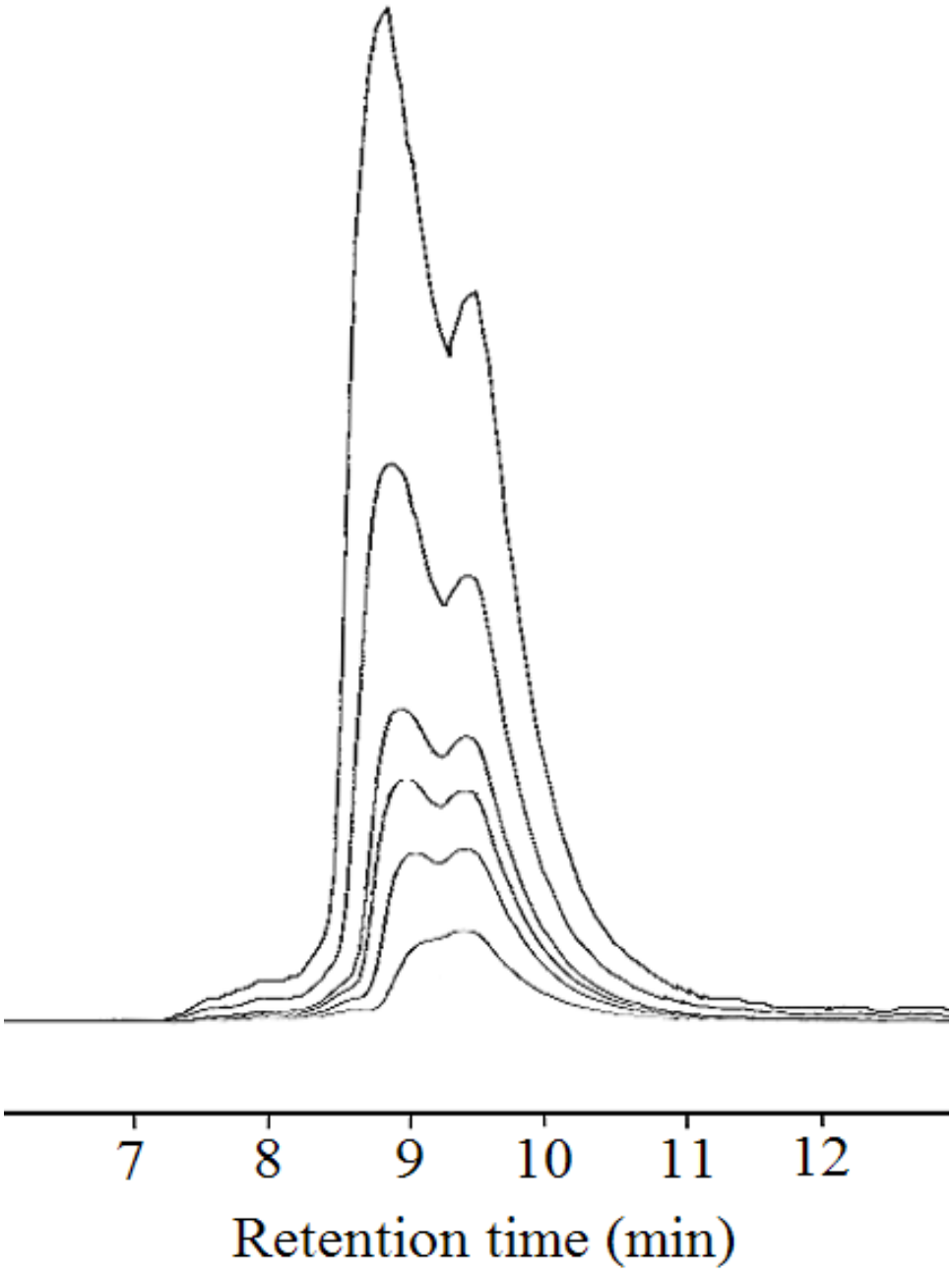

Figure 4-4. SEC analysis of quaternary structure of ASB with different amount of enzyme injected (2.5-40 μL)

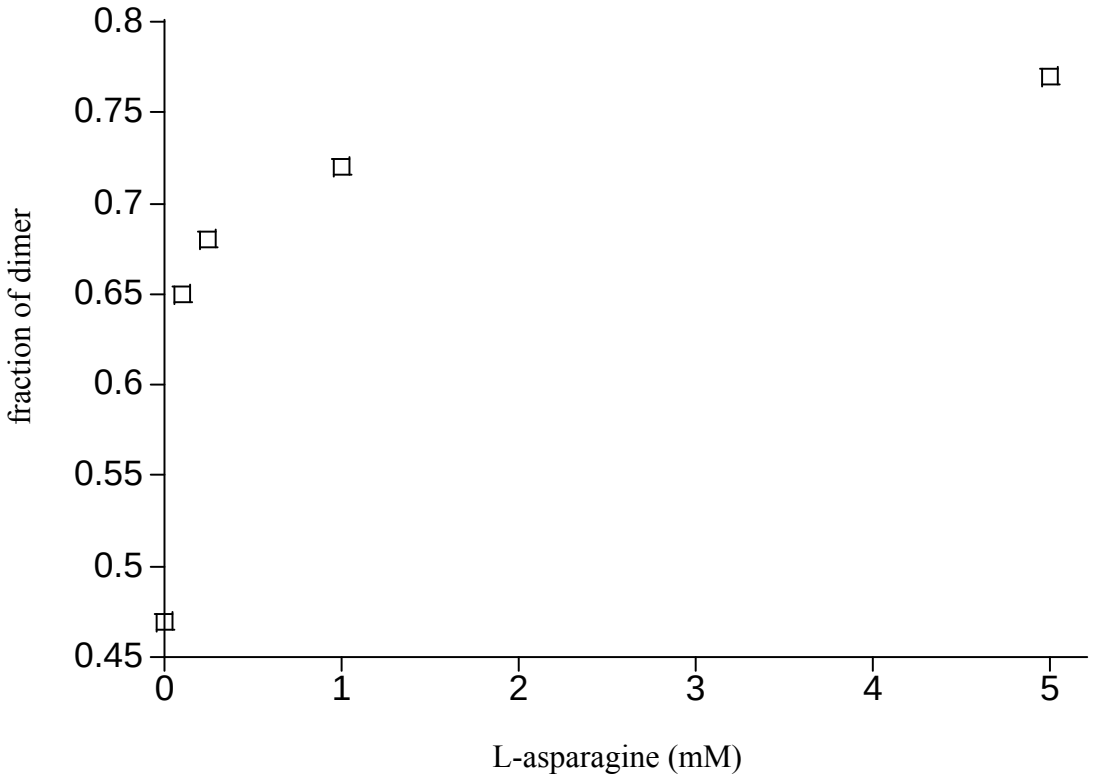

Figure 4-5. Fraction of dimer vs concentration of asparagine

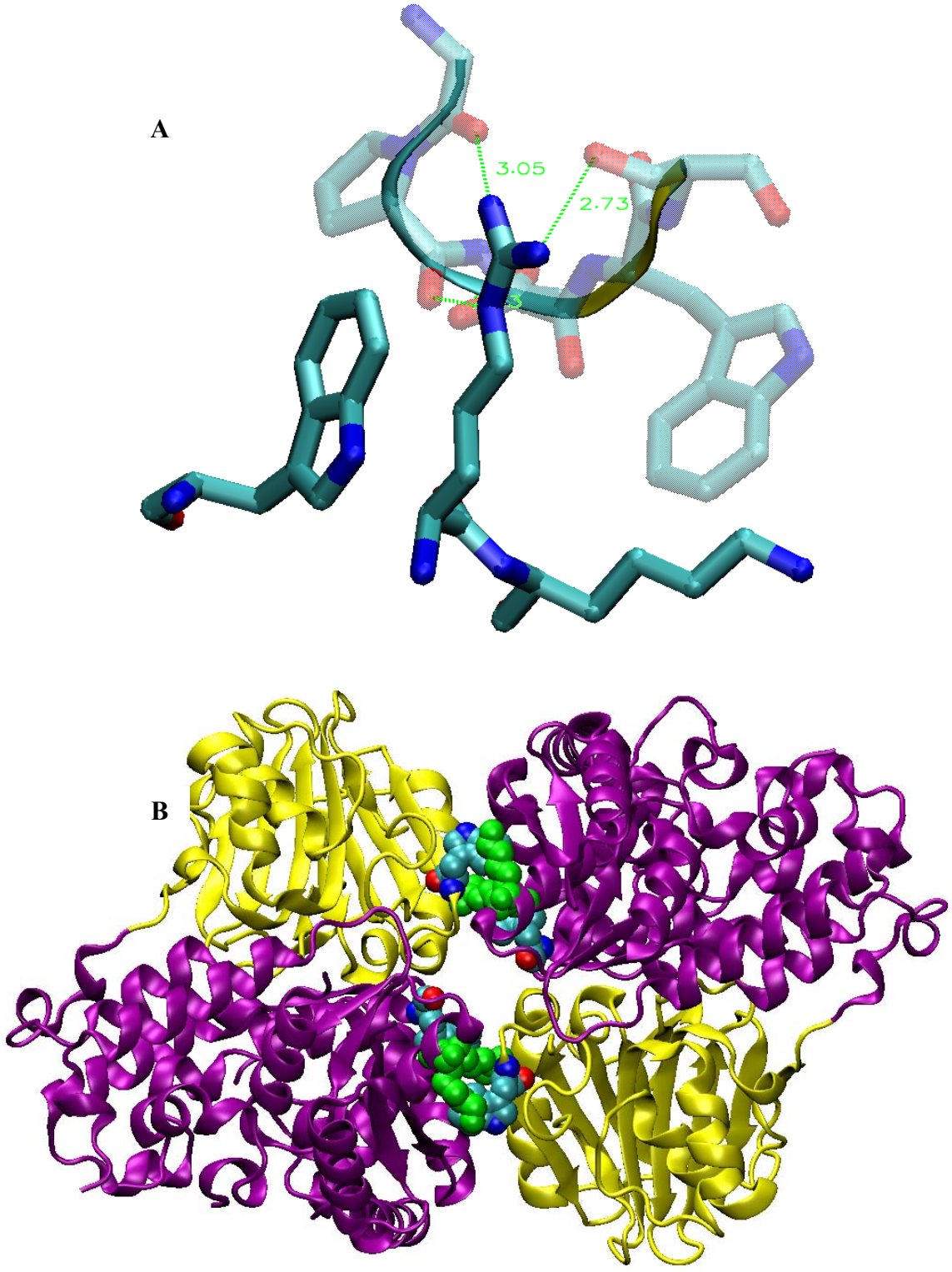

Figure 4-6. The interface of the two subunits

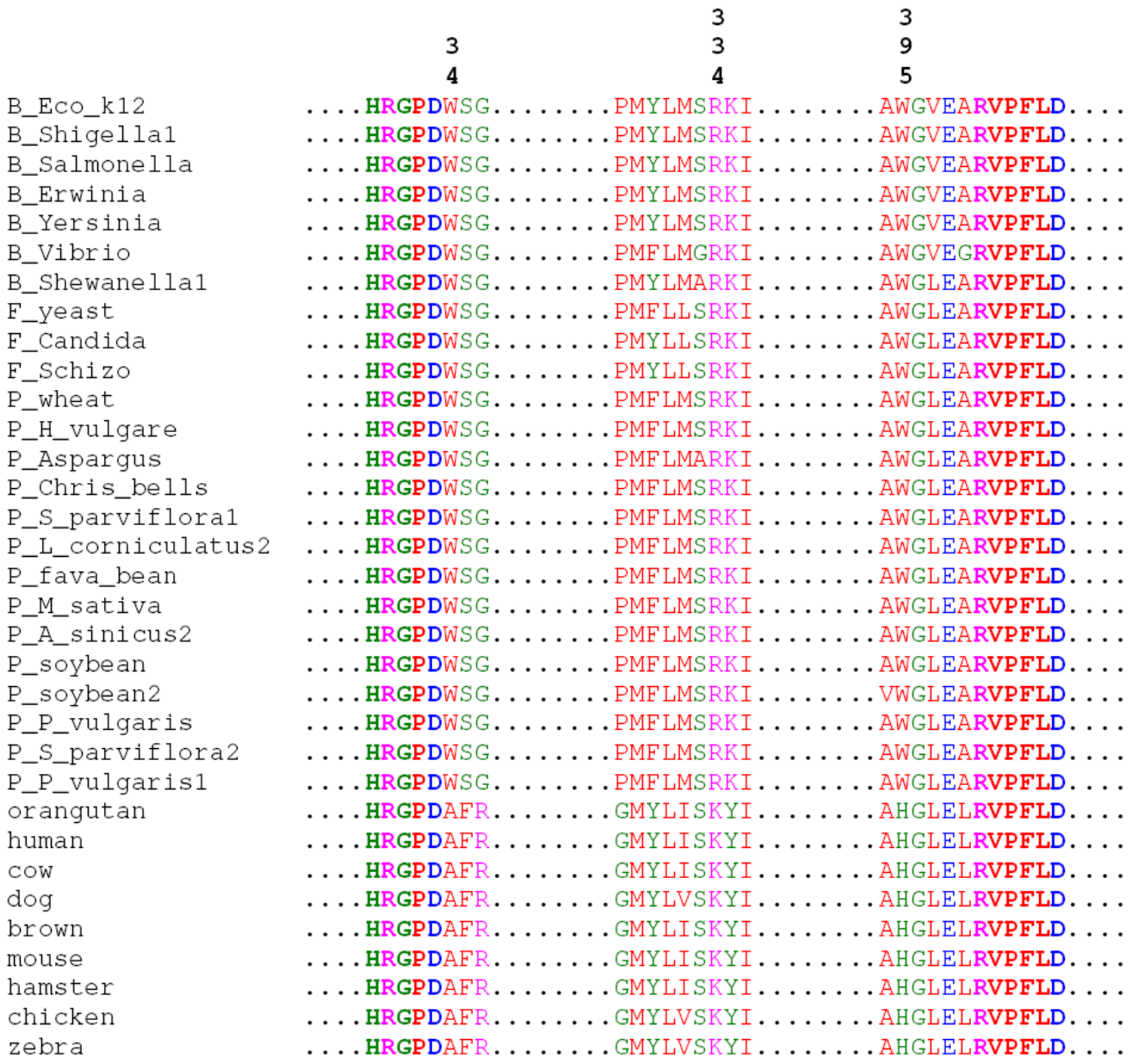

Figure 4-7. Sequence alignment of the interface residues

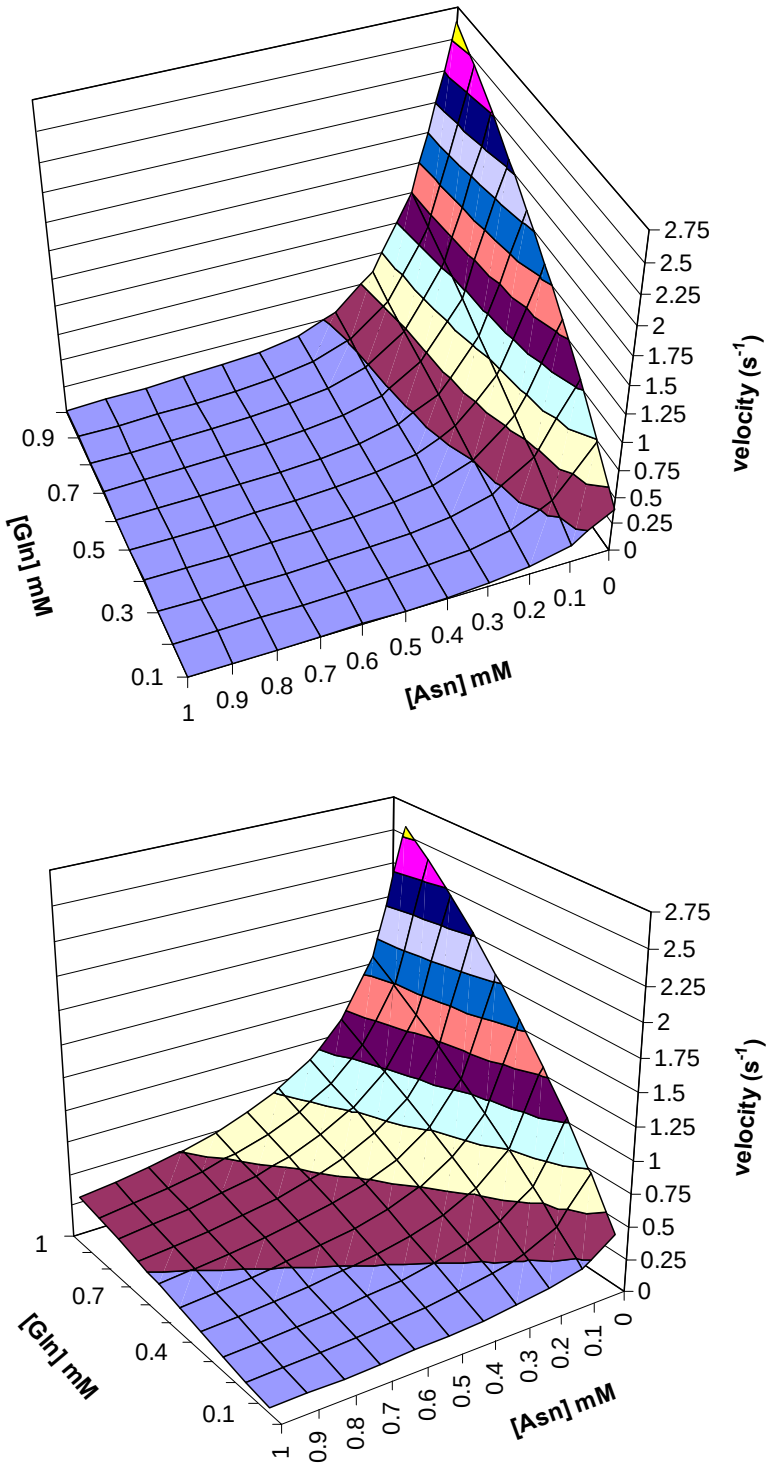

Figure 4-8. The glutaminase activity of ASNS around physiological conditions

CHAPTER 5
THE UTILIZATION OF DIFFERENT NITROGEN SOURCES BY ASPARAGINE SYNTHETASE: EVOLUTION FROM *Escherichia coli* TO HUMAN

Introduction

Glutamine-dependent asparagine synthetase (EC 6.3.5.4) catalyzes ATP-dependent synthesis of asparagine from aspartate, utilizing either glutamine or ammonia as nitrogen source. For more than 15 years, the mechanisms of enzymatic reaction and ammonia tunneling by asparagine synthetase was extensively studied using asparagine synthetase B from *Escherichia coli*. Furthermore, due to the difficulties in expression of human asparagine synthetase (hASNS), ASB also served as a model system for designing inhibitor of asparagine synthetase, since the amount of human asparagine synthetase is directly related to the resistance of leukemia cell to the asparaginase chemotherapy. So far, only one crystal structure was resolved for the C1A mutant of ASB. It is a homodimer with two active sites in each subunit. The two sites, glutaminase site and synthetase site, are separated with an intramolecular tunnel that is about 20 Å long. The way substrates bind to the active sites is like from back door and front door. Glutaminase site is a αββα four layer sandwich structure, which is common in the class II glutamine dependent amidotransferase. The synthetase site consists mostly of α-helices. Human enzyme has 37% identity to ASB based on their primary structure. And most of the functional residues, including those in the active sites and those tunnel residues for ammonia channeling, are conserved in both enzymes. Both hASNS and ASB are supposed to have same catalytic mechanism and overall structure. On the other hand, since they are from different sources, one from bacterial, the other from human, the two enzymes are evolutionarily different from each other. With more studies on hASNS after it was successfully prepared using a baculovirus expression system in Richards' lab (*57*), more results showed the differences between them. In

previous chapter, studies about asparagine inhibition showed different regulatory mechanisms to the glutaminase activity of hASNS and ASB. Asparagine inhibits the glutaminase activity of hASNS by a simple competitive mechanism to glutamine, while it regulates the glutaminase activity of ASB through a cooperative binding mechanism. The first binding constant is close to that of hASNS, implying asparagine binds to the same active site first in both enzymes. Consequently, asparagine has higher inhibition effect on ASB due to consecutively binding of three asparagine molecules to the enzyme. Since ASB is a homodimer and each subunit has only two possible asparagine binding sites, the cooperative binding of three asparagine molecules suggests the communications between the two subunits, as well as between the two domains. In the latter case, the binding of asparagine to the glutaminase active site affects synthetase site. Furthermore, ATP itself, or ATP with aspartate, stimulates the glutaminase activity of ASB, which support the idea that the two catalytic domains communicate with each other and substrate binding to synthetase site results in the changes in the glutaminase site. Therefore, the communication between the two domains in ASB is two-way effect. The studies on the quaternary structure of ASB showed that the asparagine binding stimulates dimerization, implying the conformational changes for the interface residues between the two subunits. This may provide the structural basis for the inter-subunit communication. As for hASNS, its glutaminase activity is further decreased with both ATP and aspartate present (Beeson, unpublished results). The communication between the two domains is from synthetase site to glutaminase site. The results about asparagine binding showed no communication from glutaminase site to synthetase site. This is also supported by the fact that asparagine binding did not change the quaternary structure of human enzyme. In this Chapter, I investigated the utilization of two different nitrogen sources, glutamine or ammonium, by hASNS using the new

developed NMR assay. Compared with the results of ASB, I will discuss the evolutionary differences between hASNS and *Escherichia coli* enzyme (ASB).

Material and Methods

The experiments were performed as described in Chapter 2 Materials and Methods part.

Materials

See Chapter 2 Materials and Methods part. Recombinant, wild type hASNS was expressed and purified following literature procedures (*57*).

Competition Experiment

Reaction mixtures consisted of 100 mM HEPPS buffer (pH 8.0), 60 mM $MgCl_2$, 10 mM ATP, 20 mM aspartate and different concentrations of $^{15}NH_4Cl$ (pH 8.0) or glutamine in total volume of 2 mL. In experiments where the concentration of $^{15}NH_4Cl$ (pH 8.0) was varied as 10 mM, 25 mM, 50 mM, 75 mM and 100 mM, L-glutamine was fixed at 20 mM. Alternatively, when L-glutamine was varied as 0 mM, 2.5 mM, 5mM, 10 mM, 20 mM and 40 mM, $^{15}NH_4Cl$ was added at an initial concentration of 100 mM. Reactions were initiated by the addition of hASNS (18 μg) and the resulting samples incubated for 10 min at 37 ^{o}C before being quenched by the addition of trichloroacetic acid (TCA) (60 μL). After centrifugation for 5 min at 3000 rpm to remove precipitated protein, the supernatant was adjusted to pH 5 by the addition of 10 M aq. NaOH and an aliquot of this solution (650 μL) transferred to a 5 mm NMR tube for analysis. At higher pH values, amide NH exchange precluded the derivation of any quantitative relationship between peak area and ^{15}N-Asn concentration. The standard samples contained 100 mM HEPPS buffer (pH 8.0), 60 mM $MgCl_2$, 10 mM ATP, 100 mM $^{15}NH_4Cl$ (pH 8.0), 20 mM glutamine and different concentrations of ^{15}N-L-Asn from 0.05 mM to 2.5 mM, without adding hASNS.

NMR Measurements, HPLC assay and Kinetic Simulations

See Chapter 2 Materials and Methods part.

Results and Discussion

When both ammonium and glutamine are present in the reaction mixture, the two nitrogen sources compete with each other for the β-aspartyl-AMP intermediate to produce asparagine. If $^{15}NH_4^+$ and ^{14}N-glutamine are used, the ability of utilization of different nitrogen source by hASNS and the efficiency of ammonia transfer can be investigated by quantification of ^{15}N-asparagine, produced from $^{15}NH_4^+$, and ^{14}N-asparagine, from glutamine, using the new developed NMR assay, combining with HPLC assay reported before (Fig. 5-1).

As shown in Table 5-1, the incorporation of ^{15}N into asparagine is increased with more $^{15}NH_4^+$ present in the solution, with constant concentration of glutamine (20 mM). The ^{14}N-asparagine/^{15}N-asparagine ratio dropped down from 4.6 to 0.4. When the concentration of $^{15}NH_4Cl$ was fixed as 100 mM, at low concentration of glutamine, the ^{14}N-asparagine produced increased with glutamine. Unfortunately, due to the low amount of ^{14}N-Asn, the error is big. However, we can see the positive relationship between the concentration of glutamine and the ^{14}N-Asn/^{15}N-Asn ratio. While at high concentration of glutamine, the ratio droped down, which suggests that the production of ^{14}N-Asn slowed down, based on the results that ammonia dependent synthetase activity keep constant. This may result from the inhibition to the glutaminase acitivity of this enzyme. Both glutamine and asparagine are potential inhibitors. The glutamine inhibition (substrate inhibition) was oberserved when I determined kinetic parameters for its glutaminase activity by varing the concentration of glutamine (0-80 mM), which suggest that a second molecule of glutamine binds to the enzyme and inhibits its glutaminase activity. Previous work also showed that asparagine is a good inhibor to its glutaminase activity with K_I value of 120 μM. However, under 1 mM concentration, the inhibition appears competitive to glutamine and didn't affect k_{cat} value. Since the total production of asparagine is less than 0.5

mM, and relatively small compared to the concentration of the substrate, this inhibition is very likely caused by glutamine inhibition.

As described in Chapter 2, if ammonia can not access the active site with the presence of glutamine, all the asparagine would be ^{14}N product at saturating concentration of glutamine. In this case, free ammonia is suppressed by glutamine. The ratio of ^{14}N asparagine to ^{15}N asparagine would be infinite. This ratio will be decreasing with the extent of suppression becomes less. When there is no suppression at all, the $^{14}NH_3$ will compete with $^{14}NH_3$ freely. If ammonia tunneling is fast and efficient enough, then the ratio of ^{14}N asparagine to ^{15}N asparagine would be determined by the ratio of production rates using ammonia and glutamine. That is,

$$\frac{[^{14}N-Asn]}{[^{15}N-Asn]}=\frac{v_{14}}{v_{15}}=\frac{(k_{cat}/K_{m-tunneling})[\mathrm{Gln}][E]_{G\ln}}{(k_{cat}/K_{m-binding})[^{15}NH_3][E]_{NH_3}}\propto\frac{[\mathrm{Gln}][E]_{G\ln}}{[^{15}NH_3][E]_{NH_3}}\approx\frac{[\mathrm{Gln}][E]_{G\ln}}{[^{15}NH_3]_i[E]_{NH_3}}$$

Therefore,

$$\frac{[^{14}N-Asn]}{[^{15}N-Asn]}\propto\frac{[G\ln][E]_{G\ln}}{[^{15}NH_3]_i[E]_{NH_3}}\ \text{or}\ \frac{[^{15}N-Asn]}{[^{14}N-Asn]}\propto\frac{[^{15}NH_3]_i[E]_{NH_3}}{[G\ln][E]_{G\ln}}$$

Where,

$[E]_{NH_3}$ is the enzyme form that can bind exogenous ammonia and produce asparagine.

$[E]_{G\ln}$ is the enzyme form that can bind glutamine and produce asparagine.

Alternatively, if the tunnel is not efficient, the ratio of ^{14}N asparagine to ^{15}N asparagine would decreases. Most of the asparagine would be labeled form and the ratio of $^{14}N/^{15}N$ in asparagine would be close to zero if the $^{14}NH_3$ intermediate leaks and equilibrates with $^{15}NH_3$ from bulk solution, since $[^{15}NH_3]$ was much bigger than $[^{14}NH_3]$.

The kinetic model was constructed based on the assumption that glutamine competes with exogenous ammonium, which includes 1) asparagine inhibition, 2) glutamine inhibition, and 3)

competition between ^{14}N source and ^{15}N source (Figure 5-2). The inhibition constants for aspargine and glutamine were set to 120 μM and 120 mM respectively. The simulation results were consistent with the experimental results (Figur 5-3AB), which support the hypothesis that glutamine is a competitive substrate to exgenous ammonium and the ammonia tunneling is fast and efficient enough in hASNS so that ammonia intermediate produced from the hydrolysis of glutamine is competing with $^{15}NH_3/^{15}NH_4^+$. The binding of glutamine did not suppress the utilization of ammonium by hASNS.

Compared with the results of ASB, hASNS showed less preference of using glutamine as nitrogen source. Under the same experimental conditions, the ^{14}N-Asn/^{15}N-Asn ratio in the ASB catalyzed reaction is bigger than that in hASNS catalyzed reaction (Figure 5-4A), or inversely, the ^{15}N-Asn/^{14}N-Asn ratio is less (Figure 5-4B). Relatively less ^{15}N was incorporated into asparagine by ASB, suggesting more preference to glutamine by ASB relative to human enzyme. The presence of glutamine partially suppresses the utilization of exogenous ammonia by ASB. In another word, ASB prefers using glutamine than ammonium, while human enzyme is more capable of using ammonium as nitrogen source to synthesize asparagine than ASB. This difference may evolve from the need of utilizing different nitrogen sources. In *Escherichia coli*, both ammonia dependent and glutamine dependent asparagine synthetase were discovered. The two enzymes have little similarities in structure and not evolutionary related (*11*). The ammonia dependent asparagine synthetase (ASA), encoded from *asnA*, can only use ammonium as nitrogen source. And glutamine dependent asparagine synthetase (ASB) can use both ammonium and glutamine, with a preference of glutamine. In human cell, only glutamine dependent asparagine synthetase was found, which is homologous to the *Escherichia coli* enzyme, ASB. The human enzyme can also use both ammonium and glutamine, with higher ability for using

ammonium, relative to ASB. Since no ammonia dependent asparagine synthetase was found in human genome, this kinetic difference may result from the need of ammonia utilizing enzyme in human cells. During the process of evolution, human enzyme gradually developed more ability to utilize exogenous ammonium, and kept its glutamine dependent asparagine synthetase activity, while ASB functions mainly as glutamine dependent enzyme since *Escherichia coli* cell can express ammonia dependent asparagine synthetase.

Conclusions

The studies on human asparagine synthetase showed that when both ammonia and glutamine are present in the reaction mixture, ammonia competes freely with glutamine as the nitrogen source. The simulated results based on this study are consistent with the experimental results. In previous chapter, *Escherichia coli* asparagine synthetase showed partial suppression of ammonia by glutamine. Compared to hASNS, the bacterial enzyme has higher preference to use glutamine, and relatively less preference of ammonia. This may result from evolution due to the fact that in *Escherichia coli*, there is ammonia dependent asparagine synthetase. It is not necessary for glutamine dependent enzyme to utilize ammonia. However, no ammonia dependent AS was found in human cells. The human enzyme may function as both ammonia and glutamine dependent enzyme during the evolution.

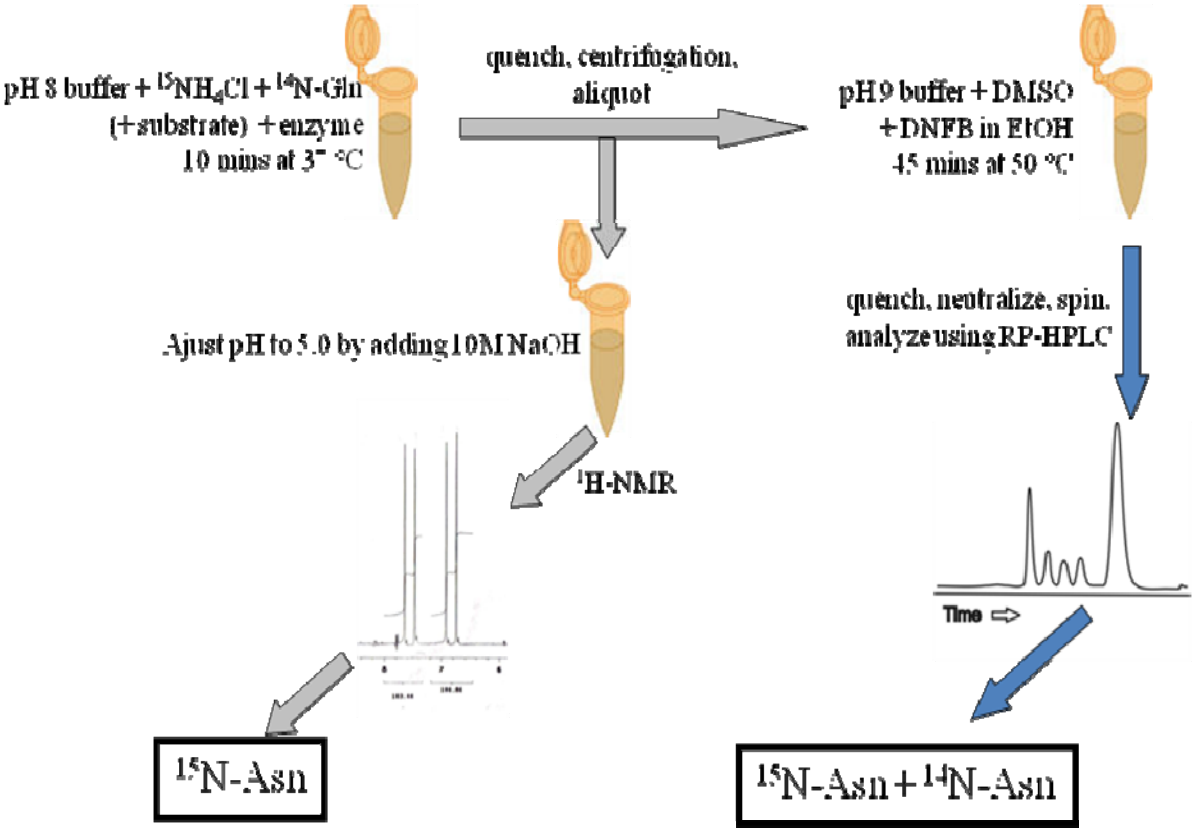

Figure 5-1. Quantification of ^{15}N-asparagine and ^{14}N-asparagine using NMR assay and HPLC assay. The enzyme can use both $^{15}NH_4Cl$ and ^{14}N-glutamine as nitrogen source. With both in the reaction mixture, both ^{15}N-asparagine and ^{14}N-asparagine were produced. The amount of ^{15}N-asparagine produced can be directly determined using NMR assay. The total amount of asparagine can be quantified by HPLC assay. The difference is the amount of ^{14}N-asparagine produced.

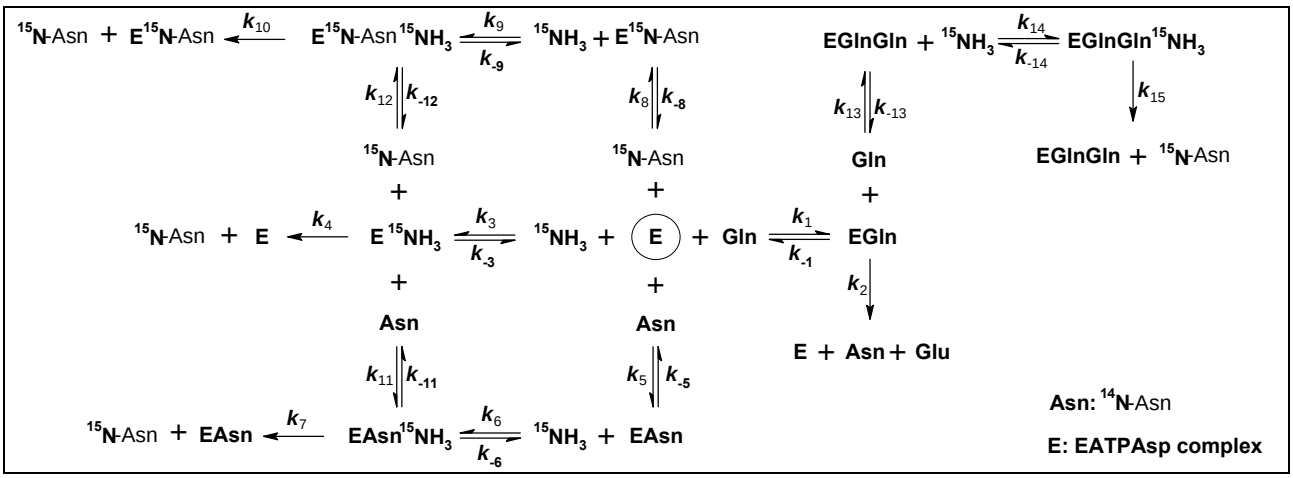

Figure 5-2. Simulation model for the competition reactions catalyzed by hASNS.

A)

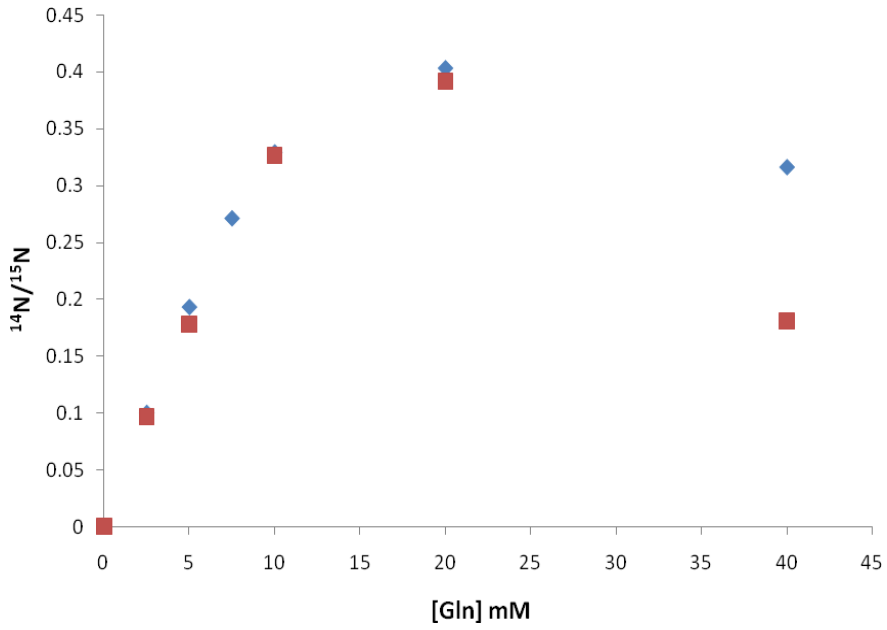

B)

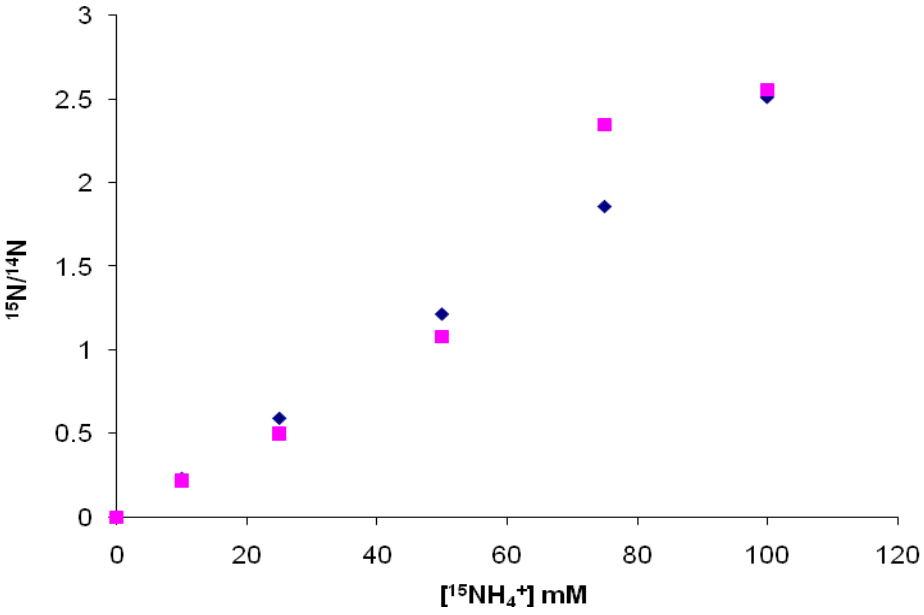

Figure 5-3. Simulations of competition reactions catalyzed by hASNS. A) varing glutamine, brown square: experimental results; blue, simulation. B) varing ammonium, blue: simulation; purple square: experimental

A)

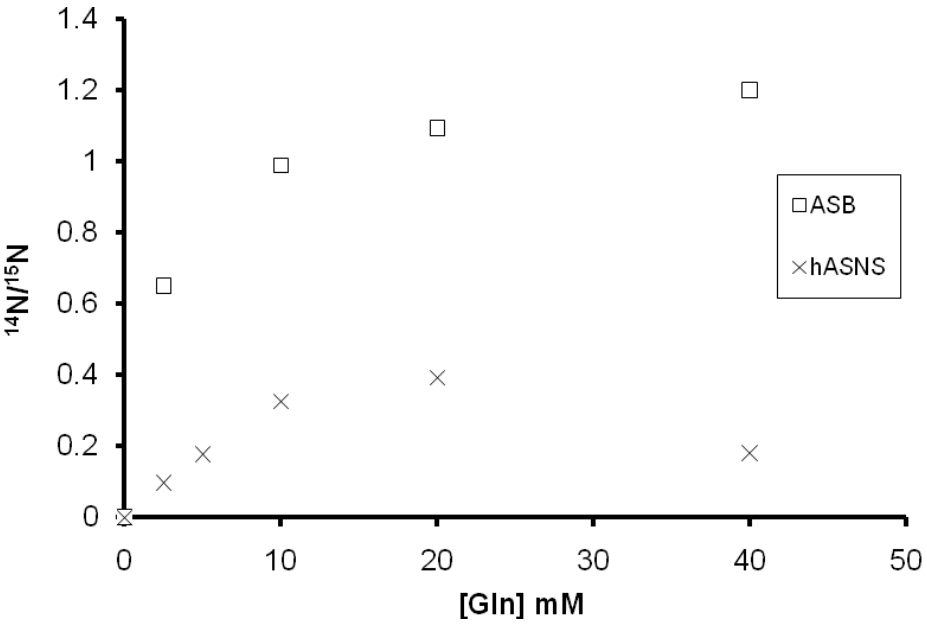

B)

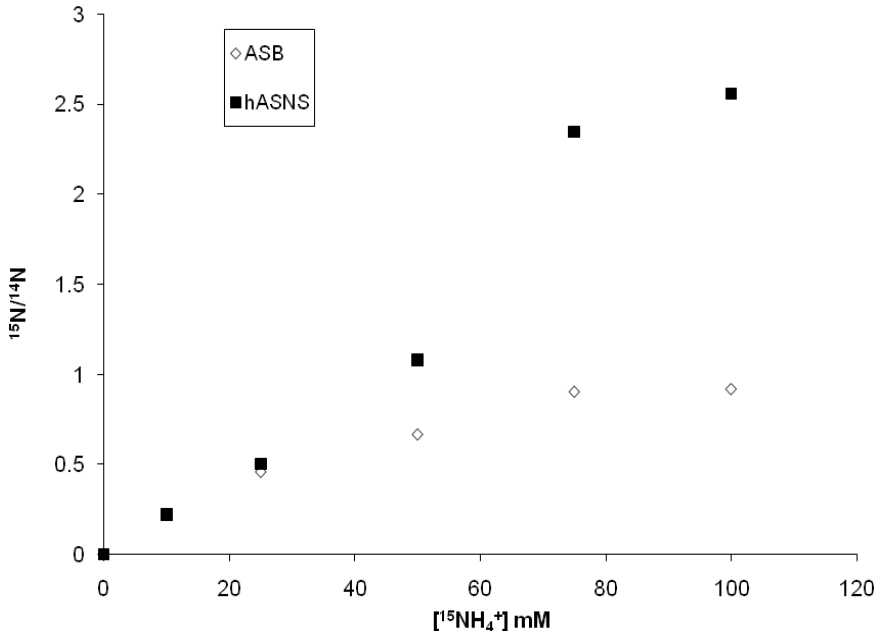

Figure 5-4. Utilization of ammonia and glutamine as nitrogen source by ASB and hASNS. In general, ASB showes higher preference to use glutamine as nitrogen source. A) varing glutamine, square: ASB; cross, hASNS. B) varing ammonium, blank diamond: ASB; square: hASNS

Table 5-1. hASNS catalyzed production of ^{15}N into L-asparagine in the steady-state competition assays.[a]

Gln (mM)	$^{15}NH_4Cl$ (mM)	^{15}N-Gln (mM)[b]	^{15}N-Asn (mM)[b,c]	Total Asn (mM)[d]	^{14}N-Asn/^{15}N-Asn
0	100	ND[e]	0.21 ± 0.02	0.215± 0.009	0
2.5	100	0.025 ± 0.004	0.19 ± 0.05	0.21± 0.02	0.1 ± 0.2
5.0	100	0.05 ± 0.02	0.21 ± 0.03	0.244 ± 0.007	0.2 ± 0.2
10	100	0.060 ± 0.002	0.21 ± 0.02	0.28 ± 0.02	0.3 ± 0.1
20	100	0.054 ± 0.006	0.198 ± 0.006	0.28± 0.02	0.4 ± 0.1
40	100	0.07 ± 0.01	0.228 ± 0.003	0.269 ± 0.002	0.2 ± 0.02
20	0	ND[e]	ND[e]	0.105 ± 0.004	NA[e]
20	10	ND[e]	0.031 ± 0.005	0.175 ± 0.002	4.6 ± 0.7
20	25	ND[e]	0.074 ± 0.010	0.222 ± 0.009	2.0 ± 0.3
20	50	0.02 ± 0.01	0.14 ± 0.02	0.26 ± 0.02	0.9 ± 0.2
20	75	0.047 ± 0.002	0.1721 ± 0.0007	0.25 ± 0.02	0.4 ± 0.1
20	100	0.054 ± 0.006	0.198 ± 0.006	0.28 ± 0.02	0.4 ± 0.1

[a] All reactions contained 10 mM MgATP, 20 mM aspartate, 60 mM $MgCl_2$ and 280 nM hASNS in 100 mM HEPPS buffer, pH 8 (2 mL total volume).

[b] As determined by gHMQC NMR spectroscopy. Errors are estimated on the basis of measurements employing known concentrations of authentic ^{15}N-Asn.

[c] This value is corrected for the amount of ^{15}N-Asn that would be formed from ^{15}N-Gln at natural abundance, but the contribution of ^{14}N-Asn formed from any $^{14}NH_3$ released from the enzyme, as a result of the glutaminase activity of AS-B, is assumed to be negligible.

[d] Mean value and standard deviation computed from two separate determinations on duplicate samples using reverse-phase HPLC.

[e] ND – not detected; NA – not applicable.

CHAPTER 6
PREPARATION OF LIGAND BOUND hASNS – INHIBIITION AND BINDING STUDIES

Introduction [1]

Glutamine dependent asparagine synthetase (ASNS, EC 6.3.5.4) catalyzes ATP dependent conversion of aspartate to asparagine using glutamine as the nitrogen source. One of the interests in asparagine synthetase lies in the correlation of this enzyme to the resistance of the acute lymphoblastic leukemia cells after treated with L-asparaginase. For a long time, the *Escherichia coli* asparagine synthetase B (ASB) was studied as a model for the human enzyme because of its readiness to be expressed in a large amount. ASNS belongs to class II amidotransferase, with two active sites that are separated by an intramolecular tunnel. Each of the two active sites catalyzes a half reaction. At glutaminase site, ammonia is released from glutamine through a thioester intermediate formed by the nucleophilic attack of the thiolate group of Cys1 residue to the amide group of glutamine. At the other end of the tunnel, the γ-carboxylic acid group of aspartate is activated by ATP and form the β-aspartyl-AMP intermediate, followed by ammonia attacking to its γ-carbonyl group to produce asparagine (Figure 6-1). Although both human ASNS and ASB show same properties from the point view of chemistry, the kinetic studies of human enzyme revealed several differences from that of *E. coli* enzyme, which were discussed in the previous chapter. So far, the crystal structure of C1A mutant of *Escherichia coli* asparagine synthetase B (ASB) is the only one that was reported for asparagine synthetase (ASNS). Since the function of biomolecules can only be fully understood under the structural context, more crystal structure of ASNS, especially of hASNS, need to be studied. Recently, human asparagine synthetase (hASNS) was successfully expressed in a baculovirus system using *sf9* insect cells.

[1] This work was done with Alexandria Berry, an undergraduate. Li designed the experiments and analyzed the results. Li and Berry performed the work.

This makes possible to have enough protein for X-ray crystallographic studies of human enzyme.

In this work, efforts were made to prepare inhibitor-bound hASNS. 4-diazo-5-oxo-L-norleucine (DON) is a glutamine analog. It irreversibly inhibits the glutaminase activity of class II amidotransferases by reacting with the thiol group of the catalytic Cys1 residue in the glutaminase active site and forming a covalent C-S bond (Figure 6-2). The transition state analog Adenylated sulfoximine, mimicing that β-aspartyl-AMP is attacked by ammonia, was a good inhibitor for human asparagine synthetase with K_I at nM level (*71*) (Figure 6-3). My results showed that both inhibitors can bind to the enzyme, with DON in the glutaminase site and sulfoximine in the other.

Materials and Methods

Materials

Unless otherwise stated, all chemicals and reagents were purchased from Sigma (St. Louis, MO). L-Glutamine was recrystallized prior to use as previously described (*53*). C-terminally tagged human ASNS were expressed in and purified from a baculovirus/insect cell expression system as previously described (*16, 57*). Adenylated sulfoximine (as a 1:1 mixture of diasterioisomers) were obtained from Japan.

Enzyme Assays

The glutaminase activity of hASNS was determined by measuring the production of glutamate using glutamate dehydrogenase (L-GLDH) coupled assay. ASNS reaction mixtures (200 μL total volume) contained 100 mM NaCl, 10 mM $MgCl_2$, and 25 mM L-glutamine in 100 mM EPPS. Reactions were initiated upon the addition of hASNS and incubated at 37°C for 10 minutes, and terminated by addition of 30 μL 20% (v/v) trichloroacetic acid (TCA). The reaction mixtures was added to 770 μL coupling assay mixture, which consisted of pH 9.0 buffer (300 mM glycine, 250 mM hydrazine), 1.5 mM NAD^+, and 1 mM ADP. The absorbance was recorded

before and after the addition of 2.2 units of glutamate dehydrogenase (0 and 30 minutes). Glutamate was quantified using standard curve. The synthetase activity with either glutamine or ammonia as nitrogen source was assayed by determining the formation of PPi using PPi reagent (Sigma Technical Bulletin BI-100), based on the fact that PPi and asparagine were produced at 1:1 ratio in the hASNS catalyzed reaction.

Loss of Glutaminase Activity with Time at Different Temperature

The stability of hASNS was first investigated to determine the best incubation time. Time-based glutaminase activity of hASNS was tested at three different incubation temperatures, in ice, room temperature and 37 ^{o}C. After 10 μL of deionized water being added to one tube (approximately 100 μL) of the stock enzyme solution (1 mg/mL, 50 mM EPPS, pH 8, 5 mM DTT, and 20% glycol), the solution was aliquoted into 3 tubes, which were incubated on ice(0-4 ^{o}C, at room temperature (approximately 22°C), and at 37°C respectively. At a series of time points (0-61 minutes), 2 μL incubated enzyme from each aliquot were removed and immediately added into 198 μL of glutaminase reaction mixture to test its glutaminase activity.

DON Inhibition

The inhibition mixture was prepared by mixing stock enzyme solution (1.0 mg/mL) and DON aqueous solution (50 mM), which contained 0.9 mg/mL hASNS and 5.88 mM DON, while the control was made by mixing stock enzyme solution and deionized water. EPPS solution was filtered using Fisherbrand® 25 mm Syringe Filter, 0.2 μm, nylon. Solutions were incubated at room temperature and 15 μL aliquots were removed simultaneously from both inhibition mixture and control at varying time points (4-30 minutes), and then the enzyme was separated from free DON by using 30,000 nominal molecular weight limit (Daltons) Microcon® Centrifugal Filter Devices spin columns (Millipore Corporation, Bedford, MA). After each aliquot was spun down for 1 minute at 10,000 rpm, the enzyme was rinsed twice using 100 μL of 100 mM filtered EPPS

(4 minutes at 13,000 rpm). The purified enzyme was recovered in a new centrifuge tube by 30 μL of 100 mM filtered EPPS, which was added to the bottom side of the filter (1 minute at 7,000 rpm). All enzymes recovered were immediately assayed for their glutaminase activity (10 μL recovered enzyme). The DON inhibited enzyme was also checked for synthetase activity versus control enzyme synthetase activity using the pyrophosphate assay and concentration using the Bradford assay.

Loss of Synthetase Activity with Time at different Temperature

The time dependent loss of synthetase activity was determined at both room temperature and 37 ^{o}C. About 12% deionized water was added to the stock enzyme. The enzyme solution then was aliquoted into 8 different tubes and stored in a $^{-}$80°C freezer. These tubes were removed from the freezer one by one and sit at room temperature (approximately 22°C) for different times (0-70 minutes), or at 37°C over a 60 minute period, followed by testing their synthetase activity (incubated at 37°C in 100 mM EPPS, pH 8, containing 10 mM $MgCl_2$, 100 mM NH_4Cl, 20 mM aspartate, and 2.5 mM ATP over a period of 10 minutes with a 1 mL final volume).

Inhibition of the DON Inhibited Enzyme by Sulfoximine

The DON inhibited enzyme was prepared as described above, with incubation time being 20 minutes. The synthetase activity of the DON inhibited enzyme was assayed using the pyrophosphate assay with 0-10 μM sulfoximine. As for the control enzyme, the synthetase activity was measured with 0 μM or 10 μM sulfoximine inhibitor.

Results

Stability Experiment

Previous studies by size exclusion chromatography showed that hASNS dissociates into monomer from dimer with time. The structural changes may result in the loss of its activity. Furthermore, the unstable tholate group of Cys1 is readily oxidized in the solution, which causes

loss of the glutaminase activity of the enzyme. Here we investigated the stability of the enzyme before we characterized the inhibition to hASNS by DON and sulfoximine.

hASNS lost glutaminase activity with time at room temperature and 37 ^{o}C

Aliquots of hASNS were incubated in ice, at room temperature (about 22 ^{o}C) and at 37 ^{o}C respectively. The glutaminase activity of hASNS was immediately tested after being incubated for a certain time by previously reported assay method (*17*). Our results showed that hASNS lost its glutaminase activity faster at higher temperature. When incubated in ice, its activity decreased by 15% after 60 minutes (data not shown). While after 20 minutes' incubation at 37 ^{o}C, the enzyme lost 50% of its glutaminase activity (Figure 6-4, Table 6-1). After 60 minutes at 37 ^{o}C, more than 85% activity was lost. At room temperature, hASNS still kept 57% of its activity after 60 minutes. The percent activity left decreased exponentially with time, which indicates a first order reaction for the lost of glutaminase activity. The calculated half-life for glutaminase activity of hASNS are 74 minutes and 20 minutes for room temperature and 37 ^{o}C respectively.

The loss of NH_3 dependent synthetase activity with time at room temperature and 37 ^{o}C

The ammonia dependent synthetase activity was also checked after hASNS was incubated at room temperature or at 37 ^{o}C (Figure 6-5, Table 6-2). After being incubated for certain time, hASNS was added to assay mixture to initiate the reaction. The results showed that hASNS lost its ammonia dependent activity in different patterns for short time incubation and long time incubation. At room temperature, the enzyme lost little synthetase activity until being incubated for more than 30 minutes, and then its activity dropped exponentially. Similar results were observed for the enzyme incubated at 37 ^{o}C. When the incubation time was shorter than 15 minutes, the synthetase activity went down more like linearly than exponentially. After being incubated for more than 15 minutes, the activity decrease exponentially.

Inhibition to hASNS by DON

It has been reported that DON reacts with thiol group of Cys1 residue of several other class II amidotransferases and forms covalent bonded complex (E-ON). While few studies about DON inhibition to asparagine synthetase were reported, we did this experiment to support the hypothesis that DON is a glutaminase inhibitor for all the class II amidotransferases and has little effect on synthetase activity of hASNS.

DON inhibits 90% of glutaminase activity of hASNS after incubating for 20 minutes.

$$\mathbf{E} \xrightarrow[[DON] = 5.88\ mM]{k[DON] = 0.0026\ s^{-1}} \mathbf{EDON}$$

Before measuring its glutaminase activity after hASNS was incubated with 5.88 mM for a series of time, we separated E-ON from DON by using spin column (see methods part) because our results suggested that DON is a substrate of coupling enzyme glutamate dehydrogenase (L-GLDH) and affect the glutaminase assay. The protein concentration was tested using modified Coomassie assay and the percent recovery of hASNS for separation step was 71 ± 5 %. For each time point, we used incubated enzyme without DON as control to eliminate the effect caused by separation step (Figure 6-6, Table 6-3). After 20 minutes' incubation, the glutaminase activity of DON inhibited hASNS was only about 10% of control enzyme. The percent activity decreased exponentially with time. This indicates a first-order reaction for the inactivation of hASNS by 5.88 mM DON and the rate constant was calculated as 0.0026 s^{-1}.

DON had little effect on the rate of ammonia dependent synthesis of asparagine.

In this work, we did not try to characterize the ammonia dependent synthetase activity of DON incubated enzyme. We simply compared the production rate of pyrophosphate by DON incubated enzyme with that by control enzyme (incubated without DON) at saturating level of all

the substrates (except ammonia at 100 mM). Several reports showed that Asn:PPi ratio close to 1:1 for free enzyme or inhibited enzyme. Therefore, we here assume that DON incubated hASNS will not affect Asn:PPi ratio during the enzyme catalyzed synthesis. Note: In order to fully characterize the inhibition mechanism, this assumption need to be confirmed by using HPLC-based end point assay (*23*) and PPi assay (*22*). The concentration of the recovered enzyme solutions was determined to be 0.78 mg/mL using the Bradford assay. The volume of recovered enzyme solution varied from about 12 to 18 μL (approximately 0.0117 mg of enzyme), versus the initial volume of 15 μL of 1.0 mg/mL of stock enzyme (0.015 mg). With all the substrate at saturating level, the production rate of pyrophosphate had no significant changes between E-ON complex and control enzyme, which implies little changes for ammonia dependent synthetase activity (Table 6-4).

Inhibition by Adenylated Sulfoximine

The transition state analog adenylated sulfoximine is a good inhibitor with K_I at nanomolar level. It was reported to suppress proliferation of an L-asparginase-resistant leukemia cell line and is a potential solution for drug resistance in lymphoblastic and myeloblastic leukemia cells (*71*). Here we examined its inhibition to DON incubated hASNS and checked the difference between its inhibition effect on DON incubated hASNS and on free enzyme.

Inhibition to the ammonia dependent synthetase activity of stock hASNS

The inhibition to hASNS by sulfoximine has been studied regarding its ammonia dependent synthetase activity as well as glutaminase acitivity. While sulfoximine was reported as a good inhibitor to synthetase activity of hASNS, little effect on glutaminase activity of hASNS by sulfoximine was discovered. As control experiment for the studies of its inhibition to DON incubated hASNS, we tested ammonia dependent synthetase activity of stock hASNS with 3 different concentrations of sulfoximine, 0, 5, and 10 uM respectively. The initial rate was 0.0404

± 0.0007 μM/s. The production of PPi catalyzed by hASNS without sulfoximine linearly increased with time. With the presence of inhibitor, the production gradually slowed down with time (Figure 6-7).

Data were processed based on the slow onset inhibition model as reported in literature (*71, 80*). Three parameters, v_{ss}, v_0 and k were determined by fitting the data using KaleidaGraph v3.5 from Synergy Software, where v_{ss} and v_0 are initial and steady-state velocities respectively, and k is the apparent first-order rate constant for isomerization of EI to EI^*. k_6 was calculated using the following equations with these three parameter determined at different concentrations of inhibitor:

$$k_6 = k \times \frac{v_{ss}}{v_0} \qquad (1)$$

The average value of k_6 then was used to estimate K_I and k_5 by fitting to the equation below.

$$k = k_6 + k_5 \times \frac{\frac{[I]}{K_I}}{1 + \frac{[ATP]}{K_a} + \frac{[I]}{K_I}} \qquad (2)$$

The calculated kinetic results were listed in Table 6-5 as well as those reported in the literature.

Inhibition to the ammonia dependent synthetase activity of DON incubated hASNS

The ammonia dependent synthetase activity of DON incubated hASNS was tested with different concentrations of sulfoximine (0-10uM), immediately after purified E-ON was prepared. The incubated hASNS without DON was used as control. The production of PPi without sulfoximine linearly increased with time for both DON incubated enzyme and control enzyme, with k_{cat} value of 0.09 ± 0.01 uM/s and 0.047 ± 0.005 uM/s respectively (Figure 6-8 and 6-9). With sulfoximine, the production of PPi versus time was consistent with the slow onset inhibition model, same as what we got before for stock enzyme (Figure 6-8). Based on the results

for control enzyme, the rate constants for conversion of EI to EI* were calculated and listed in Table. Here we assume the control enzyme has same K_I value as stock enzyme. Little difference was found between these rate constants for control enzyme and for stock enzyme (Table 6-6). This showed that the binding property of hASNS to sulfoximine had no significant changes after the control enzyme was prepared. Unfortunately, for DON incubated enzyme, we could only accurately determine the initial velocity ν_0 by fitting the data using KaleidaGraph, not ν_{ss} and k. All the fitting gave a big error for ν_{ss} and k, which has no practical meaning, except k was fitted as 4.9×10^{-4} s^{-1} at 10 μM of sulfoximine (Figure 6-9).

Discussion

The catalytic mechanism can only be completely understood under structural context. hASNS has two active sites, glutaminase site and synthetase site. In order to prepare inhibitor bound hASNS and make crystal structure, we did kinetic studies about hASNS using two inhibitors, DON and sulfoximine. DON is a glutamine analog. DON incubated enzyme showed significant decrease for its glutaminase activity after being separated from DON and diluted for more than 30 fold in the enzyme catalyzed reaction. The first order rate constant was calculated as 0.0026 s^{-1} in the presence of 5.88 mM DON at room temperature. After 20 minutes' incubation with DON, 90% of hASNS was inhibited based on its glutaminase activity while its ammonia dependent synthetase activity decreased about 10%. This result supports the idea that DON reacts with the thiolate group of Cys1 residue of hASNS and form covalently bound enzyme, although no direct evidence shows the inhibition is irreversible for hASNS. The covalently bound enzyme complex has been observed for other class II amidotransferases, such as glutamine phosphoribosylpyrophosphate (PRPP) amidotransferase, glutamate synthase and glucosamine-4-phosphate synthetase (GlmS) (*28, 54, 81, 82*). All this evidence indicates that DON incubated hASNS is E-ON complex. The fact that DON incubated enzyme lost

glutaminase activity without affecting its synthetase activity significantly proves that DON, as a glutamine analog, binds glutaminase active site, not synthetase site. This conclusion was further supported by the result that the ammonia dependent synthetase activity of DON incubated enzyme was inhibited by sulfoximine, an analog of transition state that formed in the synthetase site, which had little effect on the glutaminase activity of hASNS by previous studies. The apparent first order rate constant was calculated as 0.00049 s^{-1} for the inhibition of DON incubated enzyme with the presence of 10 μM sulfoximine. The calculated half-life was 24 minutes and the time for 90% inhibition was 78 minutes.

hASNS is not stable. After one hour at room temperature, the enzyme lost 43% of its glutaminase activity and 11% of synthetase activity. When the enzyme was kept at 37 ^{o}C, these numbers are 87% and 67% respectively. The lost of its glutaminase activity may result from the oxidation of the thiolate group of Cys1. However, it is unexpected that its ammonia dependent synthetase activity also decreased with time. Maybe this is caused by structural changes of the enzyme at higher temperature because its molecular weight changed from dimer form to monomer form by size exclusion chromatography.

The sulfoximine inhibition to DON incubated hASNS is different from the control. Only k value for the highest concentration of sulfoximine (10 μM) was estimated as 0.000489 s^{-1}. It is decreased by 5 times compared to that of control enzyme, which means the formation of EI* became slower for DON incubated enzyme. Since stock enzyme and control enzyme showed similar binding affinity to sulfoximine. We can exclude the possibility that this was caused by incubation for 20 minutes at room temperature as well as separation step. Therefore, we can conclude that the formation of the covalent complex from the reaction of DON with enzyme at glutaminase site resulted in some conformational changes of the synthetase site. Since k can be

expressed as a function of k_5, k_6 and K_I at certain concentration of ATP, and $k_6 << k$ or k_5 for control enzyme, the decreasing of the k value is likely caused by the decreasing of k_5, or increasing of K_I or both. This implies that DON inhibited enzyme has some structural changes either that affect the binding of sulfoximine or that make the "on" rate of EI to EI* slower. This can be supported by the following analysis.

If incubation with DON does not affect its binding to sulfoximine, that is, K_I is a constant with value of 0.181 μM, so

$$k_5 = (k - k_6) \times \frac{1 + \frac{[ATP]}{K_a} + \frac{[I]}{K_I}}{\frac{[I]}{K_I}} < k \times \frac{1 + \frac{[ATP]}{K_a} + \frac{[I]}{K_I}}{\frac{[I]}{K_I}}$$

$$k_5 < 4.9 \times 10^{-4}\, s^{-1} \times \frac{1 + \frac{5mM}{0.2mM} + \frac{10\mu M}{0.181\mu M}}{\frac{10\mu M}{0.181\mu M}} = 7.2 \times 10^{-4}\, s^{-1}$$

Therefore, k_5 is less than 7.2×10^{-4} s^{-1}. This value is one fourth of that for control.

$$k_6 = k - k_5 \times \frac{\frac{[I]}{K_I}}{1 + \frac{[ATP]}{K_a} + \frac{[I]}{K_I}} < k$$

So k_6 must be less than 4.9×10^{-4} s^{-1}. Compared to original value of 1.9×10^{-4} s^{-1}, the change of k_6 cannot significantly affect k value to be changed from 2.3×10^{-3} s^{-1} to 4.9×10^{-4} s^{-1}. So k_5 is the one of the factors that affect k value significantly.

Since k_6 is not a major factor that affect k value, we can neglect the k_6 term in the equation 2. Then

$$k \approx k_5 \times \frac{\frac{[I]}{K_I}}{1+\frac{[ATP]}{K_a}+\frac{[I]}{K_I}}$$

So k is negatively related to K_I value. The increasing of K_I results in the decreasing of k.

For DON incubated enzyme, it is more difficult to determine ν_{ss} and k by fitting the data measured within 15 minutes. The concentration of the pyrophosphate produced can be expressed using following equation for slow onset inhibition model.

$$P = v_{ss}t + (1-e^{-kt}) \times \frac{v_0 - v_{ss}}{k}$$

When time is long enough, $P = v_{ss}t + \frac{v_0 - v_{ss}}{k}$. This means the production of pyrophosphate is linearly related to the time with ν_{ss} as slope and $\frac{v_0 - v_{ss}}{k}$ as intercept on y-axis. Therefore, to determine ν_{ss} and k, especially ν_{ss}, we need to measure the production of pyrophosphate for enough time. Unfortunately, hASNS is not stable enough for a long time assay.

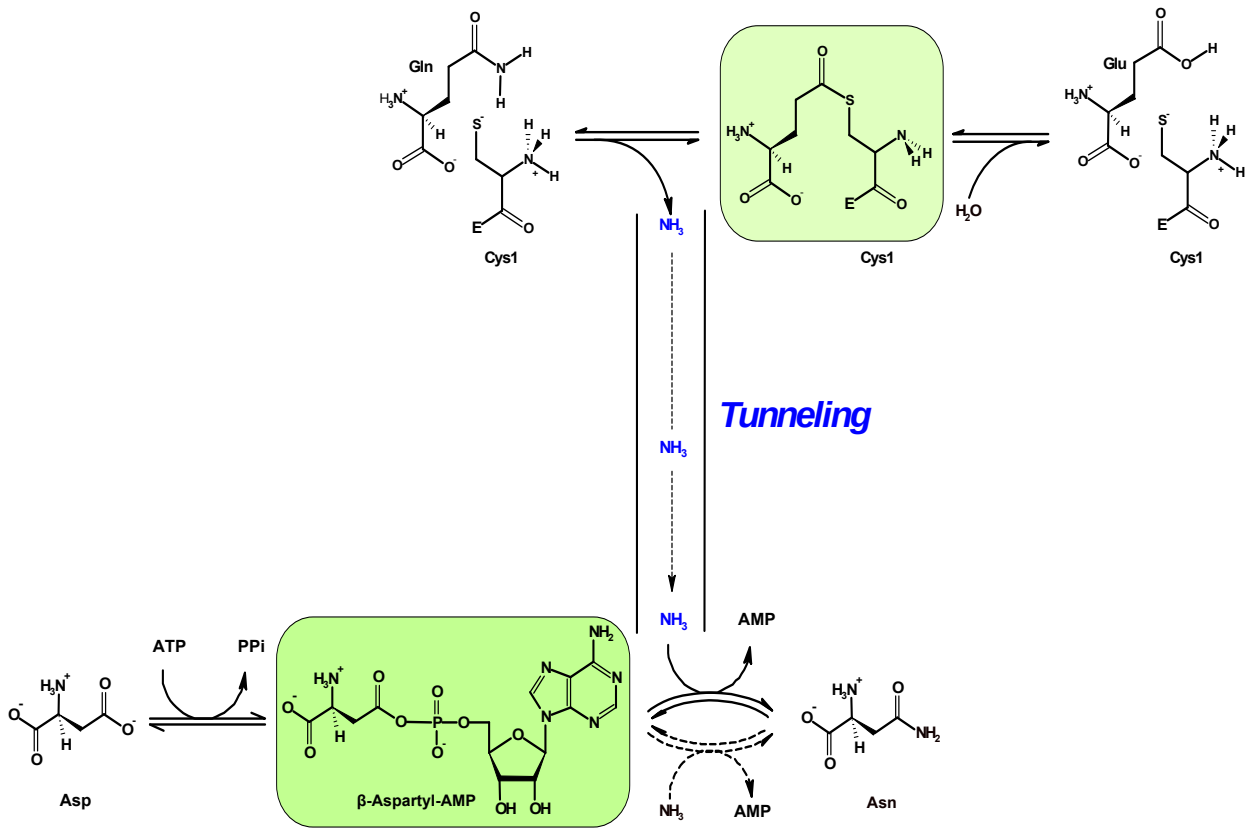

Figure 6-1. The mechanisms of ASNS catalyzed reaction. At glutaminase site, ammonia is released from glutamine through a thioester intermediate formed by the nucleophilic attack of the thiolate group of Cys1 residue to the amide group of glutamine. Then the thioester is hydrolyzed into glutamate and reproduce free enzyme. At the other end of the tunnel, the γ-carboxylic acid group of aspartate is activated by ATP and form the β-aspartyl-AMP intermediate, followed by ammonia attacking to its γ-carbonyl group to produce asparagine.

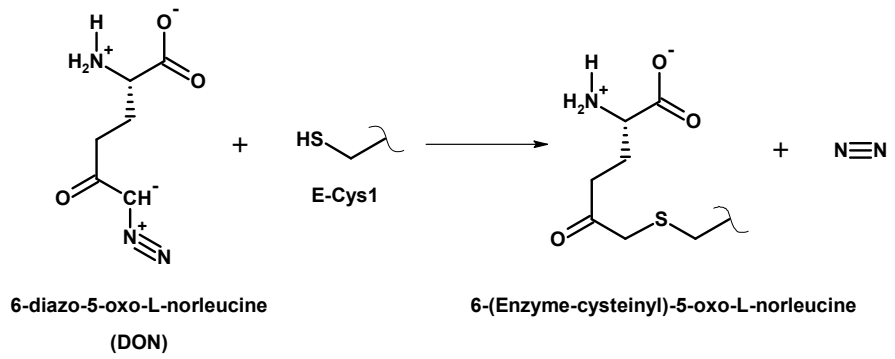

Figure 6-2. DON reacts with Cys1 residue of ASNS and forms covalent adduct.

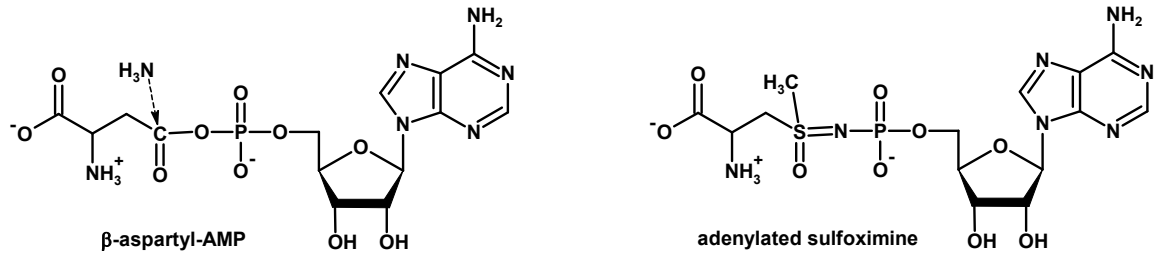

Figure 6-3. The inhibitor adenylated sulfoximine (right) mimics the nucleophilic attacking of β-aspartyl-AMP by ammonia.

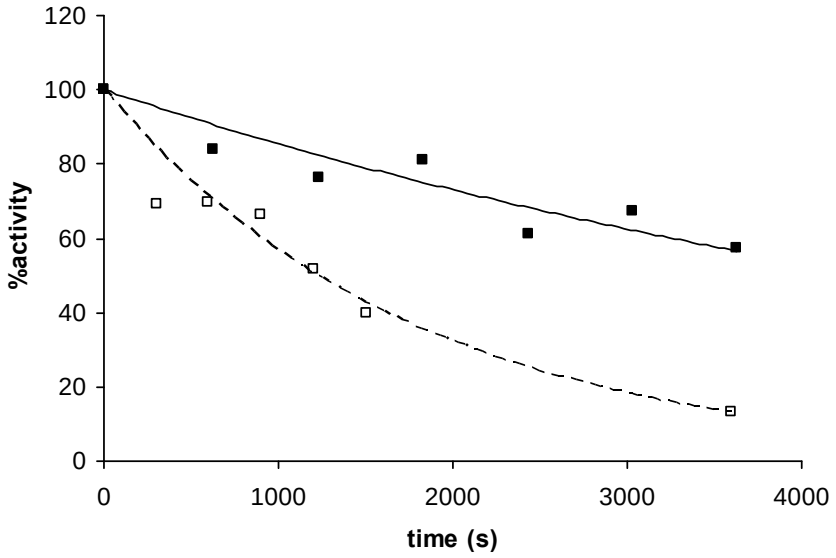

Figure 6-4. The glutaminase activity of hASNS decreased exponentially with time. Solid line (data: filled square): 22 ^{o}C; Dashed line (data: blank square): 37 ^{o}C..

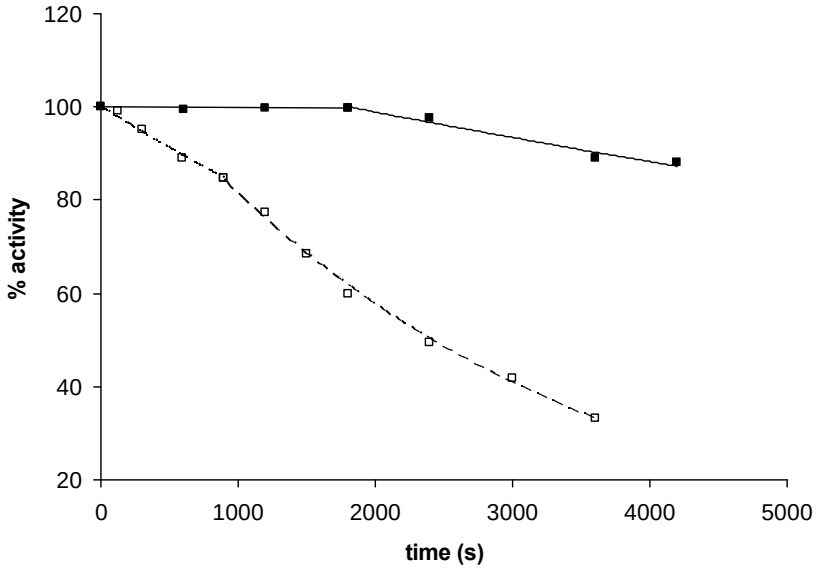

Figure 6-5. The ammonia dependent synthetase activity of hASNS decreased with time. Solid line (data: filled square): 22 ^{o}C; Dashed line (data: blank square): 37 ^{o}C.

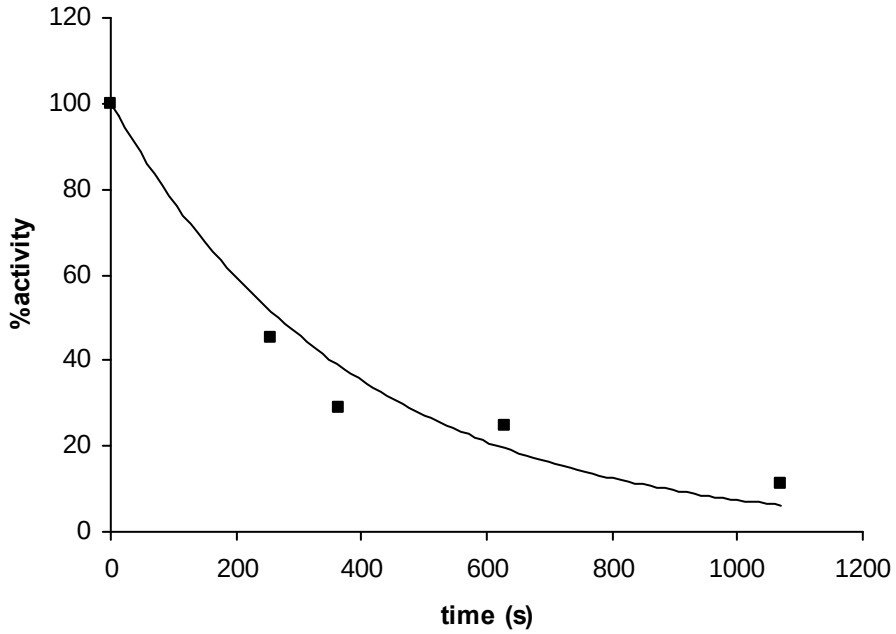

Figure 6-6. The glutaminase activity of DON inhibited hASNS decreased exponentially with time. The curve was fitted using the first four data.

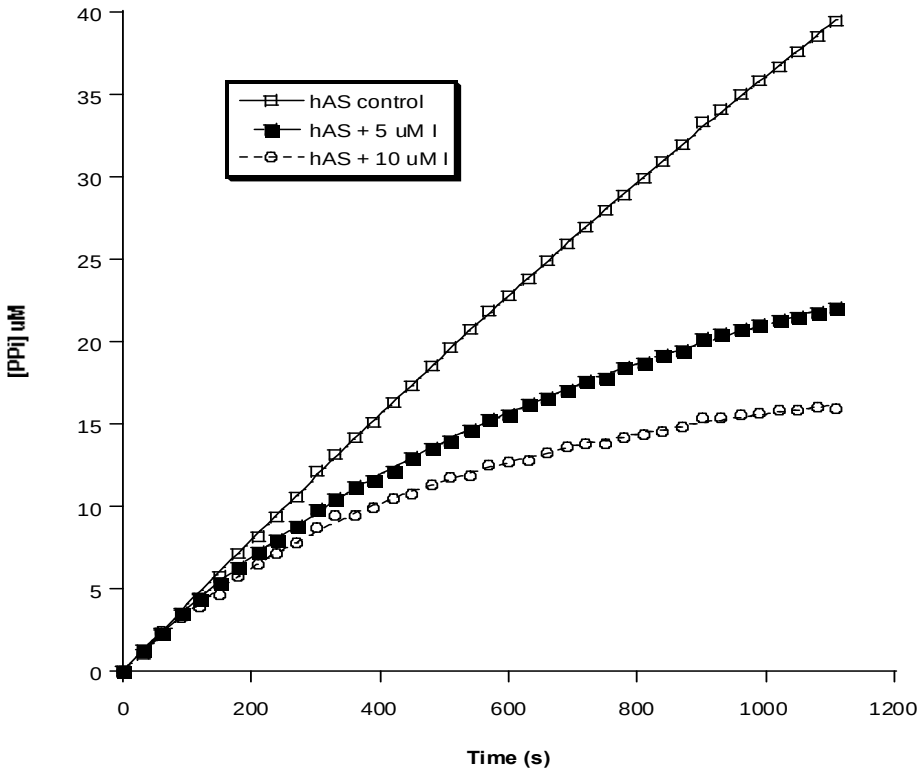

Figure 6-7. The inhibition to free hASNS by sulfoximine

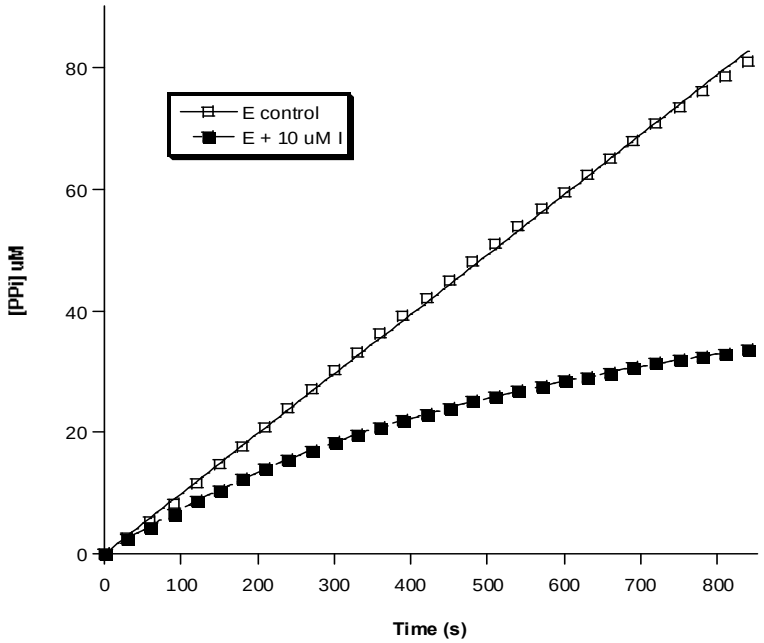

Figure 6-8. Inhibition to control hASNS by sulfoximine

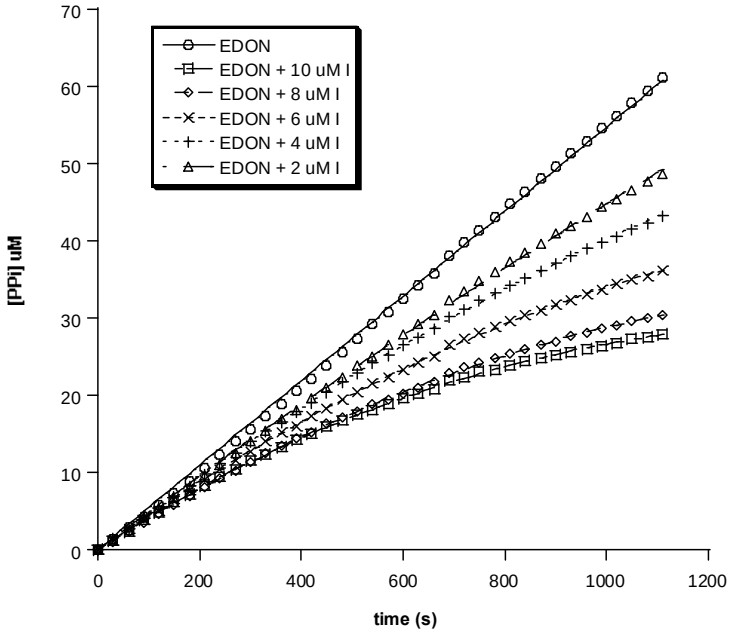

Figure 6-9. Inhibition to DON inhibited hASNS by sulfoximine

Table 6-1. Percent glutaminase activity at different incubation time without DON

Room Temperature (~22 ^{o}C)		37 ^{o}C	
Time (s)	%activity	Time (s)	%activity
0	100	0	100
630	83.8	300	69.4
1230	76.2	600	69.6
1830	81.2	900	66.3
2430	61.0	1200	51.5
3030	67.1	1500	39.6
3630	57.3	3600	13.4

Table 6-2. Percent ammonia dependent synthetase activity without inhibitors

Room Temperature (~22 °C)		37 °C	
Time (s)	%activity	Time (s)	%activity
0	100	0	100
		120	99.12864
		300	95.05294
600	99.59384	598	89.15113
		893	84.74562
1200	99.69538	1201	77.24632
		1500	68.41563
1800	99.72076	1800	59.92223
2400	97.56304	2400	49.46501
		3000	41.84203
3600	88.95752	3600	33.09285
4200	88.06905		

Table 6-3. The loss of glutaminase activity due to DON inhibition

Room Temperature (~22 ^{o}C)	
Time (s)	%activity
0	100
254	45
365	29
630	25
1070	11
1324	13
1883	12

Table 6-4. Synthetase activity of the DON inhibited and control enzyme after incubation determined using the pyrophosphate assay

Enzyme Solution	Rate of Reaction uM/s	
	Trial 1	Trial 2
hASNS + 5.88 mM DON	3.99E-02	4.37E-02
hASNS control	4.80E-02	4.60E-02

Table 6-5. Kinetical constant for sulfoximine inhibition to ammonia dependent synthetase activity of hASNS

data source	K_I (nM)	k_5 (s^{-1})	k_6 (s^{-1})	$k_{obs}/[I]_{tot}$ (M^{-1} s^{-1})	K^*_I (nM)
repeat	181	3.51×10^{-3}	2.6×10^{-4}	-	13.4
literature	285	2.98×10^{-3}	2.6×10^{-5}	436	2.46

Table 6-6. Parameters for inhibition of stock hASNS and control hASBS by sulfoximine

hASNS	K_I (nM)	k_5 (s^{-1})	k_6 (s^{-1})	$K_{obs}/[I]_{tot}$ (M^{-1} s^{-1})	K^*_I (nM)
stock	181	3.51×10^{-3}	2.6×10^{-4}	-	13.4
control	181*	3.12×10^{-3}	1.9×10^{-4}	-	11.0

APPENDIX A
SEQUENCE ALIGNMENT OF TUNNEL RESIDUES IN ASB

SPECIES Tunnel Residues

```
                                 1 1 2 3 3 3 3 3 3 3 3 3 3 3 4
                 2 3 5 7 7 2 4 3 4 4 4 5 5 8 8 8 9 9 9 0
                 9 1 0 4 6 0 3 8 4 6 8 0 2 0 5 9 3 7 9 1

                               1 2 3 3 3 3 3 3 3 3 3 3 4 4
                   3 3 5 7 7 4 3 2 4 4 4 5 5 8 8 9 9 9 0 0
                 1 0 2 2 5 8 2 2 9 5 7 9 1 7 4 8 2 6 8 0 4
plant_456_e-133  CHRGPLINGEYIVTLDMVISGEGSDEYLDCANTFGLEARVL
plant2_525_e-153 CHRGPLINGEYIVTLDMVISGEGSDEYLDCANTSGLEARVL
mustard_plant_456_e-125 CHRGPLVNGEYIVTLDMVLSGEGADEYLDCANTSGLEARVL
pea_586_e-160    CHRGPLINGEYIVTLDMVISGEGSDEYLDCANTYGLEARVL
bacteria2_564_e-180 CHRGPLINGEYIVVLDMVLSGEGSDEYLDCANMMGVEPRVL
plant3_586_e-168 CHRGPLINGEYMICLDMVISGEGSDEYLDCANTSGVEARVL
fruit_fly_558_e-120 CHRGPLINGEYMIILDMILSGEGADEYLDCANAMGVELRVL
Ecoli_           CHRGPLINGEYMIILDMVLSGEGSDEYLDCANMSGVEARVL
bacteria_554     CHRGPLINGEYMIILDMVLSGEGSDEYLDCANMSGVEARVL
Salmonella_554   CHRGPLINGEYMIILDMVLSGEGSDEYLDCANMSGVEARVL
Yersinia_554     CHRGPLINGEYMIILDMVLSGEGSDEYLDCANMSGVEARVL
Paramecium_588_e-132 CHRGPLINGEYMIIFDMCLTGEGSDEYLDLANCLGIETRPM
fungus_571_e-133 CHRGPLINGEYMVTLDMVLSGEGSDEYLDCANTMGLEARVL
fungus2_574_e-136 CHRGPLINGEYMITLDMVLSGEGSDEYLDCANTMGLEARVL
Neurospora_581_e-148 CHRGPLINGEYMITLDMVLSGEGSDEYLDCANTSGLEARVL
sunflower_589_e-163 CHRGPLVNGEYMITLDMVISGEGSDEYLDCANTSGLEARVL
mosquito_533_e-112 CHRGPLINGEYMIVLDVVLSGEGADEYLDCANCAGLELRVL
C_elegans_567_e-105 CHRGPLINGEYVVKLDMVLSGEGADEYLDCADSMSVEVRVL
hamster_561_e-81 CHRGPLVNGEYVVRLDMIFSGEGSDEYLDVADTAGLELRVL
mouse_561_e-81   CHRGPLVNGEYVVRLDMIFSGEGSDEYLDVADTAGLELRVL
Human_562_e-80   CHRGPLVNGEYVVRLDMIFSGEGSDEYLDVADTAGLELRVL
                 ****** ****   ***  **** ***** *   * * ***
```

Red asterisk shows absolutely conserved residue; black asterisk shows those residues that conserved in 20 out 21 species.

Red letter: conserved residue in at least 20 out of 21 species. Blue background letter show different residue(s) other than conserved residues
Yellow column: conserved residue in at least 15 out of 21 species.
Purple column: conserved residue in at least 10 out of 21 species.

Note: 1. An absolutely conserved Gly is right before Met 120 and Ile 142.
2. Ile 52 (16 I, 5 V), Met 120 (12 M, 5 I, 4 V), Ile 142 (11 I, 10 V)
Asn 389 (17 N, 4 D), Val 397 (12 L, 8 V, 1 I), Cys 385 (17 C, 3 V, 1 L)
Val 344 (16 V, 4 I, 1 C), Ser 350 (17 S, 4 A)

APPENDIX B
THE KINETIC MODEL FOR EXCHANGE EXPERIMENT

The model for exchanging experiment was analyzed as following:

$$E + Gln \underset{k_2}{\overset{k_1}{\rightleftharpoons}} Eester + NH_4^+ \quad \text{(i)}$$

$$Eester + {}^{15}NH_4^+ \underset{k_1}{\overset{k_2}{\rightleftharpoons}} E + {}^{15}N{-}Gln \quad \text{(ii)}$$

$$Eester + H_2O \xrightarrow{k_3} E + Glu \quad \text{(iii)}$$

Since [Gln] >> [^{15}N-Gln] and [$^{15}NH_4^+$] >> [NH_4^+], the reverse reaction of (i) and (ii) are negligible. So the model is simplified as:

$$E + Gln \xrightarrow{k_1} Eester + NH_4^+ \quad \text{(I)}$$

$$Eester + {}^{15}NH_4^+ \xrightarrow{k_2} E + {}^{15}N{-}Gln \quad \text{(II)}$$

$$Eester + H_2O \xrightarrow{k_3} E + Glu \quad \text{(III)}$$

Based on the steady state theory,

$$\frac{d[Eester]}{dt} = k_1[E][G\ln] - k_2[Eester][{}^{15}NH_4^+] - k_3[Eester][H_2O] = 0$$

$$k_1[E][G\ln] = k_2[Eester][{}^{15}NH_4^+] + k_3[Eester][H_2O]$$

$$k_1[E][G\ln] = [Eester](k_2[{}^{15}NH_4^+] + k_3[H_2O])$$

$$[E] = \frac{[Eester](k_2[{}^{15}NH_4^+] + k_3[H_2O])}{k_1[G\ln]}$$

Since $[E]_T = [E] + [Eester]$

Then $[E]_T = \frac{[Eester](k_2[^{15}NH_4^+] + k_3[H_2O])}{k_1[G\ln]} + [Eester]$

$$= \frac{[Eester](k_1[G\ln] + k_2[^{15}NH_4^+] + k_3[H_2O])}{k_1[G\ln]}$$

Therefore,

$$[Eester] = \frac{k_1[E]_T[G\ln]}{(k_1[G\ln] + k_2[^{15}NH_4^+] + k_3[H_2O])}$$

So the production rate of [^{15}N-Gln] is:

$$v = k_2[Eester][^{15}NH_4^+] = \frac{k_1k_2[E]_T[G\ln][^{15}NH_4^+]}{(k_1[G\ln] + k_2[^{15}NH_4^+] + k_3[H_2O])}$$

When [$^{15}NH_4^+$] is kept constant and [Gln] is varied,

$$v = \frac{(k_2[E]_T[^{15}NH_4^+])[G\ln]}{(\frac{k_2}{k_1}[^{15}NH_4^+] + \frac{k_3}{k_1}[H_2O]) + [G\ln]}$$

$$= \frac{V_{\max-G\ln}[G\ln]}{K_{M-G\ln} + [G\ln]}$$

Where

$$V_{\max-G\ln} = k_2[E]_T[^{15}NH_4^+]$$

$$K_{M-G\ln} = \frac{k_2}{k_1}[^{15}NH_4^+] + \frac{k_3}{k_1}[H_2O]$$

When [Gln] is kept constant and [$^{15}NH_4^+$] is varied,

$$v = \frac{(k_1[E]_T[G\ln])[^{15}NH_4^+]}{(\frac{k_1}{k_2}[G\ln] + \frac{k_3}{k_2}[H_2O]) + [^{15}NH_4^+]}$$

$$= \frac{V_{\max -{}^{15}NH_4^+}[{}^{15}NH_4^+]}{K_{M-{}^{15}NH_4^+} + [{}^{15}NH_4^+]}$$

Where

$$V_{\max -{}^{15}NH_4^+} = k_2[E]_T[G\ln]$$

$$K_{M-{}^{15}NH_4^+} = \frac{k_1}{k_2}[{}^{15}NH_4^+] + \frac{k_3}{k_2}[H_2O]$$

LIST OF REFERENCES

1. Hyde, C. C.; Ahmed, S. A.; Padlan, E. A.; Miles, E. W.; Davies, D. R., Three-Dimensional Structure of the Tryptophan Synthase R2â2, Multienzyme Complex from Salmonella typhimurium. *J Biol Chem* **1988,** *263*, 17857-71.

2. Huang, X.; Holden, H. M.; Raushel, F. M., Channeling of substrates and intermediates in enzyme-catalyzed reactions. *Annu Rev Biochem* **2001,** *70*, 149-80.

3. Raushel, F. M.; Thoden, J. B.; Holden, H. M., Enzymes with molecular tunnels. *Acc Chem Res* **2003,** *36*, (7), 539-48.

4. Lunn, F. A.; Bearne, S. L., Alternative substrates for wild-type and L109A E. coli CTP synthases -- Kinetic evidence for a constricted ammonia tunnel. *Eur J Biochem* **2004,** *271*, 4204-12.

5. Zalkin, H., The amidotransferases. *Adv Enzymol Relat Areas Mol Biol* **1993,** *66*, 203-309.

6. Zalkin, H.; Smith, J. L., Enzymes utilizing glutamine as an amide donor. *Adv Enzymol Relat Areas Mol Biol* **1998,** *72*, 87-144.

7. Haskell, C. M.; Canellos, G. P., l-asparaginase resistance in human leukemia--asparagine synthetase. *Biochem Pharmacol* **1969,** *18*, (10), 2578-80.

8. Prager, M. D.; Peters, P. C.; Janes, J. O.; Derr, I., Asparagine synthetase activity in malignant and non-malignant human kidney and prostate specimens. *Nature* **1969,** *221*, (185), 1064-5.

9. Nakamura, M.; Yamada, M.; Hirota, Y.; Sugimoto, K.; Oka, A.; Takanami, M., Nucleotide sequence of the asnA gene coding for asparagine synthetase of E. coli K-12. *Nucleic Acids Res* **1981,** *9*, (18), 4669-76.

10. Felton, J.; Michaelis, S.; Wright, A., Mutations in two unlinked genes are required to produce asparagine auxotrophy in Escherichia coli. *J Bacteriol* **1980,** *142*, (1), 221-8.

11. Scofield, M. A.; Lewis, W. S.; Schuster, S. M., Nucleotide sequence of Escherichia coli asnB and deduced amino acid sequence of asparagine synthetase B. *J Biol Chem* **1990,** *265*, (22), 12895-902.

12. Humbert, R.; Simoni, R. D., Genetic and biomedical studies demonstrating a second gene coding for asparagine synthetase in Escherichia coli. *J Bacteriol* **1980,** *142*, (1), 212-20.

13. Richards, N. G.; Schuster, S. M., Mechanistic issues in asparagine synthetase catalysis. *Adv Enzymol Relat Areas Mol Biol* **1998,** *72*, 145-98.

14. Schnizer, H. G.; Boehlein, S. K.; Stewart, J. D.; Richards, N. G.; Schuster, S. M., Formation and isolation of a covalent intermediate during the glutaminase reaction of a class II amidotransferase. *Biochemistry* **1999,** *38*, (12), 3677-82.

15. Larsen, T. M.; Boehlein, S. K.; Schuster, S. M.; Richards, N. G.; Thoden, J. B.; Holden, H. M.; Rayment, I., Three-dimensional structure of Escherichia coli asparagine synthetase B: a short journey from substrate to product. *Biochemistry* **1999,** *38*, (49), 16146-57.

16. Boehlein, S. K.; Richards, N. G.; Schuster, S. M., Glutamine-dependent nitrogen transfer in Escherichia coli asparagine synthetase B. Searching for the catalytic triad. *J Biol Chem* **1994a,** *269*, (10), 7450-7.

17. Boehlein, S. K.; Richards, N. G.; Walworth, E. S.; Schuster, S. M., Arginine 30 and asparagine 74 have functional roles in the glutamine dependent activities of Escherichia coli asparagine synthetase B. *J Biol Chem* **1994b,** *269*, (43), 26789-95.

18. Boehlein, S. K.; Schuster, S. M.; Richards, N. G., Glutamic acid gamma-monohydroxamate and hydroxylamine are alternate substrates for Escherichia coli asparagine synthetase B. *Biochemistry* **1996,** *35*, (9), 3031-7.

19. Stoker, P. W.; O'Leary, M. H.; Boehlein, S. K.; Schuster, S. M.; Richards, N. G., Probing the mechanism of nitrogen transfer in Escherichia coli asparagine synthetase by using heavy atom isotope effects. *Biochemistry* **1996,** *35*, (9), 3024-30.

20. Boehlein, S. K.; Walworth, E. S.; Richards, N. G.; Schuster, S. M., Mutagenesis and chemical rescue indicate residues involved in beta-aspartyl-AMP formation by Escherichia coli asparagine synthetase B. *J Biol Chem* **1997,** *272*, (19), 12384-92.

21. Boehlein, S. K.; Walworth, E. S.; Schuster, S. M., Identification of cysteine-523 in the aspartate binding site of Escherichia coli asparagine synthetase B. *Biochemistry* **1997,** *36*, (33), 10168-77.

22. Boehlein, S. K.; Stewart, J. D.; Walworth, E. S.; Thirumoorthy, R.; Richards, N. G.; Schuster, S. M., Kinetic mechanism of Escherichia coli asparagine synthetase B. *Biochemistry* **1998,** *37*, (38), 13230-8.

23. Tesson, A. R.; Soper, T. S.; Ciustea, M.; Richards, N. G., Revisiting the steady state kinetic mechanism of glutamine-dependent asparagine synthetase from Escherichia coli. *Arch Biochem Biophys* **2003,** *413*, (1), 23-31.

24. Fresquet, V.; Thoden, J. B.; Holden, H. M.; Raushel, F. M., Kinetic mechanism of asparagine synthetase from Vibrio cholerae. *Bioorg Chem* **2004,** *32*, (2), 63-75.

25. Buchanan, J. M., The amidotransferases. *Adv Enzymol Relat Areas Mol Biol* **1973,** *39*, 91-183.

26. Nakamura, A.; Yao, M.; Chimnaronk, S.; Sakai, N.; Tanaka, I., Ammonia channel couples glutaminase with transamidase reactions in GatCAB. *Science* **2006,** *312*, (5782), 1954-8.

27. Oshikane, H.; Sheppard, K.; Fukai, S.; Nakamura, Y.; Ishitani, R.; Numata, T.; Sherrer, R. L.; Feng, L.; Schmitt, E.; Panvert, M.; Blanquet, S.; Mechulam, Y.; Soll, D.; Nureki, O., Structural

basis of RNA-dependent recruitment of glutamine to the genetic code. *Science* **2006,** *312*, (5782), 1950-4.

28. Mouilleron, S.; Badet-Denisot, M. A.; Golinelli-Pimpaneau, B., Glutamine binding opens the ammonia channel and activates glucosamine-6P synthase. *J Biol Chem* **2006,** *281*, (7), 4404-12.

29. Anand, R.; Hoskins, A. A.; Stubbe, J.; Ealick, S. E., Domain organization of Salmonella typhimurium formylglycinamide ribonucleotide amidotransferase revealed by X-ray crystallography. *Biochemistry* **2004,** *43*, (32), 10328-42.

30. Endrizzi, J. A.; Kim, H.; Anderson, P. M.; Baldwin, E. P., Crystal structure of Escherichia coli cytidine triphosphate synthetase, a nucleotide-regulated glutamine amidotransferase/ATP-dependent amidoligase fusion protein and homologue of anticancer and antiparasitic drug targets. *Biochemistry* **2004,** *43*, (21), 6447-63.

31. Myers, R. S.; Jensen, J. R.; Deras, I. L.; Smith, J. L.; Davisson, V. J., Substrate-induced changes in the ammonia channel for imidazole glycerol phosphate synthase. *Biochemistry* **2003,** *42*, (23), 7013-22.

32. van den Heuvel, R. H.; Ferrari, D.; Bossi, R. T.; Ravasio, S.; Curti, B.; Vanoni, M. A.; Florencio, F. J.; Mattevi, A., Structural studies on the synchronization of catalytic centers in glutamate synthase. *J Biol Chem* **2002,** *277*, (27), 24579-83.

33. Douangamath, A.; Walker, M.; Beismann-Driemeyer, S.; Vega-Fernandez, M. C.; Sterner, R.; Wilmanns, M., Structural evidence for ammonia tunneling across the (beta alpha)(8) barrel of the imidazole glycerol phosphate synthase bienzyme complex. *Structure* **2002,** *10*, (2), 185-93.

34. Raushel, F. M.; Thoden, J. B.; Holden, H. M., The amidotransferase family of enzymes: molecular machines for the production and delivery of ammonia. *Biochemistry* **1999,** *38*, (25), 7891-9.

35. Richards, N. G.; Kilberg, M. S., Asparagine synthetase chemotherapy. *Annu Rev Biochem* **2006,** *75*, 629-54.

36. Binda, C.; Bossi, R. T.; Wakatsuki, S.; Arzt, S.; Coda, A.; Curti, B.; Vanoni, M. A.; Mattevi, A., Cross-talk and ammonia channeling between active centers in the unexpected domain arrangement of glutamate synthase. *Structure* **2000,** *8*, (12), 1299-308.

37. Massiere, F.; Badet-Denisot, M. A., The mechanism of glutamine-dependent amidotransferases. *Cell Mol Life Sci* **1998,** *54*, (3), 205-22.

38. Weeks, A.; Lund, L.; Raushel, F. M., Tunneling of intermediates in enzyme-catalyzed reactions. *Curr Opin Chem Biol* **2006,** *10*, (5), 465-72.

39. Mullins, L.; Raushel, F., Channeling of ammonia through the intermolecular tunnel contained within carbamoyl phosphate synthetase. *JOURNAL OF THE AMERICAN CHEMICAL SOCIETY* **1999,** *121*, (15), 3803-3804.

40. Myers, R. S.; Amaro, R. E.; Luthey-Schulten, Z. A.; Davisson, V. J., Reaction coupling through interdomain contacts in imidazole glycerol phosphate synthase. *Biochemistry* **2005,** *44*, (36), 11974-85.

41. Willemoes, M., Competition between ammonia derived from internal glutamine hydrolysis and hydroxylamine present in the solution for incorporation into UTP as catalysed by Lactococcus lactis CTP synthase. *Arch Biochem Biophys* **2004,** *424*, (1), 105-11.

42. Bera, A. K.; Chen, S.; Smith, J. L.; Zalkin, H., Temperature-dependent function of the glutamine phosphoribosylpyrophosphate amidotransferase ammonia channel and coupling with glycinamide ribonucleotide synthetase in a hyperthermophile. *J Bacteriol* **2000,** *182*, (13), 3734-9.

43. Miles, B. W.; Raushel, F. M., Synchronization of the three reaction centers within carbamoyl phosphate synthetase. *Biochemistry* **2000,** *39*, (17), 5051-6.

44. Kim, J.; Raushel, F. M., Perforation of the tunnel wall in carbamoyl phosphate synthetase derails the passage of ammonia between sequential active sites. *Biochemistry* **2004,** *43*, (18), 5334-40.

45. Thoden, J. B.; Huang, X.; Raushel, F. M.; Holden, H. M., Carbamoyl-phosphate synthetase. Creation of an escape route for ammonia. *J Biol Chem* **2002,** *277*, (42), 39722-7.

46. Chaudhuri, B. N.; Lange, S. C.; Myers, R. S.; Davisson, V. J.; Smith, J. L., Toward understanding the mechanism of the complex cyclization reaction catalyzed by imidazole glycerolphosphate synthase: crystal structures of a ternary complex and the free enzyme. *Biochemistry* **2003,** *42*, (23), 7003-12.

47. Amaro, R. E.; Myers, R. S.; Davisson, V. J.; Luthey-Schulten, Z. A., Structural elements in IGP synthase exclude water to optimize ammonia transfer. *Biophys J* **2005,** *89*, (1), 475-87.

48. Luthey-Schulten, Z. A.; Amaro, R., Molecular dynamics simulations of substrate channeling through an α/β barrel protein. *Chem. Phys.* **2004,** *307*, 147-155.

49. Amaro, R.; Tajkhorshid, E.; Luthey-Schulten, Z., Developing an energy landscape for the novel function of a (beta/alpha)8 barrel: ammonia conduction through HisF. *Proc Natl Acad Sci U S A* **2003,** *100*, (13), 7599-604.

50. Smith, J. L., Structures of glutamine amidotransferases from the purine biosynthetic pathway. *Biochem Soc Trans* **1995,** *23*, (4), 894-8.

51. Brannigan, J. A.; Dodson, G.; Duggleby, H. J.; Moody, P. C.; Smith, J. L.; Tomchick, D. R.; Murzin, A. G., A protein catalytic framework with an N-terminal nucleophile is capable of self-activation. *Nature* **1995,** *378*, (6555), 416-9.

52. Bieganowski, P.; Pace, H. C.; Brenner, C., Eukaryotic NAD+ synthetase Qns1 contains an essential, obligate intramolecular thiol glutamine amidotransferase domain related to nitrilase. *J Biol Chem* **2003,** *278*, (35), 33049-55.

53. Sheng, S.; Moraga-Amador, D. A.; van Heeke, G.; Allison, R. D.; Richards, N. G.; Schuster, S. M., Glutamine inhibits the ammonia-dependent activities of two Cys-1 mutants of human asparagine synthetase through the formation of an abortive complex. *J Biol Chem* **1993,** *268*, (22), 16771-80.

54. Kim, J. H.; Krahn, J. M.; Tomchick, D. R.; Smith, J. L.; Zalkin, H., Structure and function of the glutamine phosphoribosylpyrophosphate amidotransferase glutamine site and communication with the phosphoribosylpyrophosphate site. *J Biol Chem* **1996,** *271*, (26), 15549-57.

55. Badet, B.; Vermoote, P.; Haumont, P. Y.; Lederer, F.; LeGoffic, F., Glucosamine synthetase from Escherichia coli: purification, properties, and glutamine-utilizing site location. *Biochemistry* **1987,** *26*, (7), 1940-8.

56. van den Heuvel, R. H.; Curti, B.; Vanoni, M. A.; Mattevi, A., Glutamate synthase: a fascinating pathway from L-glutamine to L-glutamate. *Cell Mol Life Sci* **2004,** *61*, (6), 669-81.

57. Ciustea, M.; Gutierrez, J. A.; Abbatiello, S. E.; Eyler, J. R.; Richards, N. G., Efficient expression, purification, and characterization of C-terminally tagged, recombinant human asparagine synthetase. *Arch Biochem Biophys* **2005,** *440*, (1), 18-27.

58. Hurd, R. E.; John, B. K., Gradient-enhanced proton-detected heteronuclear multiple-quantum coherence spectroscopy. *J. Magn. Reson.* **1991,** *91*, 648-653.

59. Schnizer, H. G.; Boehlein, S. K.; Stewart, J. D.; Richards, N. G.; Schuster, S. M., gamma-Glutamyl thioester intermediate in glutaminase reaction catalyzed by Escherichia coli asparagine synthetase B. *Methods Enzymol* **2002,** *354*, 260-71.

60. Bradford, M. M., A rapid and sensitive method for the quantitation of microgram quantities of protein utilizing the principle of protein-dye binding. *Anal Biochem* **1976,** *72*, 248-54.

61. Mendes, P., Biochemistry by numbers: simulation of biochemical pathways with Gepasi 3. *Trends Biochem Sci* **1997,** *22*, (9), 361-3.

62. Mendes, P., GEPASI: a software package for modelling the dynamics, steady states and control of biochemical and other systems. *Comput Appl Biosci* **1993,** *9*, (5), 563-71.

63. Bearne, S. L.; Hekmat, O.; Macdonnell, J. E., Inhibition of Escherichia coli CTP synthase by glutamate gamma-semialdehyde and the role of the allosteric effector GTP in glutamine hydrolysis. *Biochem J* **2001,** *356*, (Pt 1), 223-32.

64. Levitzki, A.; Koshland, D. E., Jr., Cytidine triphosphate synthetase. Covalent intermediates and mechanisms of action. *Biochemistry* **1971,** *10*, (18), 3365-71.

65. Zalkin, H.; Truitt, C. D., Characterization of the glutamine site of Escherichia coli guanosine 5'-monophosphate synthetase. *J Biol Chem* **1977,** *252*, (15), 5431-6.

66. Dossena, L.; Curti, B.; Vanoni, M. A., Activation and coupling of the glutaminase and synthase reaction of glutamate synthase is mediated by E1013 of the ferredoxin-dependent enzyme, belonging to loop 4 of the synthase domain. *Biochemistry* **2007,** *46*, (15), 4473-85.

67. Isupov, M. N.; Obmolova, G.; Butterworth, S.; Badet-Denisot, M. A.; Badet, B.; Polikarpov, I.; Littlechild, J. A.; Teplyakov, A., Substrate binding is required for assembly of the active conformation of the catalytic site in Ntn amidotransferases: evidence from the 1.8 A crystal structure of the glutaminase domain of glucosamine 6-phosphate synthase. *Structure* **1996,** *4*, (7), 801-10.

68. Vanoni, M. A.; Curti, B., Structure--function studies on the iron-sulfur flavoenzyme glutamate synthase: an unexpectedly complex self-regulated enzyme. *Arch Biochem Biophys* **2005,** *433*, (1), 193-211.

69. Su, N.; Pan, Y. X.; Zhou, M.; Harvey, R. C.; Hunger, S. P.; Kilberg, M. S., Correlation between asparaginase sensitivity and asparagine synthetase protein content, but not mRNA, in acute lymphoblastic leukemia cell lines. *Pediatr Blood Cancer* **2007**.

70. Cui, H.; Darmanin, S.; Natsuisaka, M.; Kondo, T.; Asaka, M.; Shindoh, M.; Higashino, F.; Hamuro, J.; Okada, F.; Kobayashi, M.; Nakagawa, K.; Koide, H.; Kobayashi, M., Enhanced expression of asparagine synthetase under glucose-deprived conditions protects pancreatic cancer cells from apoptosis induced by glucose deprivation and cisplatin. *Cancer Res* **2007,** *67*, (7), 3345-55.

71. Gutierrez, J. A.; Pan, Y. X.; Koroniak, L.; Hiratake, J.; Kilberg, M. S.; Richards, N. G., An inhibitor of human asparagine synthetase suppresses proliferation of an L-asparaginase-resistant leukemia cell line. *Chem Biol* **2006,** *13*, (12), 1339-47.

72. Horowitz, B.; Meister, A., Glutamine-dependent asparagine synthetase from leukemia cells. Chloride dependence, mechanism of action, and inhibition. *J Biol Chem* **1972,** *247*, (20), 6708-19.

73. Gong, S. S.; Guerrini, L.; Basilico, C., Regulation of asparagine synthetase gene expression by amino acid starvation. *Mol Cell Biol* **1991,** *11*, (12), 6059-66.

74. Cedar, H.; Schwartz, J. H., The asparagine synthetase of Escherhic coli. I. Biosynthetic role of the enzyme, purification, and characterization of the reaction products. *J Biol Chem* **1969,** *244*, (15), 4112-21.

75. Cedar, H.; Schwartz, J. H., The asparagine synthetase of Escherichia coli. II. Studies on mechanism. *J Biol Chem* **1969,** *244*, (15), 4122-7.

76. Herrera-Rodriguez, M. B.; Perez-Vicente, R.; Maldonado, J. M., Expression of asparagine synthetase genes in sunflower (Helianthus annuus) under various environmental stresses. *Plant Physiol Biochem* **2007,** *45*, (1), 33-8.

77. Herrera-Rodriguez, M. B.; Maldonado, J. M.; Perez-Vicente, R., Role of asparagine and asparagine synthetase genes in sunflower (Helianthus annuus) germination and natural senescence. *J Plant Physiol* **2006,** *163*, (10), 1061-70.

78. Herrera-Rodriguez, M. B.; Maldonado, J. M.; Perez-Vicente, R., Light and metabolic regulation of HAS1, HAS1.1 and HAS2, three asparagine synthetase genes in Helianthus annuus. *Plant Physiol Biochem* **2004,** *42*, (6), 511-8.

79. Herrera-Rodríguez, M. B.; Carrasco-Ballesteros, S.; Maldonado, J. M.; Pineda, M.; Aguilar, M.; Pérez-Vicente, R., Three genes showing distinct regulatory patterns encode the asparagine synthetase of sunflower (*Helianthus annuus*). *New Phytologist* **2002,** *155*, 33-45.

80. Koroniak, L.; Ciustea, M.; Gutierrez, J. A.; Richards, N. G., Synthesis and characterization of an N-acylsulfonamide inhibitor of human asparagine synthetase. *Org Lett* **2003,** *5*, (12), 2033-6.

81. Krahn, J. M.; Kim, J. H.; Burns, M. R.; Parry, R. J.; Zalkin, H.; Smith, J. L., Coupled formation of an amidotransferase interdomain ammonia channel and a phosphoribosyltransferase active site. *Biochemistry* **1997,** *36*, (37), 11061-8.

82. van den Heuvel, R. H.; Svergun, D. I.; Petoukhov, M. V.; Coda, A.; Curti, B.; Ravasio, S.; Vanoni, M. A.; Mattevi, A., The active conformation of glutamate synthase and its binding to ferredoxin. *J Mol Biol* **2003,** *330*, (1), 113-28

BIOGRAPHICAL SKETCH

Kai Li was born in Zouping, China on August 2, 1974. After he got his Bachelor of Science degree in biochemistry from Nankai University in Tianjin, China, he went to Beijing, China, and became a graduate student in Plant medicine in China Academy of Agriculture Sciences (CAAS), where he got his Master of Science degree. From 1998 to 2001, he worked in China Institute of Veterinary Drug Control (IVDC) and did residue analysis of veterinary drugs in food such as meat, egg and milk. In September 2002, he was enrolled in graduate school of State University of New York at Albany. Due to family reason, he transferred to University of Florida after being in Albany for about 9 months. From 2003 to 2007, he studied asparagine synthetase under the supervision of Dr. Nigel G. J. Richards.